

# POLITECNICO DI TORINO

Corso di Laurea Magistrale  
in Ingegneria Civile

Tesi di Laurea Magistrale

## Critical review and data modelling of interlayer shear resistance in asphalt pavements



### Relatori

Ezio Santagata

Pier Paolo Riviera

Lucia Tsantilis

*firma del relatore (dei relatori)*

prof. Nome del Relatore

.....

.....

### Candidato

*firma del candidato*

Juan David Gutierrez

December 2020

## Table of Contents

<i>Abstract:</i> .....	3
1. Chapter 1 – Introduction. ....	1
1.1. Introduction to chapter.....	2
1.2. Objectives and scope of work.....	5
1.3. Outline and organization of the document.....	6
2. Chapter 2 – Literature Review. ....	9
2.1. Introduction to chapter.....	10
2.2. Prior studies on the interface bond strength of interlayer of flexible pavements. ....	10
2.3. Prior studies on modelling the interlayer of flexible pavements .....	25
2.4. The Leutner Shear test.....	32
2.4.1. Shear bond test according to Standard BS EN 12697 – 48.....	34
3. Chapter 3 – Constitutive models .....	37
3.1. Introduction to chapter.....	38
3.2. Simple Shear models. ....	38
3.2.1. Bonded segment of the curve.....	39
3.2.2. Debonded segment of the curve.....	41
3.2.3. The interlayer reaction modulus, $K$ . ....	42
3.2.4. Peak shear stress and corrected displacement at peak shear stress. ....	44
3.3. Models considering shear and normal stresses. ....	44
3.3.1. Contribution of $\tau d$ .....	46
3.3.2. Contribution of $\tau res$ .....	47
4. Chapter 4 – Analysis of measured data. ....	49
4.1. Introduction to chapter.....	50
4.2. Experimental program and data obtention.....	50
4.3. Experimental results analysis .....	52
4.4. Stress – displacement curves. ....	53
4.5. Interlayer reaction modulus ( $K$ ) analysis.....	62
5. Chapter 5 -Software analysis.....	71
5.1. Introduction to chapter.....	72
5.2. Assessment of the bonding conditions in pavement analysis software. ....	72
5.2.1. BISAR (Bitumen Structures Analysis in Roads). ....	72

5.2.2.	EVERSTRESS .....	75
5.2.3.	EVERSTRESSFE.....	76
5.2.4.	KENPAVE .....	78
5.3.	Proposed method to calibrate the <i>Interlayer Stiffness K</i> and input in different pavement analysis software. ....	79
5.3.1.	Difference between considering <b><i>Kmax</i></b> and <i>K</i> . ....	88
5.4.	Interlayer reaction modulus effect on asphalt pavement modelling.....	91
5.4.1.	Modelling in BISAR 3.0 .....	92
5.4.2.	Modelling in EVERSTRESSFE.....	97
5.4.3.	Importance of calibrating adequately the interlayer bonding condition. ....	101
5.4.4.	Input values from measured Leutner data.....	102
6.	Chapter 6 - Conclusions .....	105
7.	Bibliography.....	109
8.	Appendix.....	113
8.1.	Appendix A – Stress – displacement curves with <i>Kmax</i> and <i>K</i> lines. ....	114
8.1.1.	ME_1 plots.....	114
8.1.2.	ME_2 plots.....	116
8.1.3.	TE_1 plots.....	117
8.1.4.	TE_2 plots.....	119
8.1.5.	NT plots.....	121
8.2.	Appendix B – MATLAB script.....	123
9.	Acknowledgments.....	124

### Table of figures

Figure 1.1:	Typical flexible pavement cross-section.....	2
Figure 1.2:	Slippage cracking on a surface of flexible pavement. ....	4
Figure 2.1	AC pavement cross-section used by Shahin et al. ....	10
Figure 2.2	Effect of interlayer slippage on maximum horizontal strain at the bottom of the old AC layer.....	11

Figure 2.3: Comparisons of horizontal strains at overlay surface when a shear load is present. ...12

Figure 2.4: Tests methods to assess the interlayer bond properties both in the Lab and in-situ. ...13

Figure 2.5: Factors that affect the interlayer’s behavior, as proposed by Raab and Partl. ....17

Figure 2.6: Shear strength vs displacement relationship .....18

Figure 2.7: Modelled shear stress vs displacement. ....18

Figure 2.8: (a) Specimens compacted through Continuous paving. (b) Specimens compacted through discontinuous paving, used by Zhang et al. ....23

Figure 2.9: Failure envelopes obtained by Cutica for interfaces treated with a cationic emulsion. ....24

Figure 2.10: Layout of the real-scale pavement sections used for the APT program, (Ozer et al., 2012). ....26

Figure 2.11: Failure envelope used to describe the interface behavior under various loading conditions, (Ozer et al., 2012). ....27

Figure 2.12: Cross-section of the 3D FE model done (Ozer et al., 2012). ....27

Figure 2.13: Modelled vertical deformations under loading (Williamson, 2015). ....29

Figure 2.14: : Schematics of the Leutner device, Review of applicable bond strength tests for assessing asphalt delamination potential (Tseng, Street and Vic, 2019). ....33

Figure 2.15: Typical stress – displacement curve from Leutner test. ....34

Figure 2.16: Schematics on the Shear Testing Apparatus (BSI group, 2019). ....35

Figure 2.17: Specimen Geometry according to standard. ....35

Figure 2.18: Stress – Displacement curve parameters (bsi group, 2019). ....36

Figure 3.1: (a) Initial state of the double-layered specimens in direct shear tests .....38

Figure 3.2: Example of shear stress versus displacement plot, obtained from a Leutner test. ....39

Figure 3.3: Bonded segment of the shear – displacement curve. ....40

Figure 3.4: Stress – displacement curve (bsi group, 2019). ....43

Figure 3.5: (a) Undeformed state of the double-layered specimens. (b) Deformed state of the double-layered specimens under shear load and normal load. ....45

Figure 3.6: Detail of the interlocking between surfaces at the interlayer level. ....46

Figure 4.1 Setup of the pavement test section and sub-sections. ....51

Figure 4.2: Schematics of the double – layered cores obtained from the pavement test section. ...52

Figure 4.3: Stress – displacement curves for ME\_1 cores. ....54

Figure 4.4: Stress – displacement curves for ME\_2 cores. ....55

Figure 4.5: Stress – displacement curves for TE\_1 cores. ....57

Figure 4.6: Stress – displacement curves for TE\_2 cores. ....58

Figure 4.7: Stress displacement curves for NT cores.....	60
Figure 4.8: $T_{peak,avg}$ for all of the analyzed cores.....	61
Figure 4.9 (a): Lines used to find $K_{max}$ and $K$ in ME_1_1.....	63
Figure 4.10: Stress – displacement curves, TE_1_3.....	66
Figure 4.11: Interlayer reaction modulus results for all categories.....	68
Figure 5.1: Input screen to define slippage between layers in BISAR 3.0 (Bitumen Business group, 1998).....	73
Figure 5.2: Location of the interface contact configuration screen in Everstress.....	76
Figure 5.3: Interface condition configuration in EverStressFE.....	77
Figure 5.4: KENPAVE main screen.....	78
Figure 5.5: Type of Interface screen in KENPAVE.....	79
Figure 5.6(a): Stress – displacement curve plot obtained from the MATLAB script, ME_1_1....	82
Figure 5.7: ME_1_1 bonded segment of the curve plotted by MATLAB script to select points. .	84
Figure 5.8: $K_{max}$ line plotted over the bonded segment of the curve.....	85
Figure 5.9: Bonded segment of the curve, $K_{max}$ and $K$ lines, ME_1_1.....	87
Figure 5.10: Bonded segment of the curve, $K_{max}$ line, ME_1_1.....	89
Figure 5.11: ME_1_1 Bonded segment of the curve and $K$ line.....	90
Figure 5.12: Scheme of the modelled pavement section in BISAR 3.0.....	92
Figure 5.13: Modelled pavement section on EVERSTRESSFE.....	98
Figure 5.14 (a): Displacements and strains obtained for $K_{max}$ .....	99
Figure 5.15 (a): Displacements and strain for fully bonded condition.....	100
Figure 8.1: Bonded segment of the curve with $K_{max}$ and $K$ lines, ME_1_1.....	114
Figure 8.2: Bonded segment of the curve with $K_{max}$ and $K$ lines, ME_1_2.....	115
Figure 8.3: Bonded segment of the curve with $K_{max}$ and $K$ lines, ME_1_3.....	115
Figure 8.4: Bonded segment of the curve with $K_{max}$ and $K$ lines, ME_2_1.....	116
Figure 8.5: Bonded segment of the curve with $K_{max}$ and $K$ lines, ME_2_2.....	116
Figure 8.6: Bonded segment of the curve with $K_{max}$ and $K$ lines, ME_2_3.....	117
Figure 8.7: Bonded segment of the curve with $K_{max}$ and $K$ lines, TE_1_1.....	117
Figure 8.8: Bonded segment of the curve with $K_{max}$ and $K$ lines, TE_1_2.....	118
Figure 8.9: Bonded segment of the curve with $K_{max}$ and $K$ lines, TE_1_3.....	118
Figure 8.10: Bonded segment of the curve with $K_{max}$ and $K$ lines, TE_2_1.....	119
Figure 8.11: Bonded segment of the curve with $K_{max}$ and $K$ lines, TE_2_2.....	119
Figure 8.12: Bonded segment of the curve with $K_{max}$ and $K$ lines, TE_2_3.....	120

Figure 8.13: Bonded segment of the curve with Kmax and K lines, NT\_1. ....121  
Figure 8.14: Bonded segment of the curve with Kmax and K lines, NT\_2. ....121  
Figure 8.15: Bonded segment of the curve with Kmax and K lines, NT\_3. ....122

## Table of tables

Table 2.1: Direct Shear tests summary proposed by Raab and Partl (1).....	14
Table 2.2: Direct shear tests summary proposed by Raab and Partl (2). ....	15
Table 2.3: Simple shear tests summary, as proposed by Raab and Partl. ....	16
Table 2.4: Leutner test limit values proposed by various authors. ....	20
Table 2.5: Summary of the experimental program performed by Canestrari et al.....	21
Table 2.6: Experimental program proposed (Raab and Partl, 2004).....	22
Table 2.7: Variables used to calibrate the statistical models developed by (Das et al., 2018).....	31
Table 2.8: Regression model parameters (Das et al., 2018).....	32
Table 3.1: Interlayer stiffness boundary values to describe the interlayer bonding condition.....	42
Table 3.2: Constitutive equations that rule the interlayer shear behavior. ....	48
Table 4.1: Peak values for ME_1 .....	54
Table 4.2: Average of Tpeak for ME_1 .....	55
Table 4.3: Peak values for ME_2. ....	56
Table 4.4: Average of Tpeak, ME_2.....	56
Table 4.5: Peak values for TE_1. ....	57
Table 4.6: Average of Tpeak for TE_1. ....	57
Table 4.7: Peak values for TE_2. ....	59
Table 4.8: Average Peak values for TE_2.....	59
Table 4.9: Peak values for NT cores. ....	60
Table 4.10: Average Peak value for NT cores. ....	60
Table 4.11: Summary of the results obtained in terms of Tpeak for all cores .....	61
Table 4.12: Kmax, K and corrected peak displacement, all tests in ME_1 specimens. ....	65
Table 4.13: Results for Kmax, K and $\epsilon_{max}$ for all tests of ME_2. ....	65
Table 4.14: Results for Kmax, K and $\epsilon_{max}$ for all tests of TE_1. ....	66
Table 4.15: Results for Kmax, K and $\epsilon_{max}$ for all tests of TE_2. ....	67
Table 4.16 Results for Kmax, K and $\epsilon_{max}$ for all tests of NT.:.....	67
Table 4.17: Summarized results of the interlayer reaction modulus for all categories of specimens. .....	68
Table 5.1: Software and parameters to calibrate. ....	80
Table 5.2: Prompts in the MATLAB script to initialize the calculations.....	81
Table 5.3: Results of the linear regression on the selected points.....	86
Table 5.4: Input values in the analyzed software. ....	91

Table 5.5: Interlayer reaction modulus (MPa/mm) to shear spring compliance ( $m^3/N$ ) conversion. .....	93
Table 5.6: Interlayer bonding condition boundary limits in terms of the shear spring compliance .....	93
Table 5.7: BISAR results for a horizontal load equal to 1 kN. ....	94
Table 5.8: BISAR results for a horizontal load equal to 20 kN. ....	95
Table 5.9: BISAR results for a vertical load equal to 40 kN.....	96
Table 5.10: Layer specifications for model in EVERSTRESSFE .....	98
Table 5.11: Interlayer stiffness boundary values in EVERSTRESSFE. ....	101
Table 5.12: Obtained input values from experimental data. ....	103

## Table of equations

(2.1) .....	11
(2.2) .....	26
(2.3) .....	28
(2.4) .....	30
(2.5) .....	30
(2.6) .....	31
(2.7) .....	31
(2.8) .....	33
(3.1) .....	41
(3.2) .....	41
(3.3) .....	41
(3.4) .....	44
(3.5) .....	45
(3.6) .....	45
(3.7) .....	46
(3.8) .....	47
(3.9) .....	47
(3.10) .....	47
(3.11) .....	47
(3.12) .....	47
(4.1) .....	53
(5.1) .....	74
(5.2) .....	74
(5.3) .....	74
(5.4) .....	74
(5.5) .....	75
(5.6) .....	85
(5.7) .....	85
(5.8) .....	86
(5.9) .....	86
(5.10) .....	88
(5.11) .....	89





## ***Abstract:***

The ever-increasing amount of traffic is constantly forcing the society to improve the design of pavements. One particular design element that has been overlooked in this area are the interlayers of pavements. The term ‘interlayer’ refers to the exact part where two of the main layers of a pavement are in contact, and they can be treated with a tack coat/emulsion to improve the structure’s response under loading.

It has been shown that the lack of proper bonding between the pavement layers can lead to various distresses such as reflective cracking. For such reason, it is not only important to ensure the proper bonding but also to ensure that the interlayer behavior is properly characterized but it is also important to determine a proper method to calibrate effectively the interlayer bonding condition, which will result in more accurate and effective designs.

Thus, the main scope of this research was to determine a method to calibrate the interlayer bonding condition in the adequate way, based on the results obtained from one of the most common and easily accessible shear bonding tests – the Leutner shear test. To do so, a critical literature review was performed, along with a review on the existing constitutive models that reign the interlayer shear behavior.

From such review it was found that the constitutive model that better describes the interlayer behavior only under shear action (the Leutner test only admits shear loading) is *Goodman’s constitutive equation*, which states that the shear stress is equal to the displacement times the interlayer reaction modulus,  $K$ . This parameter is used to characterize the interlayer bonding condition and can be obtained from the stress – displacement curves (plotted from Leutner data). Also, the standard proposes that there are two possible values for the modulus,  $K_{max}$  and  $K$ .

To define the proper value to select, data obtained from Leutner tests in five different type of cores, characterized by different type of interlayer configurations was analyzed. The different configurations varied between a traditional cationic emulsion, a modified emulsion both at 0.15 and 0.30 kg/m<sup>2</sup> and an interlayer with no treatment. Both the peak shear stresses and the interlayer reaction modulus (both  $K_{max}$  and  $K$ ) were calculated for all types of cores. In terms of  $\tau_{peak}$ , the traditional emulsion at 0.15 kg/m<sup>2</sup> obtained the highest value, as well as in terms of  $K_{max}$  and  $K$ . For this analysis, a MATLAB script that performs the whole analysis of the Leutner data done in this document was developed.

Then, a review was performed on various asphalt pavement design software (EVERSTRESS, BISAR 3.0, EVERSTRESSFE and KENPAVE) to discuss the way in which these software permits the user to calibrate the interlayer condition. From these, BISAR 3.0 and EVERSTRESSFE were the software that allow to calibrate the interlayer condition in terms of the reaction modulus (shear spring compliance in BISAR, is the inverse of the modulus). The experimental values were used to perform models in both of these software, along with the fully bonded and completely debonded condition. From the modelling, it was found that even slight variations on the modulus can lead to variations in design/modelling purpose that can lead to underestimation or overestimation of the real effects. This enforces the idea of selecting the proper value of the modulus, which as discussed in this research was found to be the mean of the computed values of the  $K_{max}$  for a given number of tests of a specific core type,  $K_{max,avg}$ .



# **1. Chapter 1 –** **Introduction.**

## 1.1. Introduction to chapter.

Nowadays, roads constitute one of the most important parts of the infrastructure that keeps society working. Either for the need to move from one point to another, or to transport goods or materials, roads facilitate the displacement of people from one place to another, by providing the connection of places and the use of vehicles to perform these displacements. One of the most important elements on roads are pavements. These do not only provide a smooth surface along which the wheels of vehicles can roll on, but also provide a proper support and load distributing into the subgrade of the loads that originate from the traffic movements.

Pavements are defined as layered structures, which vary in composition and characteristics, moving from the surface down to the subgrade. Its main goal consists in the proper distribution of wheel loads from the top down to the bottom. Two main types of pavements exist, depending on their constitution: flexible and rigid pavement.

Flexible pavements are characterized by the use of bituminous mixtures, such as asphalt, that results on a flexible behaviour of the layers composed by these types of mixtures. On the other hand, rigid pavements are characterized by the use of concrete slabs on the top layers, which results on a rigid behaviour of the structure. The scope of this investigation is based mainly on the flexible pavements and Figure 1.1 shows the typical cross-section for this type of pavements:

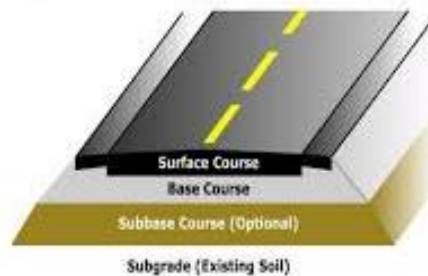


Figure 1.1: Typical flexible pavement cross-section.

As it can be observed, it is composed of various layers, which vary in thickness and each one has different characteristics, that will allow the pavement structure to work properly. A brief description on each one is given below.

- **Surface course:** This layer is composed by a dense-graded bituminous mixture, in which the aggregates are continuously graded, generating a lot of contact between stones. Its main function is to resist traffic distortions (contact between this course and traffic), to provide waterproofing to the structure, to provide skid resistance, and finally, to adequately distribute traffic loads into the underlying layers. **(3 – 5 cm)**.
- **Binder course:** Composed of dense graded bituminous mixtures, the bitumen content is less than in the surface course. Its function is to link the surface course with the base layer (therefore can be considered a transition course), and to properly distribute loads into the underlying layers. **(5 – 10 cm)**.
- **Base course:** It may be composed of a granular mixture, a stabilized mixture or a dense-

graded bituminous mixture. The function of this layer is to further distribute the loads adequately into the layers below (**10 – 30 cm**).

- **Sub-base course:** Made with an unbound granular mixture. Its functions are to distribute the loads into the subgrade, and to prevent the water to penetrate from the subgrade into the pavement (through capillarity) and to avoid the infiltration of dust particles also coming from the subgrade. (**10 – 30 cm**).

The appropriate performance of the pavement (as well as its lifespan), depends greatly on the characteristics (such as strength and stiffness) of each layer, as well as on their thicknesses. However, over the course of the years, it has been found that there are additional factors which affect the performance and lifespan in pavements, such as the bond between layers.

In flexible pavements, it is very important that layers are fully bonded between them, so that the pavement will behave as a whole, rather than as separate layers, acting together. In order to ensure the adequate bonding between layers, that will result in a better performance and life-span of a pavement, modern pavements use material or a combination of material, between layers. These mixtures used in between layers, are called *interlayers*, and one of the most common interlayers is denominated *tack coat*.

The tack coat is used in order to ensure the bonding between two bituminous layers (such as an overlay of a new asphalt course over an old one), whilst also providing a waterproofing/moisture barrier effect. Additionally, it helps to mitigate the effects of reflective cracking.

According to their material, interlayers can be either made out of:

- **Bituminous based materials** - Asphalt emulsions, paving-grade asphalt or cutback asphalts.
- **Membranes** - which can be composed out of different materials such as rubber, geotextiles or thermoplastic materials.

However, nowadays, the most popular type of interlayers used are the asphalt emulsions (bituminous based material), due to their reduced environmental impact, to the fact that they have better performance than the others. Emulsions are defined as the dispersion of small droplets of one liquid into another liquid. These liquids must be non-miscible and non-soluble. An asphalt emulsion, therefore, it is the dispersion of tiny bitumen droplets into water (Oil-in-water emulsion), plus an emulsifier agent and other elements in minor quantities.

When studying pavements, is important to understand the loads coming from the traffic, and the effect they have in each one of the layers of the pavements, as the inadequate response of any of the layers may result in what are known as *pavement distresses* and in order to obtain an effective and durable pavement, should be avoided.

In the case of flexible pavements, when studying their structural response to the applied loads, the traffic induced loads may be:

- Vertical: Dead weight, dynamic effects.
- Longitudinal: Traction, braking, horizontal forces due to friction.
- Transversal: Centrifugal effects, vehicle instability and yaw.

Although the whole pavement is affected by these types of loads, when speaking particularly about interlayers, the main types of loads to take into account are those which generate a shear stress

(longitudinal/transversal), since these types of stresses are the ones that cause slippage between layers and affect the bond between them.

When there's a lack of an adequate bonding between layers, the flexible pavement might suffer the following distresses, under repeated traffic loading:

- Premature fatigue.
- Reflective cracking.
- Top-down cracking.
- Slippage cracking.

From these, probably the most common and mostly affected by the lack of bonding between layers is the *slippage cracking* (shown in Figure 1.2). Slippage cracking is characterized by half-moon or crescent-moon shaped cracks. This type of distress is more commonly found in zones of braking/accelerating, such as curves and intersections. It can lead to an infiltration of moisture and roughness in the wearing course, which reduces consequently, the pavement's performance and lifespan.



Figure 1.2: Slippage cracking on a surface of flexible pavement.

It is important to take into account, that there are several factors that influence the adequate performance of tack coats, such as the tack coat composition, its application rate (amount of applied tack coat), temperature of application, degree of compaction, amongst others, which have been studied in the past.

For doing so, various testing methods have been used. As the main factor affecting the bonding between layer is the shear resistance, most of the tests performed were mainly shear tests, which can be catalogued into two main types of tests:

- Direct shear testing.
- Simple shear testing.

The main difference between these two types of tests, is that, while in direct shear tests the shear load is applied on the frontal surface of the specimen, in the case of the simple shear tests, the force is applied at the top of the specimen, thus shearing the upper layer against the bottom one. Additionally, usually direct shear tests don't allow the application of a normal load, whereas the

simple shear tests do allow it.

These tests allow to measure the applied forces (horizontal loads and vertical loads), which are traduced into stresses (shear or normal stresses), and the displacements in the horizontal direction and in the vertical direction (if allowed by test). From these results, the interlayer's behavior can be studied and analyzed in terms of the previous mentioned factors that influence it.

However, the final objective of studying the interlayers characteristics and behavior is not only to understand them, but rather, applying these concepts into designs. By applying such concepts into design, the result will be a more efficient pavement, in which the development of distresses is avoided as far as possible, resulting in an improved performance and lifespan of the constructed pavement.

In the area of pavement modelling or design, the most common tool used for such objective are the pavement analysis software. They are used to analyze a given pavement structure, under certain loading conditions and obtain results in terms of stresses, strains and displacements. Such results allow to design the pavement, mainly in terms of thickness of each layer, in order to avoid the principal distresses.

In order to further helping to improve the process of pavement design, this study focuses on doing a critical review on some of the existing flexible pavement analysis software and how each one of them allow to define the interlayer condition. Although some of them just allow to define if the interlayer is partially bonded, fully bonded or debonded, others allow to calibrate the interlayer reaction modulus,  $K$ .

For doing so, firstly an analysis on the existing constitutive models on the interlayers shear response will be done to provide an adequate understanding on what occurs to the interlayer under the action of loading.

Consequently, an analysis of data obtained by performing Leutner shear tests on various types of cores will be done, in order to characterize the specimens when only analyzed under shear loading and to obtain their respective values of the interlayers shear modulus and peak shear stress.

Once this is done, a critical review on some of the existing software and their method of analyzing the interlayer response will be provided, which will lead to the definition on how to calibrate a value to introduce in such software, by performing Leutner tests on double-layered specimens. Then, taking into consideration the previous information, and the results calculated from the experimental data, the calculated values of the interlayer reaction modulus will be compared by modelling a two-layered pavement system in order to assess the impact of the selecting of the interlayer reaction modulus.

Finally, with the previous information at hand, it is possible to conclude on the proper way to calibrate the interlayer bonding condition and thus, give some reference values to input in the software, based on the experimental data and on the software analysis.

## **1.2. Objectives and scope of work.**

The main objective of the current research, is to propose a method on how to calibrate the parameter that must be input in asphalt pavement design software to define the interlayer bonding condition,

based on the results obtained from the Leutner shear test.

In order to do so, firstly, a review on the constitutive methods that describe the interlayers shear response under loading is performed, in order to get a proper understanding on this phenomenon, in order to set a base for the further analysis that must be done.

Then, an analysis on each of BISAR, EVERSTRESS, EVERSTRESSFE and KENPAVE is done, both by interacting with each software, as well as by reviewing the User's guide of each one, to gather and analyze the information on how these software treats the interlayer condition. Once the analysis on the software is done and combined with the review on the constitutive models that describe the shear behavior of the interlayers, an analysis on what value must be calibrated and how is done. Also, two models will be developed in BISAR and EVERSTRESSFE in order to assess the importance of calibrating properly the interlayer bonding condition

Finally, combining the analysis done on the software, and how to calibrate the input values with the results obtained from the experimental part of the research, in order to provide the values that must be used as input in software when designing/modelling pavements that have the same interlayer conditions as the cores.

Then, based on all this, the specific objectives of this research are:

- Provide a critical review on the existing constitutive models that rule the interlayer shear behavior under different loading conditions.
- To understand how various asphalt pavement design software, allow the user to define the interlayer condition.
- From the experimental data measured by performing Leutner tests to double-layered specimens from a pavement test-section, calibrate the input values that should be used when defining a pavement with the same characteristics as the tested cores.
- Provide a MATLAB script that allows to perform the analysis of Leutner test data, in order to characterize the interlayer in terms of peak shear stress and interlayer reaction modulus.
- Through modelling, assess the importance of calibrating and adequate value that represents the interlayer bonding condition.

### **1.3. Outline and organization of the document.**

The current document has been divided into six chapters, including this first introductory chapter in which, the justification, objectives and scope of this work is given.

During Chapter 2, a literature review is performed, in order to provide the base of the work, as well as to get insight into the state-of-the-art research in this area of study. Additionally, during Chapter 2, the Leutner shear test is introduced, as well as the standard that gives the guidelines in how to perform shear bond testing on hot-mix asphalt pavements.

Chapter 3 focuses on the mechanical characterization, through constitutive equations, of the interlayer shear response under different loading conditions. The characterization mainly focuses on the response of the interlayer when analyzed solely under shear loads or when analyzed under the action of both shear and normal loads. The parameters that describe the response are also discussed in this chapter, as well as how to analyze experimental results based on such constitutive

equations.

Once the interlayer behavior has been discussed during Chapter 4, an analysis on measured data from a flexible pavement test section, in which various interlayer treatments/conditions are defined within the sub-segments of the test section. The measured data is obtained by performing Leutner tests on various cores extracted from the pavement test section.

In Chapter 5, a critical review is done on various asphalt pavement design software, in order to understand how the interlayer condition is defined in every one of them. Once the analysis on the software is done, a method to calibrate the values to define the interlayer is proposed, based on the results obtained from Leutner testing. Additionally, along this chapter, a MATLAB script that allows the user to obtain a full analysis (as proposed in previous chapters), from raw data obtained from Leutner tests.

Additionally, during this chapter, two models will be developed, one in BISAR 3.0 and EVERSTRESSFE in order to assess the importance of choosing the adequate value to calibrate the interlayer bonding condition and its impact on the obtained results, in terms of displacements, stresses and strains.

Finally, in Chapter 6, the conclusions of this research are presented, as well as some recommendations for future investigations.



## **2. Chapter 2 – Literature Review.**

## 2.1. Introduction to chapter

In order to set the proper founding pillars for any study or research, it is of the utmost importance to review and understand the work of previous authors on the field, as well as the state-of-the-art research on it. For such reason, this chapter focuses on a extensive literature review on previous studies that have focused on describing the behavior and the phenomena that surround the interlayers of asphalt pavements.

Since this study also focuses on the modelling/design asphalt pavement software, also a review on the studies that have focused in this area is provided along this chapter. Finally, since the experimental portion of this study is centered around the Leutner shear test, it will be described in detail, along with the standard that regards the shear bond testing for hot-mix asphalts.

## 2.2. Prior studies on the interface bond strength of interlayer of flexible pavements.

One of the first studies on the evaluation of the interface bond strength, was called Consequence of Layer Separation on Pavement Performance (Shahin *et al.*, 1987) and focused on determining the effect of bond loss at the interface and its consequent layer separation, on the structural behavior of pavements. Although this study may be more related to the modelling studies, rather than experimental ones, it reveals the importance of studying the interlayers and is one of the base studies that has pushed more and more authors to focus in this area of study.

This study was carried out by considering the following cross section for AC pavements, was used:

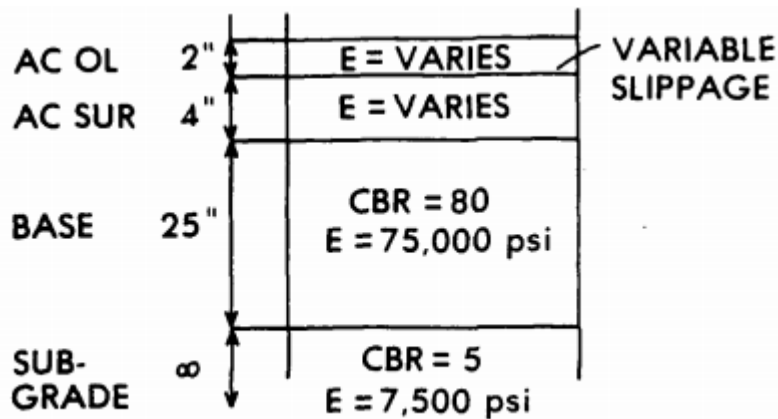


Figure 2.1 AC pavement cross-section used by Shahin *et al.*

As shown in Figure 2.1, the cross-section consisted of a new AC concrete layer overlaid (AC OL) over an already existing AC pavement surface layer (AC SUR), characterized by the quantities shown in the previous figure. This model was studied by using the SHELL software, BISAR (Bitumen Structures Analysis in Roads). It allowed to analyze strains and displacements, by varying the degree of slippage between the layers based on Equation **Error! Reference source not found.**:

$$\Delta = K \cdot \tau \quad (2.1)$$

Where:

- $\Delta$ : Relative displacement of one layer with respect to the other [mm].
- $\tau$ : Horizontal shear stress transmitted across the interface [MPa].
- $K$ : Constant of proportionality (slippage coefficient) [mm/MPa].

As its name states, the slippage coefficient allows to vary the degree of slippage between the layers, and during this study, different values of  $K$  were tested, in the range from no slippage (complete bonding), to complete slippage (frictionless).

Different cases were analyzed during this study, such as varying  $K$  values from 0 to 1000 [mm/MPa], in order to determine how the horizontal strain, varies with respect to the variation on the slippage coefficient. Additionally, the behavior of the interlayer was studied under the effect of horizontal and vertical loads.

In Figure 2.2, the variation of the horizontal strain at the bottom of the old AC layer with respect to the variation of  $K$ . The focus of this particular strain is done due to the fact that, when analyzing the pavement's fatigue life, one of the values that must be controlled, according to the author of this study, is either the horizontal tensile strain at the bottom of the overlay layer (AC OL), the horizontal tensile strain at the bottom of the old surface layer (AC SUR) or finally, the vertical compressive strain at the top of the subgrade.

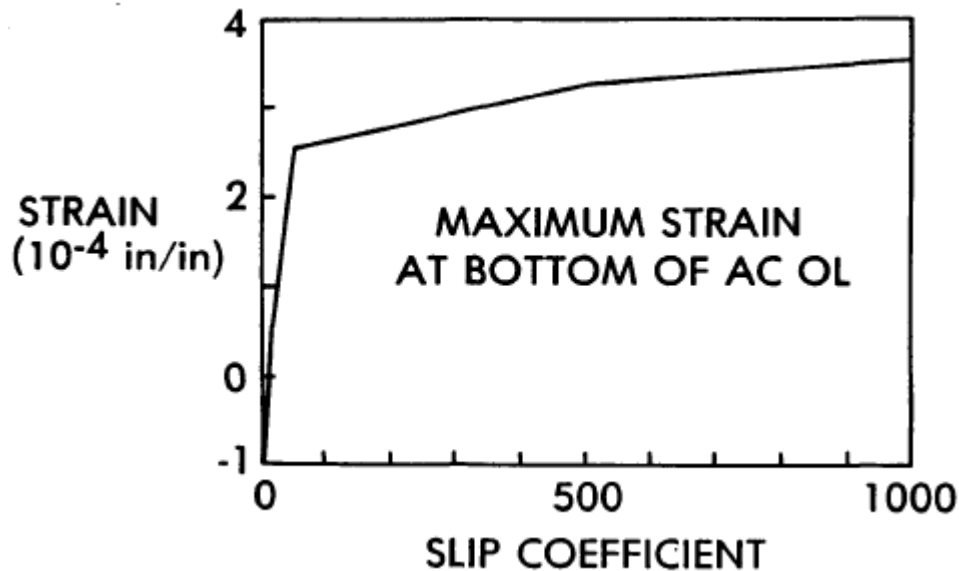


Figure 2.2 Effect of interlayer slippage on maximum horizontal strain at the bottom of the old AC layer.

In addition, a comparison of the horizontal strain when both vertical and horizontal loads (shear loads) are present, with respect to the case where only vertical loads are presents was made, when there's full slippage between layers is shown in Figure 2.3:

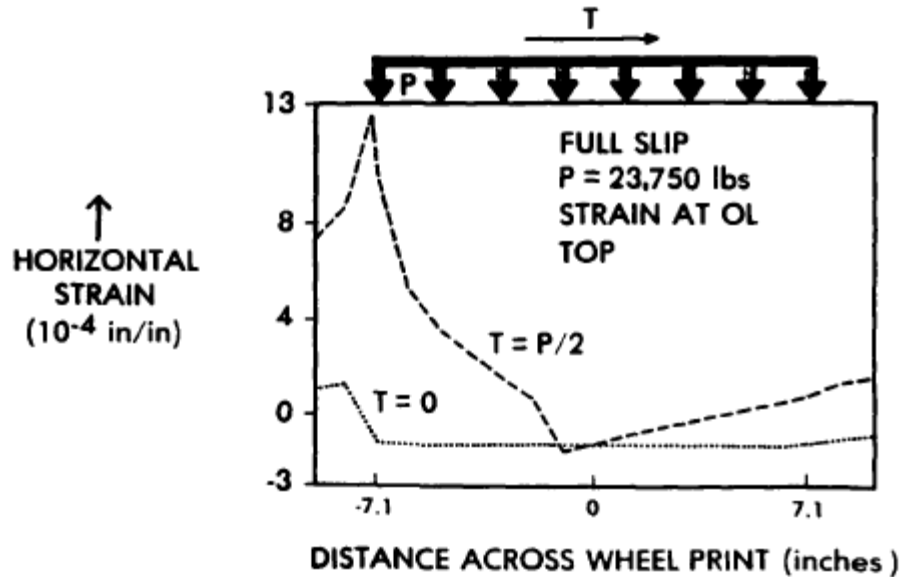


Figure 2.3: Comparisons of horizontal strains at overlay surface when a shear load is present.

From this study, some conclusions were stated, regarding both the variation of  $K$  and the effect of horizontal loads in the AC pavement, such as:

At the bottom of the overlay layer, it is clear that the horizontal strain increases rapidly for low values of  $K$ , while as this value approaches 1000, it increases slowly. Consequently, this shows that a small amount of slippage is required to mobilize the full horizontal strains.

Regarding the vertical subgrade strains, this study showed that slippage causes the layers of the pavement to behave independently from each other rather than as a whole. Since two thinner layers acting independently are not as rigid as when they work as a whole, the slippage between layers causes the compressive vertical strain at the subgrade to increase.

In presence of shear loads, greater strains are generated at the top of the overlay, and by increasing these loads, this study showed that the strains increase linearly with them. Therefore, Shahin et al. concluded that the most important determining factor of the magnitude of the strains is related directly to the magnitude of the shear loads.

When comparing the horizontal strains in presence of a shear load, in the case where there is no slip, versus the case where there is full slip, Shahin concluded that when there is full slip the strains are greater than when the two layers are fully bonded.

Finally, Shahin et al. concluded that in order to improve the pavement's response under loading and consequently its life span, a good bonding between the AC layer must be ensured.

Later on, various authors have developed different tests in order to assess the interface bonding strength on pavements, which have allowed the investigators, to evaluate different conditions that affect the interlayer's behavior. Prior to mentioning other studies, it is important to understand the type of tests available for this subject. On *Evaluation of interlayer shear bond devices for Asphalt Pavements* (Raab, Partl and El Halim, 2009), the existing testing methods for the interlayer shear bond strength are described and summarized, along with a review of the studies where these devices have been used.

Firstly, Raab discretized between two main types of tests used to assess the interlayer bond properties, both in the Lab and in-situ. In Figure 2.4, Raab and Partl showed the types of tests used, and separate them in two groups, Shear tests and Tension tests:

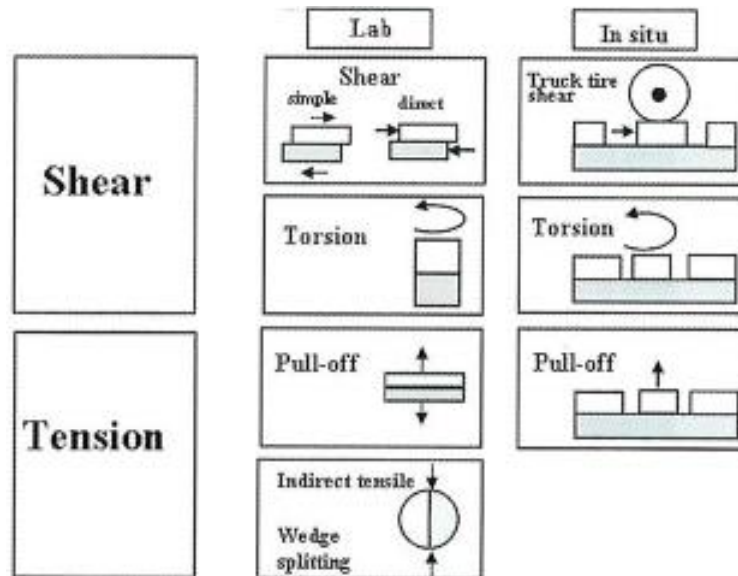


Figure 2.4: Tests methods to assess the interlayer bond properties both in the Lab and in-situ.

However, it is important to note that from these tests, the Shear testing methods are by far the most common methods to evaluate the bonding between layers. Among the shear tests, in this study, two main types of tests were distinguished: direct shear tests and simple shear tests.

Firstly, in direct shear tests, it is important to note that these are guillotine type tests and the force is induced at one side of the specimen rather than in the front surface. Additionally, the specimens are clamped or introduced in a fitting system into the device. These types of tests usually don't allow the use of a normal load, perpendicular to the shear force direction.

On the other hand, simple shear tests are characterized by the fact that in these, the shear force is applied by shearing the top of the specimen against the bottom, and the force is applied at the front surface of the specimen. Since in these tests usually the specimens are glued or fixed by tight fixture, they admit usually the application of a normal load.

In Table 2.1, Table 2.2, the summary made by Raab and Partl can be observed, in the case of the direct shear test devices, whilst in Table 2.3, the case of simple shear tests may be observed:

Table 2.1: Direct Shear tests summary proposed by Raab and Partl (1).

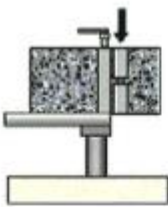
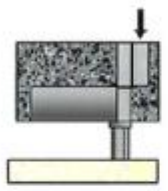
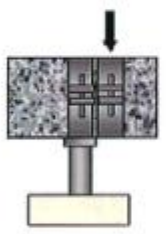
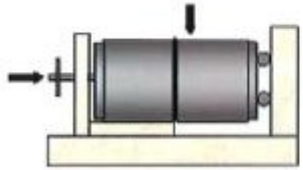
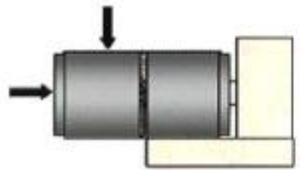
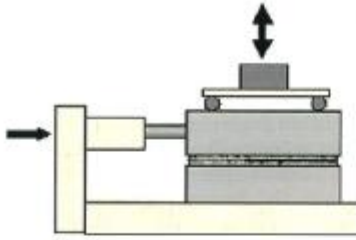
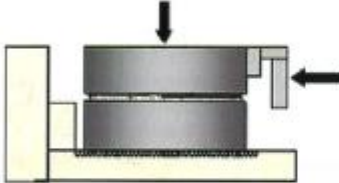
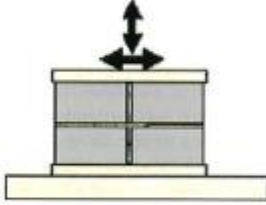
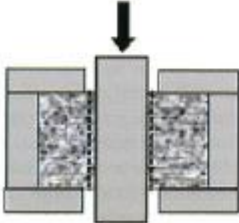
Device	Characteristics
 <p>Leutner device</p>	<p>Specimens: cylinders 150 mm or 100 mm (Austria), specimens are mechanically clamped with a latch fastener</p> <p>Gap width: 1 mm</p> <p>Testing: static</p> <p>Normal force: none</p> <p>Method for quality control in different European countries (e.g. Austria, Germany and Switzerland)</p> <p>Deformation rate: 50 mm/min</p> <p>Temperature: 20 °C (standard), for research 10 °C to 40 °C</p> <p>Result: force/deformation diagram, max force (stress)</p>
 <p>Modified device, Empa</p>	<p>Specimens: cylinders 150 mm (standard), others: 148 mm to 155 mm, and rectangular specimens 150x130 mm, specimens are hold by defined pneumatic pressure using a semicircular damp</p> <p>Gap width: 2 mm</p> <p>Testing: static</p> <p>Deformation rate: 50 mm/min</p> <p>Normal force: none</p> <p>Temperature: 20 °C (standard), other for research 40 °C</p> <p>Result: force deformation diagram, max force (stress), stiffness (max force/max slop of the force/deformation curve) in kN/mm</p>
 <p>Iowa device</p>	<p>Specimens: cylinders 150 mm, specimens are fixed in aluminium rings with pipe clamps</p> <p>Gap width: 4.8 mm</p> <p>Testing: static</p> <p>Normal force: none</p> <p>Deformation rate: 50 mm/min</p> <p>Temperature: 25 °C</p> <p>Result: force deformation diagram, max force (stress)</p>
 <p>NCAT device</p>	<p>Specimens: cylinders 150 mm, specimens are cut and placed in steel cups</p> <p>Gap width: 4.8 mm</p> <p>Testing: static</p> <p>Normal force: 0 to 550 kPa, applied by screwing the front pressure plate to the steel cups using a latch fastener</p> <p>Deformation rate: 50 mm/min</p> <p>Temperature: 10 °C, 25 °C, 60 °C</p> <p>Result: force deformation diagram, max force (stress)</p>
 <p>Romanoshi device</p>	<p>Specimens: cylinders 95 mm, specimens are cut and placed in steel cups</p> <p>Gap width: 5 mm</p> <p>Testing: static</p> <p>Normal force: 0 to 550 kPa</p> <p>Deformation rate: 12 mm/min</p> <p>Temperature: 15 °C, 25 °C, 35 °C</p> <p>Result: force deformation diagram, max force (stress)</p>

Table 2.2: Direct shear tests summary proposed by Raab and Partl (2).

	<p>Specimens: cylinders 100 mm, specimens are cut and placed in steel cups            Testing: static            Normal force: possible            Deformation rate: 12 mm/min            Temperature: 10 °C, 20 °C, 30 °C            Result: force deformation diagram, max force (stress)</p>
	<p>Specimens: cylinders 100 mm, specimens are placed in steel cup            Testing: static            Normal force: none            Deformation rate: 1.27 mm/min            Temperature: 5 °C to 45 °C            Result: force deformation diagram, max force (stress)</p>
	<p>Specimens: prismatic specimens 450×100×125 mm            Testing: static and dynamic            Normal force: none (possible)            Loading function: <math>\frac{\tau}{\tau_f} = 0,25, 8 \text{ Hz}</math>            Result: force along contact plane-slip along contact plane</p>
	<p>Specimens: cylinders 100 mm, specimen are glued into two steel semicircles            Gap width: 0 to 15 mm            Testing: dynamic            Normal force: 0–1.11 N/mm<sup>2</sup>            Loading function: sinusoidal with amplitudes of 0.005 to 0.1 mm and frequency of 1–15 Hz            Temperature: -10 °C to 30 °C            Result: force time diagram and deformation time diagram, AK = relative deformation between layers/shear stress between layers in m<sup>3</sup>/N</p>
	<p>Specimens: cylinders 100 mm, specimen are fixed into steel cups, longitudinal axis of the specimen is at 25.5° with the vertical axis            Testing: dynamic            Normal force: 0.5, 0.75, 1.0 and 1.25 MPa            Loading conditions: vertical load 10% of max load, frequency of 5 Hz, total period of 0.2 s, length of pulse of 0.05 s (simulating a vehicle pass at 50 km/h)            Temperature: 25 °C            Result: elastic and permanent displacements at the interface in normal and tangential directions for each cycle; dynamic tests were stopped when the permanent shear displacement (PSD) at the interface reached 6 mm or when it was considered that the number of cycles corresponding to a PSD of 6 mm could be extrapolated.</p>

Table 2.3: Simple shear tests summary, as proposed by Raab and Partl.

Device	Characteristics
 <p style="text-align: center;">Shear box</p>	<p>Specimens: prismatic (320×200 mm), specimens are in the mould fixed using an epoxy glue                      Gap width: approx 10–20 times the mean particle diameter of the test specimen                      Testing: dynamic and static, if dynamic test does not result in failure                      Deformation rate: 1.5 mm/min                      Normal force: applied servo hydraulically, 0, 50, 100, 200 and 250 kN/m<sup>2</sup>                      Loading function: sinusoidal shear stress with frequency of 2 Hz, vertical load 200 kN/m<sup>2</sup>. While vertical stress was kept constant, shear stress was increased in 5 levels until the specimen fails; if the specimen did not fail during dynamic testing, a static test was performed with constant deformation rate.                      Result: dynamic shear stress-relative displacement diagram</p>
 <p style="text-align: center;">ASTRA device</p>	<p>Specimens: rectangular, max cross section of 100×100 mm and cylindrical with diameters 95 to 99 mm, specimen are fixed in two steel cups                      Gap width: diameter of particle diameter of the test specimen                      Testing: static                      Normal force: 0, 0.2 and 0.4 MPa, applied by a lever and weight system                      Deformation rate: 2.5 mm/min                      Temperature: variable in climatic chamber                      Result: data-file with shear force <math>T</math>, horizontal <math>\xi</math> and vertical <math>\eta</math> displacement related to time</p>
 <p style="text-align: center;">SHRP shear test device SST</p>	<p>Specimens: cylindrical with <math>\varnothing</math>150 mm, specimen are glued onto aluminum "caps"                      Testing: static or dynamic                      Loading function: constant load mode (222.4 N/min)                      Normal force: none, possible                      Temperature: 25 °C and 55 °C                      Result: shear stress-deformation diagram</p>
 <p style="text-align: center;">MCS device</p>	<p>Specimens: three layered specimens test specimens with the dimension of 70×100×30 mm, specimen are placed in a metal frame where the side parts of the sample are fixed while the central part is subjected to a sinusoidal displacement                      Testing: dynamic                      Loading function: sinusoidal displacement, 1 Hz                      Normal force: none                      Temperature: 5 °C                      Result: shear force time and deformation time diagrams</p>

It is important to note that the majority of tests used for measuring and characterizing the interface's shear behavior, are originated from shear tests mainly used in the study of soil mechanics, modified in order to admit multi-layered specimens. In addition, almost all these tests are of static nature, but they can be modified in order to perform dynamic tests.

As mentioned earlier, these tests were designed by various authors in order to be able to characterize the interlayer's behavior. From all these, multiple studies have stemmed where the authors have been able to determine the variables that affect or influence the interlayer's behavior. Regarding these variables, also Raab and Partl proposed the following chart, shown in Figure 2.5, summarizing the variables that have been identified to affect the interlayers:

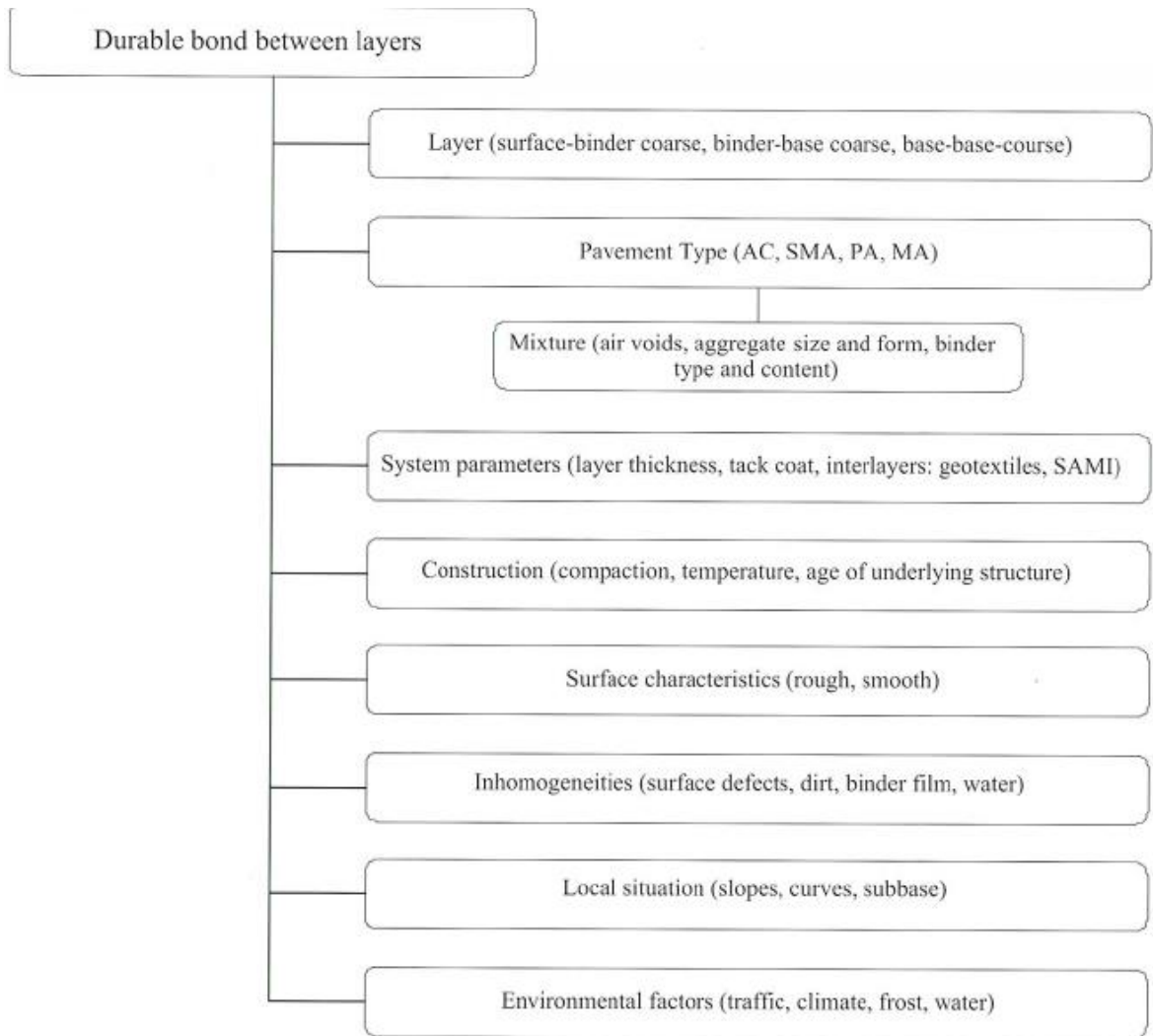


Figure 2.5: Factors that affect the interlayer's behavior, as proposed by Raab and Partl.

Following this summarization proposed by Raab and Partl, which serves as a good introduction to the studies that have been performed in this area during the last years, some other studies regarding the behavior of the interlayer are presented.

As the shear tests have been implemented, various authors have studied the shear strength versus shear displacement interactions in the interlayers, in an attempt to characterize the interlayer's behaviors. By plotting the results from these tests, some authors have been able to characterize and define the constitutive equations that govern the shear behavior in interlayers, (Uzan, Livneh and Eshed, 1978; Mohammad, Raqib and Huang, 2002; Kim *et al.*, 2011; Du, 2015).

Taking as example the graphics plotted by in *Evaluation of asphalt pavement layer bonding stress* (Du, 2015), presented in Figure 2.6, the shear behavior in the interlayer can be observed:

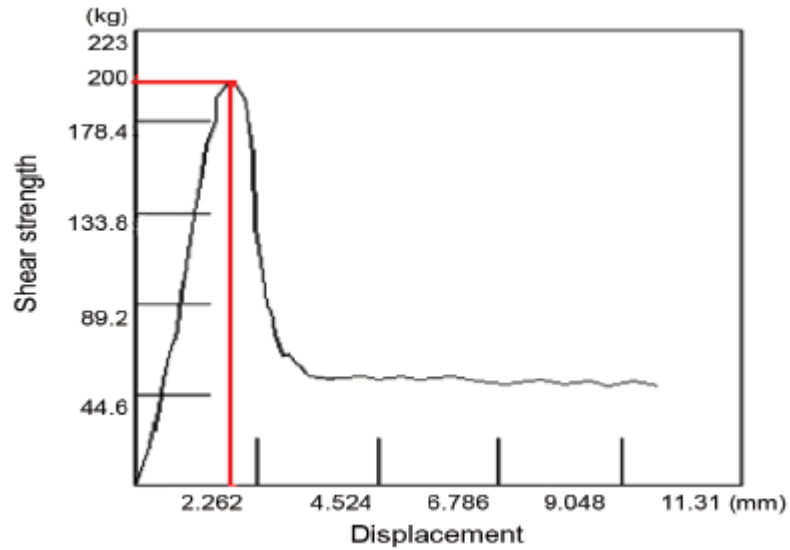


Figure 2.6: Shear strength vs displacement relationship

Now, taking into account the behavior observed by various authors, who obtained similar results to the previous figure, the shear behavior of the interlayers might be defined into three main sections. Once again, taking as an example the graphic proposed by Du in Figure 2.7 below, these sections can be described.

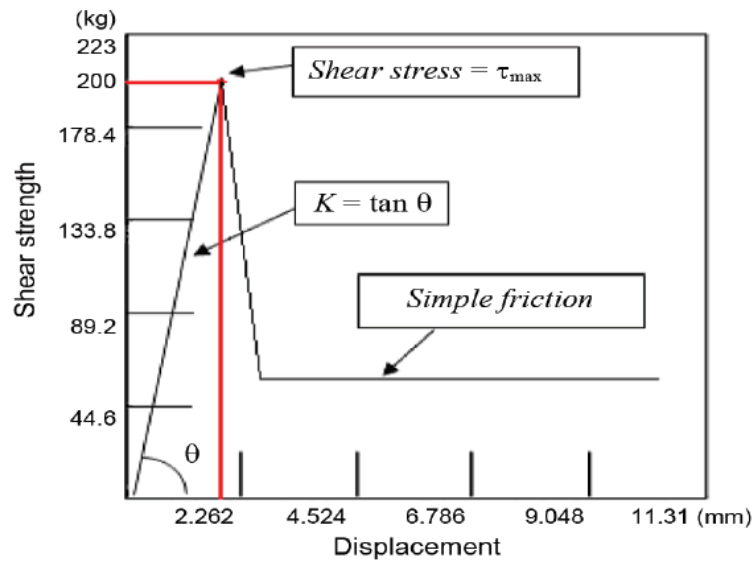


Figure 2.7: Modelled shear stress vs displacement.

The three sections in which the shear behavior of the interlayer can be defined are:

- **First section:** It is characterized by a linearly increasing function, in which the slope represents the interlayer's reaction modulus  $K$ , and the governing equation is obtained from Goodman's Constitutive law, which has been previously mentioned.
- **Second section:** Represents the point of maximum shear resistance of the interlayer, after which, failure occurs. This point is characterized by the maximum shear value obtained

during the tests.

- **Third section:** After the point of maximum shear resistance, the layers are no longer bonded and therefore, the resistance of the specimens is characterized by simple friction, which means that the binder/ tack coats are no longer contributing to the shear resistance.

In attempt to better understand how the bonding between layers occurs, and the factors which lead to a weak bonding in the pavements, in *Assessment of bond condition using the Leutner shear test* (Collop, Thom and Sangiorgi, 2002) performed a series of Leutner tests on double layered specimens, which were composed of different combinations of materials, in order to simulate the interaction between the different layers in pavements, such as wearing course over binder, binder course over base course and wearing course over base course.

Additionally, this study also aimed to obtain Leutner tests limits, in order to help future researchers, have a better understanding of typical values to obtain in a first approach to a characterization of the interlayer's shear behavior. Also, the limits obtained in this study were compared with some previous limit values proposed by other authors. Table 2.4, summarizes the limits proposed by Sangiorgi et al., as well as the values proposed by previous authors (Codjia, 1994; Stöckert, 2001), used to compare the data:

Table 2.4: Leutner test limit values proposed by various authors.

<b>Originator</b>	<b>Property</b>	<b>Wearing course/ binder course</b>	<b>Binder course/ base course</b>	<b>Wearing course/ base course</b>
<u>Codjia</u> (1994)	Shear load Displac.	15kN 1.5mm	10kN 1.0mm	13kN 1.5mm
<b>Originator</b>	<b>Property</b>	<b>Wearing course/ binder course</b>	<b>Binder course/ base course</b>	<b>Base course/ base course</b>
<u>Stöckert</u> (2001)	Shear load Displac.	25kN 2.0-4.0mm	20kN 1.5-3.0mm	16kN 1.0-3.0mm
<b>Originator</b>	<b>Property</b>	<b>Wearing course/ binder course</b>	<b>Binder course/ base course</b>	<b>Wearing course/ base course</b>
<u>Sangiorgi et al.</u> (2002): New pav.	Shear load Displac.	20kN 2.0-4.0mm	12kN 1.5-2.5mm	18kN 2.0-4.0mm
After 1-year traffic	Shear load Displac.	25kN 2.5-4.0mm	17kN 1.5-2.5mm	23kN 2.5-4.0mm

Recognizing the fact that there are several factors and situations that affect the interlayer's shear behavior, making it very difficult to evaluate, some investigations focused on the behavior of multi-layered pavements by varying several parameters (Canestrari *et al.*, 2005). To do so, the following experimental program, shown in Table 2.5, was performed during this study:

Table 2.5: Summary of the experimental program performed by Canestrari et al.

Temp. (°C)	Interface Treatment	Preparation Samples	Curing Time	Normal Stress	ASTRA	LPDS
20	Conventional Modified Without	Trial	Short (2–3 weeks)	3 values: 0. 0; 0.2; 0.4 MPa	3 specimens	
40	Conventional Modified Without					
20	Conventional Modified Without	Laboratory				
40	Conventional Modified Without					
20	Conventional Modified Without	Trial	Medium (7–8 weeks)	1 value: 0.0 MPa		10 specimens
	Conventional Modified Without					
	Conventional Modified Without	Laboratory				

As shown in the previous table, several specimens were evaluated, using two different types of tests (ASTRA and LPDS), three different types of tack coat emulsion, two different type of sample preparation and at two different temperatures. Additionally, different curing times and different values of applied normal stress were used, in an attempt to make a better understanding of how these parameters affect the interlayer's shear behavior.

From this experimental program various conclusions were drawn, such as the fact that the presence and increase of the applied normal stress causes and increase in both the interlayer modulus  $K$ , as well as an increase in the shear resistance of the specimens. Additionally, it showed that as the temperature increases, there is a decrease on the peak shear resistance at the interface, whilst the change of this parameter with respect to the temperature increase is independent of the applied normal force.

Also, taking into account that the ASTRA tests used by Canestrari et al., allows for different normal loads to be applied, it showed that the interlayer's failure criterion may be determined according to the Mohr-Coulomb law. By studying the different peak envelopes for the specimens, in this study it was concluded that friction and peak envelopes converged, suggesting that cohesion and dilatancy decreased with the increase of the normal stress.

For example, the article *Effects of asphalt mixture type on asphalt pavement interlayer shear properties* (Song et al., 2018), focused on studying the effects of the Asphalt mixture type on the interlayers shear properties. This was done by performing the comparison between the interlayer's shear properties of a pavement layer made of a Dense Asphalt Mixture and another one composed of OCFG (Open Graded Friction Course). This last one consists of a thin permeable asphalt layer placed on the traditional dense asphalt layer. It is characterized by stone-on-stone contact and highly connected air void content, alongside the use of high quality, open-graded aggregates.

During this study, a direct shear test allowing the application of normal loads, in order to evaluate the Shear strength and stiffness of the interlayer. Additionally, other evaluated characteristics were: Presence/variation of normal stress, tack coat application rate and surface characteristics.

Apart from the two different types of Asphalts used in the different specimens, the tack coat used

was an anionic, slow-setting asphalt emulsion. Also, the four tack coats residual application rates used were: 0, 0.15, 0.30 and 0.45 l/m<sup>2</sup>. The two-layered specimens were set in different combination, varying the type of asphalt mix between the following three mixes:

- BM: PG 64 -22, 6.4% asphalt binder content, Limestone.
- D: PG 70-22, 6.0% asphalt binder content, Gravel.
- OCGF: PG 76 – 22, 6.4% asphalt binder content, Gravel.

Using Goodman’s constitutive law, mentioned previously, the interface stiffness *K* was determined, and the typical shear stress versus shear displacement curve was plotted for the tests. As a result, from this study, apart from confirming some claims previously made by other authors, it showed that different combinations of Asphalt mixes in the double-layered specimens, may present different behaviors, for example, the optimal application rate variates as the combinations variate, as well as the interlayer stiffness and the peak shear resistance, showing that in effect, the type of asphalt mixes used for the different layers in pavements affect the interlayer’s behavior.

Furthermore, during this study, Song et al., also studied how the roughness of the contact surfaces in the interlayers affect the bonding properties. This was performed by analyzing the Roughness capacity, which was previously studied (Sholar *et al.*, 2004). Through this analysis, the authors concluded that those layers composed by mixes with higher air void contents presented less contact area, which led to weaker bonding properties.

In *Effect of tack coats on interlayer shear bond properties* (Raab & Partl, 2004), a study on specimens, compacted using a gyratory compactor, was done by performing tests using the Layer-Parallel Direct Shear tester (LPDS), in a two-part project.

The first part of the project focused on studying the performance of a variety of tack coats on a rough surface at the interlayer under different degrees of compaction. The second part of this project was focused on studying the effect of different surface treatments at the interlayer such as application on wet surface, high temperatures and the influence of water. Table 2.6 shows the experimental program performed during this study:

Table 2.6: Experimental program proposed (Raab and Partl, 2004).

	Compaction of top layer	Texture condition of bottom layer surface	Treatment
1. Project	50 or 204 gyrations	Rough, e.g. non-cut and sandblasted	No treatment
2. Project	204 gyrations	Smooth, e.g. cut, non-sandblasted	No treatment Tack coat application on wet surface 75 hours oven conditioning at 60°C 5 days conditioning in H <sub>2</sub> O at 40°C

The tests results, showed that the specimens subjected to 204 gyrations obtained higher values of the maximum resisting shear force than those subjected to 50 gyration. This means that a higher degree of compaction led to better interface bonding properties. On the other hand, regarding to the texture of the bottom layer surface, the results shown that higher values of maximum shear

force were obtained for the specimens that had a smooth surface than those with a rough one (non-cut and sandblasted). Finally, Raab and Partl observed that for the oven heating and the wet surface treatments, the application of a tack coat leads to an improvement in the shear bond properties. Regarding the soaking in water surface treatment, no specific conclusions were drawn.

On a similar study to determine the influence of the compaction process in the interlayer shear bonding properties (Zhang *et al.*, 2019), the authors performed a laboratory study, which aimed to understand how different compaction methods affected the interlayer. During this study, two different types of compaction were implemented; firstly, some specimens were compacted through continuous paving technology. This consists on paving and compacting with two different gradation asphalt mixtures in the upper and lower layers simultaneously, in order to obtain a better integrity and durability in the pavement. On the other hand, other specimens were compacted with discontinuous paving technique. Figure 2.8 shows the appearance of the used specimens:

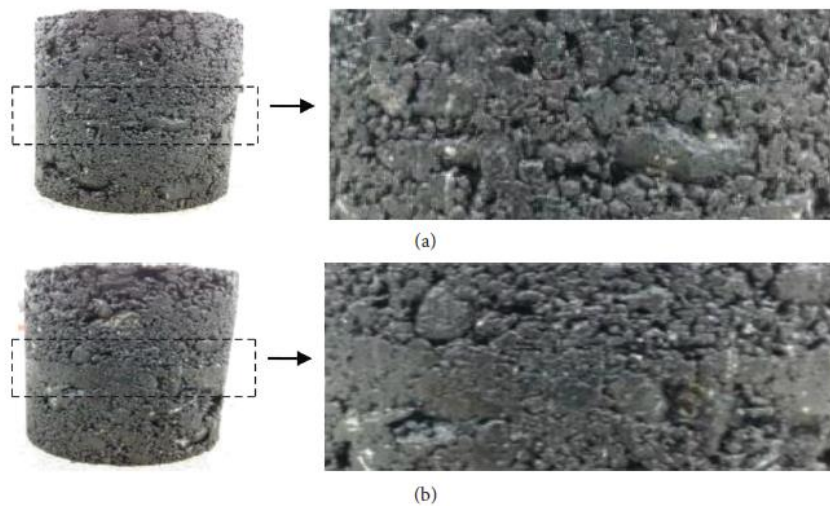


Figure 2.8: (a) Specimens compacted through Continuous paving. (b) Specimens compacted through discontinuous paving, used by Zhang *et al.*

The experimental program performed, was divided into two: tests of mechanical performance (Rut test, Bending test and Split test) and adhesion tests (interlayer adhesion test through a modified split shear test and direct shear test). Regarding the shear and adhesion properties of the interlayers, the authors came to the conclusion that the continuous paving method resulted in better bonding properties than the discontinuous one. Additionally, as the adhesion test were performed at different temperatures (freeze-thaw, room temperature and low temperature), the authors stated that, disregarding the paving method, the shear resistance was higher at low temperatures, followed by normal temperature and finally, at freeze-thaw cycles.

In his thesis dissertation, Cutica performed an experimental assessment on double-layered specimens, which were treated with different treatments/materials in the interlayer. These specimens were cores taken from a full-scale pavement, which was sub-divided into six sections and each section had a different type of treatment at the interlayer (or no treatment at all). The sectors' characteristics are as follows (*Cutica*):

- Sector I: No tack coat used
- Sector II: Cationic Emulsion – 0.15 kg/m<sup>2</sup> residual

- Sector III: Cationic Emulsion – 0.30 kg/m<sup>2</sup> residual
- Sector IV: Thermoplastic membrane
- Sector V: Modified Emulsion – 0.15 kg/m<sup>2</sup> residual
- Sector VI: Modified Emulsion – 0.30 kg/m<sup>2</sup> residual

As it can be observed, two different types of emulsions were employed (Cationic/Modified) and also for these, two different application rates were used (0.15/0.30 kg/m<sup>2</sup> residual). The other two remaining sectors were characterized by no treatment use and the use of a thermoplastic membrane.

In order to study the shear behavior of these core samples, two different laboratory tests were employed, the ASTRA and the ATREL shear testing devices, are located in Ancona (Italy) and Illinois (United States), respectively. Both devices allow to measure the shear strength at the interlayer of the specimens, by applying direct shear at constant speed, while a normal stress is fixed.

This allows to build the peak envelope by drawing Mohr's circles from the data obtained from the tests, which will allow to characterize the mechanical behavior of each one of the employed interlayer treatments. Additionally, the following parameters' influence on the shear behavior were assessed:

- Tack coat/ Application rate.
- Temperature.
- Normal Pressure.
- Dilatancy.
- Diameter.

An example of the peak envelopes obtained for the interfaces with a cationic emulsion, at different application rates and temperatures can be observed in Figure 2.9:

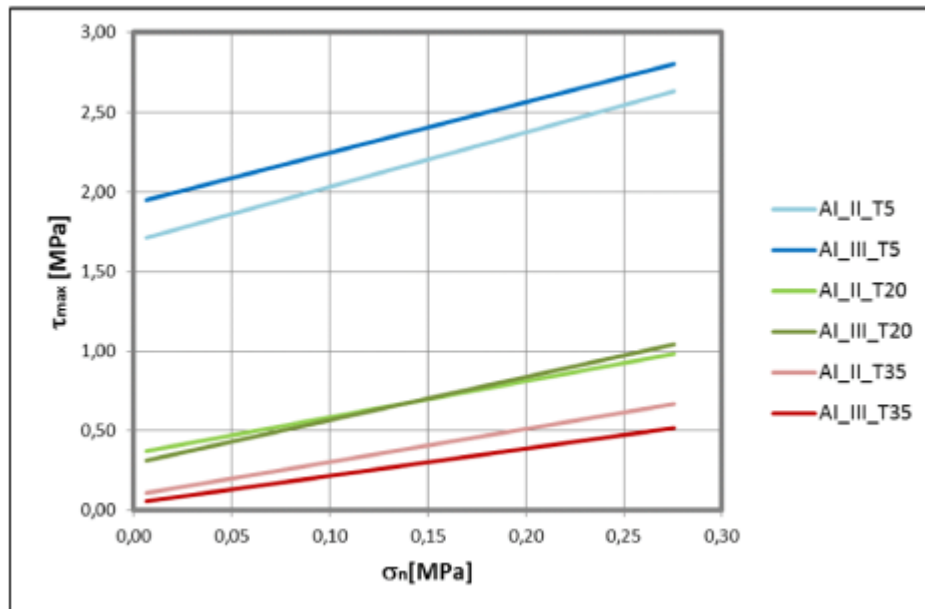


Figure 2.9: Failure envelopes obtained by Cutica for interfaces treated with a cationic emulsion.

As it can be observed, the different types of treatments in the interlayers of the specimens and their

behavior can be compared in terms of their failure envelope. By comparing the variation of the behavior among all specimens and the parameters mentioned above, some of the most important conclusions from this study were:

- The shear strength behavior in terms of temperature change, were not linear, but rather presented a breaking point at around 20°C.
- The temperature and normal stress applied parameters are independent from each other, which means that a variation in one of them, does not directly affect the behavior of the interlayer in terms of the other parameter.
- A strong correlation between the peak shear stress and the peak of dilation was found, thus confirming what has been mentioned by other authors – Maximum shear resistance is found near the peak on dilation.
- The amount of optimal residual bitumen content is not the same for all emulsions, but rather depends on the composition of the emulsion itself and on the type of emulsion (Slow setting/Medium setting/Rapid setting). For example, from the results of this study, it was observed that in the case of the modified emulsion the optimal application rate was 0.30 kg/m<sup>2</sup>.
- The treatment with thermoplastic membrane did not show any improvements in the bond properties in the interlayer.

### **2.3. Prior studies on modelling the interlayer of flexible pavements**

As the main goal of this thesis is to propose and evaluate the validity of a constitutive model that accurately describes the behavior of the interlayers, it is important to review and summarize some work of the previous authors which had worked in this field in the past. It is important to note that, the model that will be proposed during this study focuses on tests results obtained from a Leutner Shear test device, which, as will be described later on, serves only to obtain applied shear loads and displacements. However, to better understand what has been done in the past, the models that will be explained in this section range from models that only take into account the shear loads/displacement to some more complex models which have been previously proposed.

One particular author that has focused on modelling the interlayer's behavior is H. Ozer, which has performed some important researches on this particular topic, such as *Fractured based friction model for Pavement interface characterization* and later, based in this study, another one called *Characterization of interface bonding between hot-mix asphalt overlay and concrete pavements: modelling and in-situ response to accelerated loading* (Ozer et al., 2012)

On the first research mentioned on the previous paragraph, Ozer et al., presented a friction model to characterize the behavior of the interlayer, based on three parameters: Shear strength, Interface Reaction Modulus ( $K$ ) and friction. The advantage of this model, is that it describes the whole range of the interlayer shear behavior, from the initial elastic stage (fully-bonded interface), up to the purely frictional response after the debonding.

Some years later, based on their own findings and the constitutive model proposed on the 2008 study, Ozer et al. did a similar work, however this time, the scope of this study, was to conduct an experimental program, by using an Accelerated Pavement Testing (APT) program, in which 25 pavement sections were designed in order to study the effect of tack coat type/ application rate, PCC surface, HMA design, surface cleaning and non-uniform distribution of the tack coat. Figure

2.10 shows the APT program used by Ozer et al., in which the sections were studied under loading:

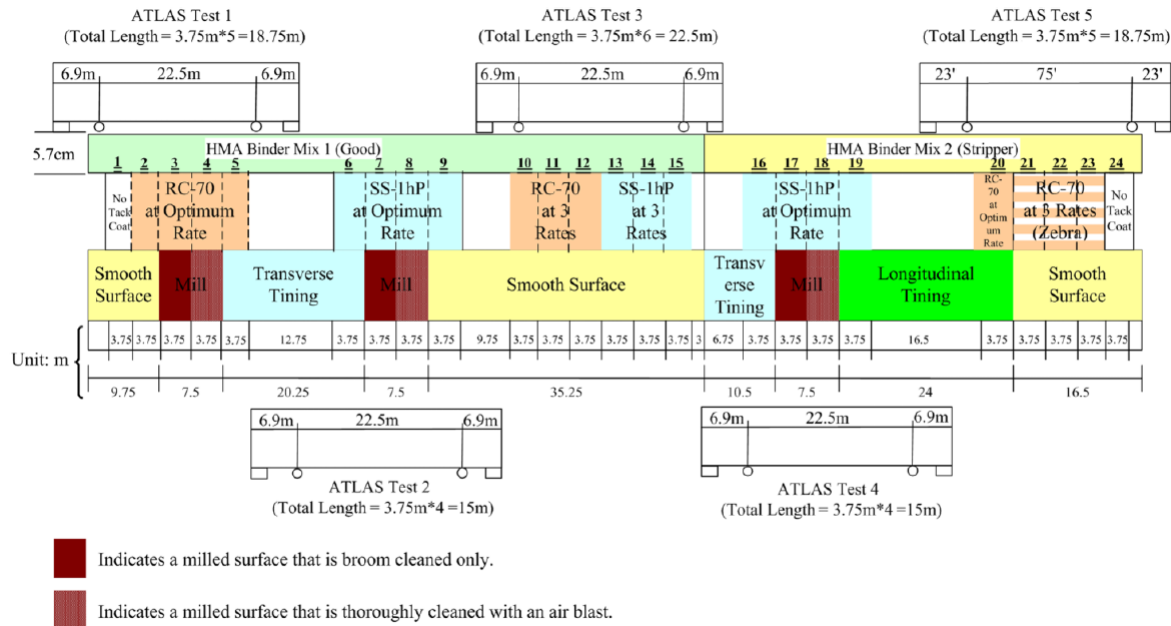


Figure 2.10: Layout of the real-scale pavement sections used for the APT program, (Ozer et al., 2012).

The main goal of the APT study, was to measure how the different configurations of each pavement section, affected the pavement's bottom tensile strain, the deformation at the interface and the rutting phenomenon.

Once this portion of the investigation was done, the other portion of the research focused on performing a Finite Element model for HMA overlays, by using the ABAQUS software. In order to model the interface, the constitutive model proposed in their previous work was used by the authors. The constitutive model for the interface, used in this research, is called the hyperbolic Mohr-Coulomb friction model, described in Equation (2.2):

$$F = \tau_{eq}^2 - (c - \sigma_{nn} \cdot \tan\varphi)^2 + (c - s \cdot \tan\varphi)^2 \quad (2.2)$$

In the previous equation,  $F$  represents the failure envelope in the Mohr-Coulomb plain, while  $\tau_{eq}$  is the equivalent tangential traction,  $\sigma_{nn}$  is the normal traction,  $s$  is the tensile strength,  $c$  is the cohesion and  $\varphi$  friction angle. Some of this interface parameters were obtained from experimental results. In particular the tensile strength was assumed equal to the shear strength, due to the absence of data. Figure 2.11 shows an example of the failure criterion used in during this study:

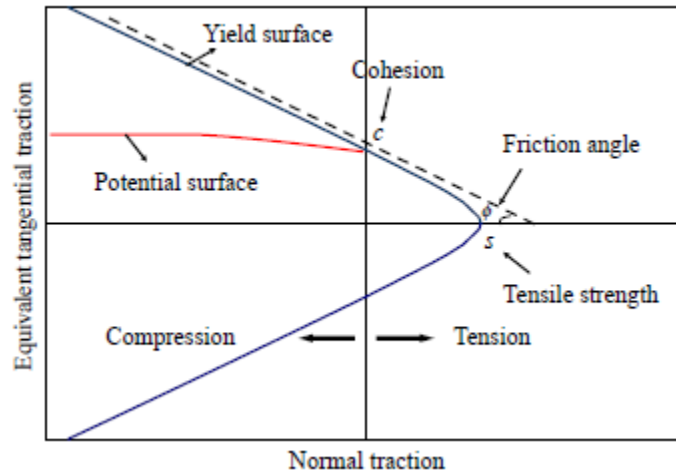


Figure 2.11: Failure envelope used to describe the interface behavior under various loading conditions, (Ozer et al., 2012).

Once these characteristics were defined, as well as the geometry and boundary conditions of the model, the base model that was elaborated is shown in Figure 2.12:

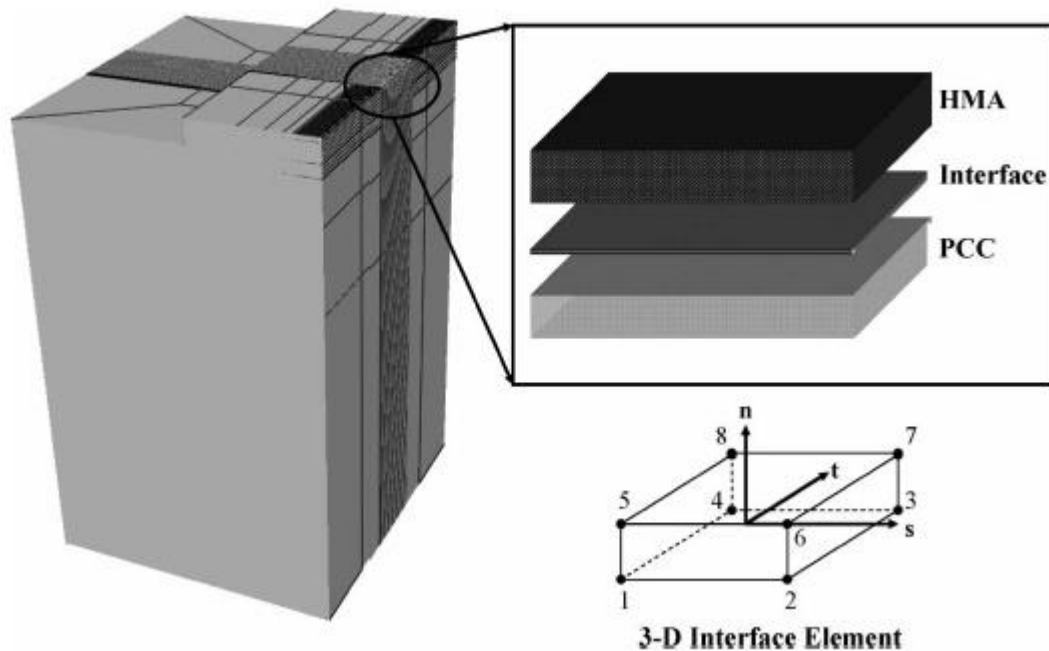


Figure 2.12: Cross-section of the 3D FE model done (Ozer et al., 2012).

Finally, once the base model was set, in order to study the stress and strains produced by dynamic loading, a dual-tire and wide-base tire configurations at different loading values and at a speed of 8km/h. Based on the modelled stresses and strains and the experimental data from the APT program, the validation process of the model was done.

In *FEM analysis of HMA interface layer interface bonding* (Williamson, 2015), once again, the

authors parted from the two-state constitutive model that has been previously proposed [Romanoschi and Metcalf, which was configured from shear stress versus displacement curves. As it has been mentioned thoroughly in this chapter, the first part is a linearly increasing relation between the two quantities, related through the interlayers' stiffness modulus  $K$ . Then, after the peak value of shear stress is reached, the shear resistance is purely frictional and characterized by the friction coefficient,  $\mu$ .

The scope of this work was to develop an accurate 3D – FEM model that would predict the response of an HMA pavement while varying the values of the interlayer stiffness modulus ( $K$ ), which is used to study different bonding conditions. Additionally, the model also was used to study the variation in the application rates of the tack coats. In order to validate the model, APT (Accelerated Pavement Testing) experimental data was employed. It is important to note that APT data is used to understand how vehicle loading induces strains in the pavement.

To perform the 3D – FEM model, the authors employed the software ABAQUS, which allows to model elements of different geometries and material properties. Regarding the materials' properties, in this particular case, the authors represented each element as solid, homogeneous and isotropic. The granular base and soil subgrade were modeled as elastic materials, whilst the plastic behavior was ignored due to the distance between these layers and the studied interface.

On the other hand, the asphalt materials were modeled as viscoplastic materials, for which the time-hardening creep parameters were obtained from previous studies. The constitutive equation selected for the asphalt materials is shown in Equation (2.3):

$$\epsilon^{vp} = A'\sigma^n t^{m+1} \quad (2.3)$$

Where  $A$ ,  $m$  and  $n$  are creep parameters that were determined through lab testing. After setting up and calibrating the model, the strains under loading were studied. An example of the results obtained can be observed in Figure 2.13:

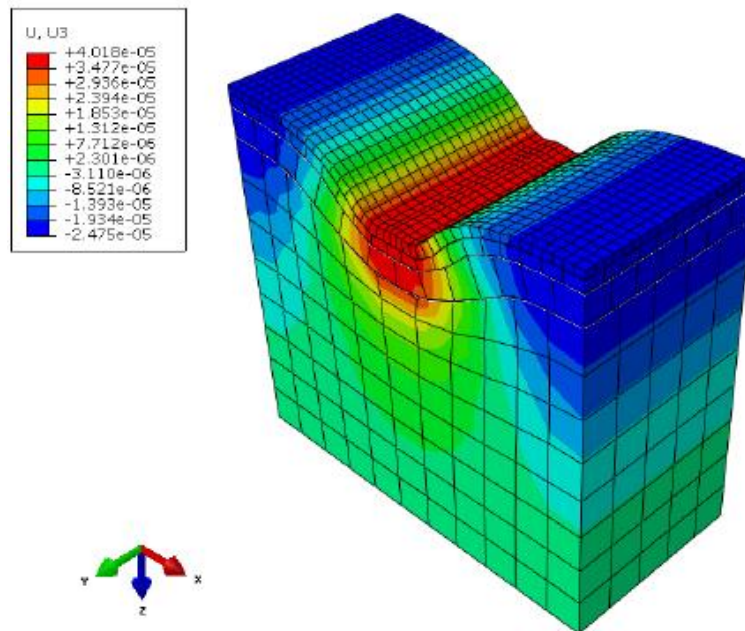


Figure 2.13: Modelled vertical deformations under loading (Williamson, 2015).

According to the authors, the model did accomplish the goal when compared to the experimental data, and drew conclusions related to the application of repetitive loads in the model. Regarding this kind of loads, it was found that the longitudinal strains directly under the load can be modeled even by disregarding the loading time, and they were mostly elastic strains.

Another similar study, *Surface Layer bond stresses and strength* (Kim *et al.*, 2015), proposed a guideline to minimize the debonding distresses in asphalt pavements. In order to do so, the authors did a computational analysis, in order to determine the stresses and strains in asphalt pavements, subjected to vehicle loads and how they affect the debonding of the layers.

In this extensive research, there were various aims, alongside to that one mentioned in the previous paragraph. Along the guidelines of this work, the authors focused on:

- A direct shear test protocol, which serve as a way to studying the bonding strength between layers.
- A database containing the shear strength of different tack coat materials, at various confining pressures, temperatures and loading rates.
- A mechanistic prediction model for the shear strength depending on the confining stress.
- Finally, the concept of Maximum Shear Ratio (MSR) is presented a form of evaluating the capacity of the interlayers of withstanding the shear stress that comes from vehicles load.

In order to accomplish all these goals, the authors used a combination of experimental data, obtained from laboratory tests, computational data, which was used in order to determine the stresses and strains derived from moving vehicle loads. Then, from this experimental data, the authors determined a predictive model for the shear strength by varying some parameters, such as application rate, temperature, and tack coat material.

In the case of the computational data used in order to find the stresses and strains in any point in

the pavement under vehicle load, the authors used the Layered ViscoElastic pavement analysis for Critical Distresses (LVECD). The simulations were done taking into account typical materials of asphalt pavements and three different typical pavements structures used in North Carolina. The different simulation scenarios included different temperatures, different vehicle speeds and different axle loads.

Through the elaboration of shear strength mastercurves, which were determined from the experimental data, the model is able to predict the shear strength under varying conditions. As proposed by the authors, this prediction could be then compared with the stresses and strains obtained through the computational analysis, to evaluate the bonding condition at any point in the pavement under moving vehicle loads.

Among the different findings in this study, it is possible to single out two main findings of the authors that are of particular interest to this research. Firstly, the predictive model for the interface shear strength, used for pavements that make use of a tack coat between the layers, at different strain rates, temperature combination and at any confining stress. Equation (2.4) shows the predictive model obtained by the authors:

$$\tau_f = (a \cdot \dot{\gamma}_R^b) \cdot \sigma_c + c \cdot \dot{\gamma}_R^d + e \cdot \sigma_c = (a \cdot \dot{\gamma}_R^b + e) \cdot \sigma_c + c \cdot \dot{\gamma}_R^d \quad (2.4)$$

In which:

- $\tau_f$ : Shear strength at the layer interface (kPa).
- $\dot{\gamma}_R$ : Reduced shear strain rate.
- $\sigma_c$ : Normal confining stress (kPa).
- $a, b, c, d, e$ : Model parameters, calibrated for different interface conditions.

Secondly, in order to define a form of evaluating the shear resistance capability at the interlayer to the applied vehicular loads, the authors proposed the term of Maximum Shear Ratio (MSR). It allows to individuate a failure criterion for the interlayers under vehicle loading. The MSR is defined in this article as the ratio between the acting shear stress, result of the loads, and the shear bond strength (previously defined by Canestrari et al.) which is function of the normal stress. Equation (2.5) **Error! Reference source not found.** represents the MSR:

$$MSR = \frac{\tau_{max}}{\tau_s} \quad (2.5)$$

Where  $\tau_{max}$  represents the quadratic combination of the shear stress in the transverse and longitudinal direction (determined using a computational analysis), while  $\tau_s$  represent the shear bond strength, function of the normal stress. If the value of the MSR is greater than 1.0, it means that the shear failure would occur at the interface, Additionally, the authors found that values close to 1.0 indicate a high potential of failure in the pavement due to repeated braking.

As it is known, there are several types of models, such as the one that was just mentioned (FEM), or they can also be statistical models, which focus on finding the relationship between independent and dependent variables. This is the type of model used in *Development and validation of a model to predict interface bonding between pavement layers* (Das et al., 2018), which is a study performed at Louisiana University, in which the objective was to obtain a model to predict the ISS (Interface

shear strength), by calibrating and validating two statistical models; one multilinear regression (MLR) and another non-linear regression (NLR).

In order to calibrate these models, experimental data obtained in field and then in laboratory tests, for which a LISST device was used. From this device, shear stress versus displacement curves can be obtained. Apart from these, the residual application rate and surface texture of the specimens were measured, as these were one of the variables to be calibrated as independent variables in the statistical model (along with some others). Table 2.7 shows a brief description of the variables that were studied during this research:

Table 2.7: Variables used to calibrate the statistical models developed by (Das et al., 2018).

Variable	Description
Interface shear strength (ISS), psi	Maximum interface shear stress
Pavement surface type (PT)	HMA and PCC
Residual application rate (RES), gal/yd <sup>2</sup>	Measured in the field during construction
Mean texture depth (MTD), mm	
Useful temperature interval (UTI), °C	Rheological properties of tack coat materials
PG high temperature (HPG), °C	
Penetration (PEN) @ 25°C, 100g, 5 s, dmm	
Softening point (SFPT), °C	
Rotational viscosity (RV) @ 135°C, Pa.s	

Note: PT was selected as a discrete variable in the analysis, assuming 0 and 1 for Portland cement concrete and hot-mix asphalt surfaces, respectively. Differences in the hot-mix asphalt pavement surface type were addressed by MTD.

Once the variables were defined and the experimental data related to them was collected, the next step was to calibrate and to validate the parameters related to each of the independent variables, as well to do a collinearity test to avoid the correlation between variables. Finally, the two models obtained (MLR and NLR) are shown in Equations (2.6) and (2.7) respectively:

$$ISS = \beta_0 + \beta_1 PT + \beta_2 RES + \beta_3 MTD + \beta_4 HPG \quad (2.6)$$

$$ISS = \delta_1 \cdot [(PT + MTD)^3 + \delta_2 RES \cdot HPG] \quad (2.7)$$

The regression model parameters that were obtained by the authors for both models are presented in Table 2.8:

Table 2.8: Regression model parameters (Das et al., 2018).

Parameter	Multiple-linear regression					Nonlinear regression	
	$\beta_0$	$\beta_1$	$\beta_2$	$\beta_3$	$\beta_4$	$\delta_1$	$\delta_2$
Value	-69.5	17.9	897.4	27.7	0.49	1.55	8.17
Standard error	11.9	3.9	142.8	4.1	0.13	0.13	0.98
t-value	-5.9	4.6	6.3	6.7	3.8	12.22	8.34
p-value	<0.0001	<0.0001	<0.0001	<0.0001	0.0007	<0.0001	<0.0001

All in all, the conclusions that could be drawn from this study, regarding the obtained models, according to the authors, shown that:

- There was a significant fitting of the results obtained with the models and the experimental data that was evaluated.
- Both models showed that there was a strong correlation with the ISS and the type of surface of the layers' materials (HMA/PCC) and the surface of the interlayers texture. In general, the results obtained for HMA were better than those of the PCC, in terms of the interlayer shear strength.
- Other parameters that showed a good correlation with the pavement's ISS were the depth of the pavement surface texture and also with the tack coat's residual application rate.

#### 2.4. The Leutner Shear test.

Nowadays, various testing devices have been proposed and implemented by researchers in this field to study the behavior of the interlayers. Particularly, the main objectives of these tests, as it was mentioned previously along this chapter, is to analyze how the interlayer of multi-layered specimens, responds to the application of loads, usually, in terms of displacement. Among all these laboratory tests, it is found the Leutner shear test device, first used in 1973 by R. Leutner in Germany.

According to the classification of Shear test devices proposed in *Evaluation of interlayer shear bond devices for asphalt pavements* (Raab, Partl and El Halim, 2009), the Leutner shear test device belongs to the Direct shear test devices, which are mainly characterized for being guillotine type test, in which, the shear force is applied at one side of the specimen, not in the front surface. In these types of tests, the specimens are clamped or introduced in a fitting system into the device. Finally, it is important to mention that they usually don't allow the application of a normal load, as it is the case of the Leutner device. Figure 2.14 shows the schematics of a Leutner device:

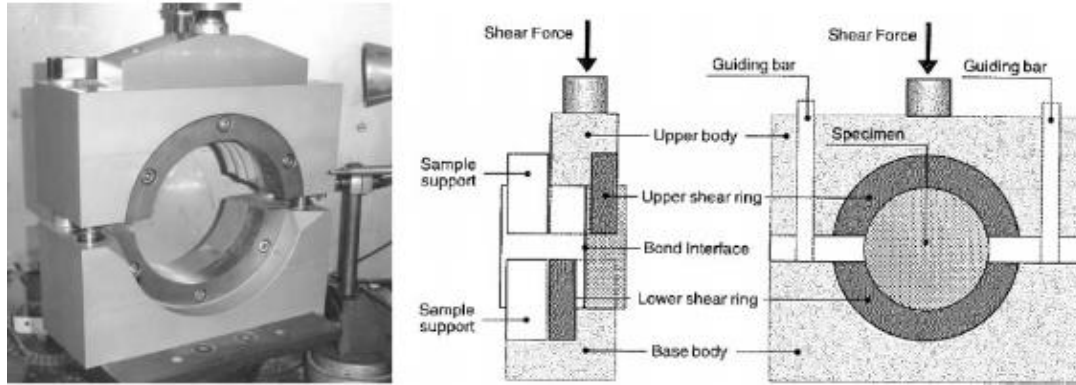


Figure 2.14: : Schematics of the Leutner device, *Review of applicable bond strength tests for assessing asphalt delamination potential* (Tseng, Street and Vic, 2019).

As it can be observed in these schematics, the specimens are mounted in the support, placing the interface just under the applied shear force. Then, one layer of the specimen is sheared against the other, causing a shear stress to be applied at the interlayer. In such configuration, the plane of failure is located at the interlayer.

The Leutner device is used for the test of double-layered specimens of various diameters [mm] under the application of a shear load [kN], at a constant rate [ $50 \pm 3$  mm/min], therefore also measuring the displacement caused by the shear load. From the previous information, firstly it is possible to obtain the shear stress applied on the interlayer by dividing the shear load over the area of the specimen's interlayer, as it is presented in Equation (2.8):

$$\tau = \frac{F}{\frac{\pi D^2}{4}} \quad (2.8)$$

Where  $\tau$  is the shear stress, usually measured in [MPa],  $D$  is the specimen's diameter [mm] and  $F$  is the shear load [kN] measured by the Leutner device. Then, once the shear stress has been obtained, it is possible to plot it against the displacement, in order to obtain a shear stress-displacement curve, which has been one of the main tools used to characterize the interlayer's shear behavior in several studies.

Apart from the characterization given in the previous chapters, it is important to measure and determine some important values that can be obtained from the stress – displacement curve, obtained from the Leutner test. Figure 2.15, displays the typical curve obtained from the test:

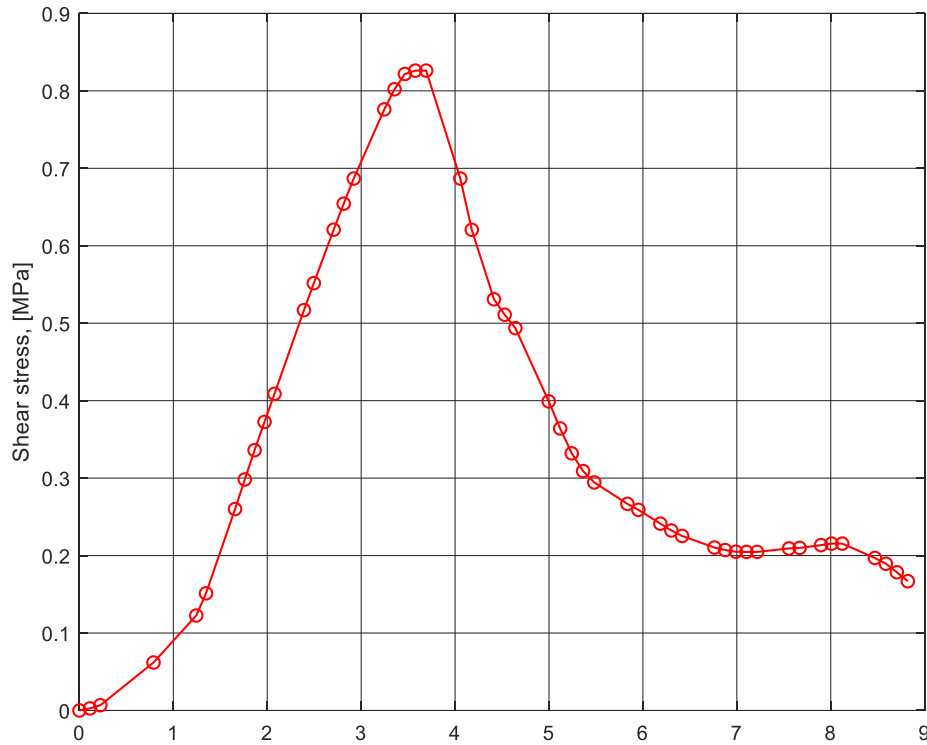


Figure 2.15: Typical stress – displacement curve from Leutner test.

This type of curve is characteristic of the shear tests, and as it was already mentioned in this chapter, some authors have previously characterized the segments of this curve in various stages. Additionally, the analysis of this curve will be done in the next chapter, which focuses on the constitutive models used to describe the interlayer’s mechanical behavior,

Additionally, there is currently a standard regarding the test methods for hot asphalts, which focuses on interlayer bonding of Bituminous mixtures. The information from this standard will be discussed in the next section of this document, to provide further insight into the Leutner shear test.

#### 2.4.1. Shear bond test according to Standard BS EN 12697 – 48.

As just mentioned, this standard for hot asphalts, focuses on providing an adequate description and methodology on the interlayer bonding test methods for bituminous mixtures.. Within it, there is a section dedicated to the Shear Bond Test (SBT), which is of particular interest for this research.

Firstly, the schematics of what is referred as ‘Shear Testing Apparatus’, but as it can be observed in Figure 2.16, these schematics have various similarities with those that were just shown in Figure 2.14, which allows to use these standards when performing Leutner testing.

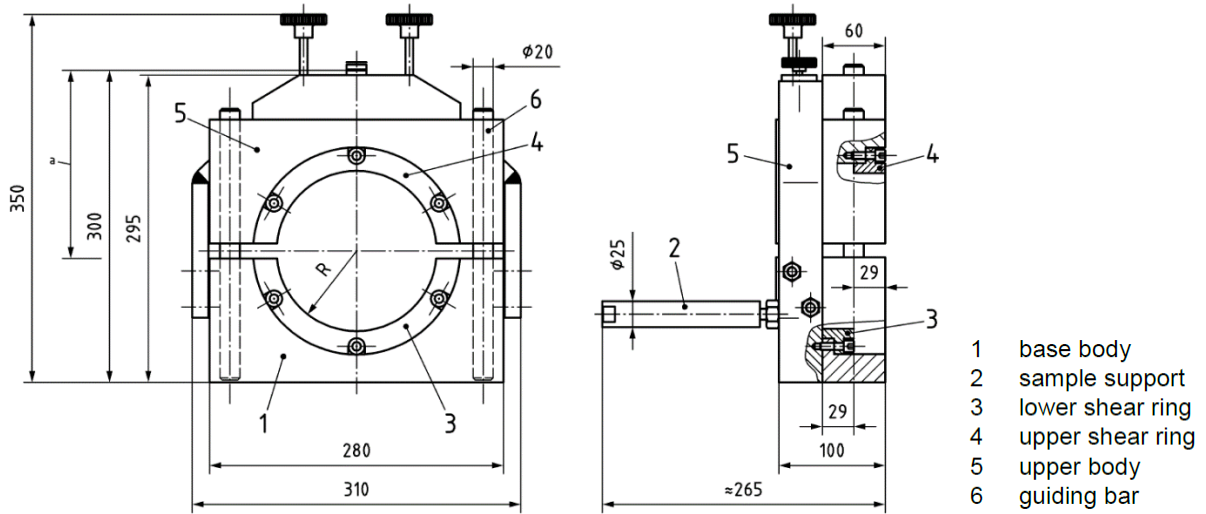


Figure 2.16: Schematics on the Shear Testing Apparatus (BSI group, 2019).

The standard, naturally provides the specifications that must be fulfilled by the testing device to be used, such as for example, a loading frame capable of applying a constant displacement rate of 50 mm/min and capable of achieving a maximum load of at least 35 kN. Also, it recommends to use the proper adhesive (like an epoxy resin), that is strong enough to avoid the failure between the adhesive and the surface of the specimen.

Then, there are specifications regarding the specimens to be used, which must be characterized by a constant diameter through the whole specimen and smooth surfaces. It is important that the interlayer shall be perpendicular to the specimen's longitudinal axis for the correct evaluation of interlayer bonding. Regarding the dimensions of the cores, Figure 2.17 shows the minimum values to be adopted for the specimens:

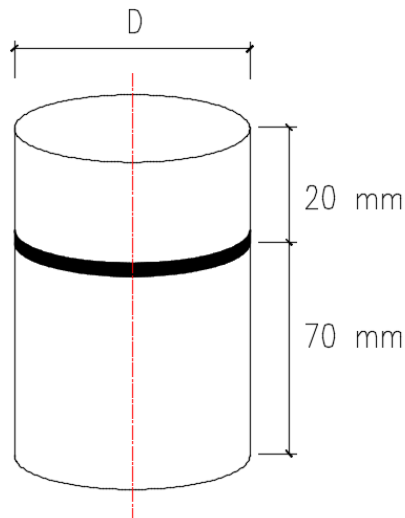


Figure 2.17: Specimen Geometry according to standard.

Where  $D$  is the diameter, that according to the standard must be either 150 ( $\pm 2$ ) mm or 100 ( $\pm 2$ ) mm.

Once the test has been performed, according to the standards, the values to take principally into account are based on the plot of the shear stress versus shear displacement, that can be elaborated by calculating the shear stress, as already has been shown in Equation (2.8). From the resulting stress – displacement curve, the following values, shown in Figure 2.18 shall be determined

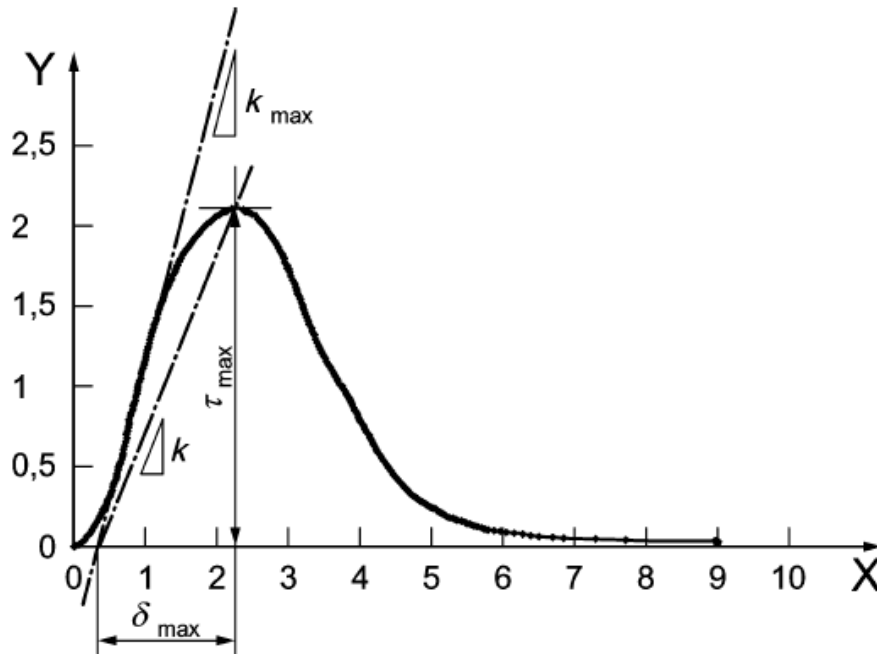


Figure 2.18: Stress – Displacement curve parameters (bsi group, 2019).

- $\tau_{max}, \delta_{max}$ : Peak shear stress [MPa] (in this document, it will be denoted as  $\tau_{peak}$ ), and corrected maximum displacement [mm].
- $K_{max}$ : Maximum interlayer reaction modulus [MPa/mm].
- $K$ : Interlayer reaction modulus [MPa/mm].

As it can be observed, the standard provides two different values of the interlayer reaction modulus, which are the slopes of two different lines. These two values will be further described in the next chapter of this document, and will be used in the analysis of the experimental data. It is worth mentioning that, the standard mentions that in the written report, only  $K_{max}$  should be reported (along with the peak values).

# **3. Chapter 3 – Constitutive models**

### 3.1. Introduction to chapter.

At this point, with the literature review, a good review and analysis of the previous authors' work has been done. The next step focuses on giving a detailed description of the existing constitutive model that describe the interlayer shear behavior. The reason behind this, is that in order to further analyze and understand how to calibrate the software's input parameters, firstly the phenomenon must be properly understood.

It is important to take into account that, although the main scope of this work is focused on the behavior obtained through Leutner Shear tests, which only allow to measure the applied shear load and its consequent shear displacement, the models presented in this chapter will not focus solely on shear quantities. The reason behind this, is the fact that there are other types of tests (as mentioned in Chapter 2), that allow for example, a normal load to be applied and therefore, the displacements in this direction will also affect the shear behavior.

However, firstly, the simple shear models will be discussed, and then, models regarding other loading conditions are analyzed.

### 3.2. Simple Shear models.

The simplest models to describe the shear behavior of the interlayers are those which only take into account the presence of a shear load and shear displacements, and they have been obtained, mainly, from experimental tests, such as the Leutner Shear test, EMPA modified device or the Iowa device, among others.

Firstly, to understand this phenomenon, it is important to note that these kinds of tests are modified versions of the typically used in the studies of soil mechanics, where a shear load is applied at a constant rate, and simultaneously, the displacements are measured. Figure 3.1 show a scheme of what occurs to double-layered specimens under simple shear action:

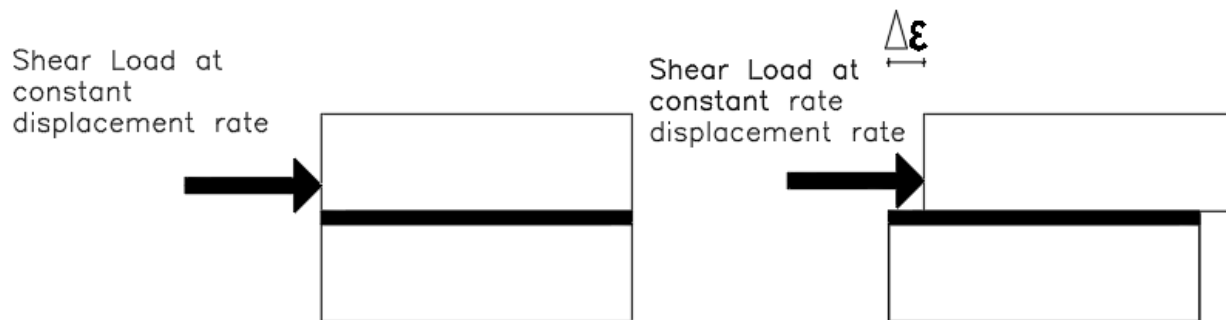


Figure 3.1: (a) Initial state of the double-layered specimens in direct shear tests

(b) Deformed state of the specimens under an applied

shear load at constant rate.

In the previous figure, it can be observed that, the applied shear load, causes the two layers to move in opposite directions, and for such reason, the quantity to take into account while studying this phenomenon is the relative displacement between the layers ( $\Delta\epsilon$ ). However, in these kinds of tests, the lower layer is fixed while the upper one moves. This means that the relative displacement ( $\Delta\epsilon$ ) is equal to the measured displacement ( $\delta$ ).

Additionally, as it can be observed, in Figure 3.1, the applied load action causes a displacement in the specimens. This laboratory test has been performed in various studies. An example of the behavior of the interlayers can be easily observed in Figure 3.2, where the typical shear stress versus displacement plot is presented.

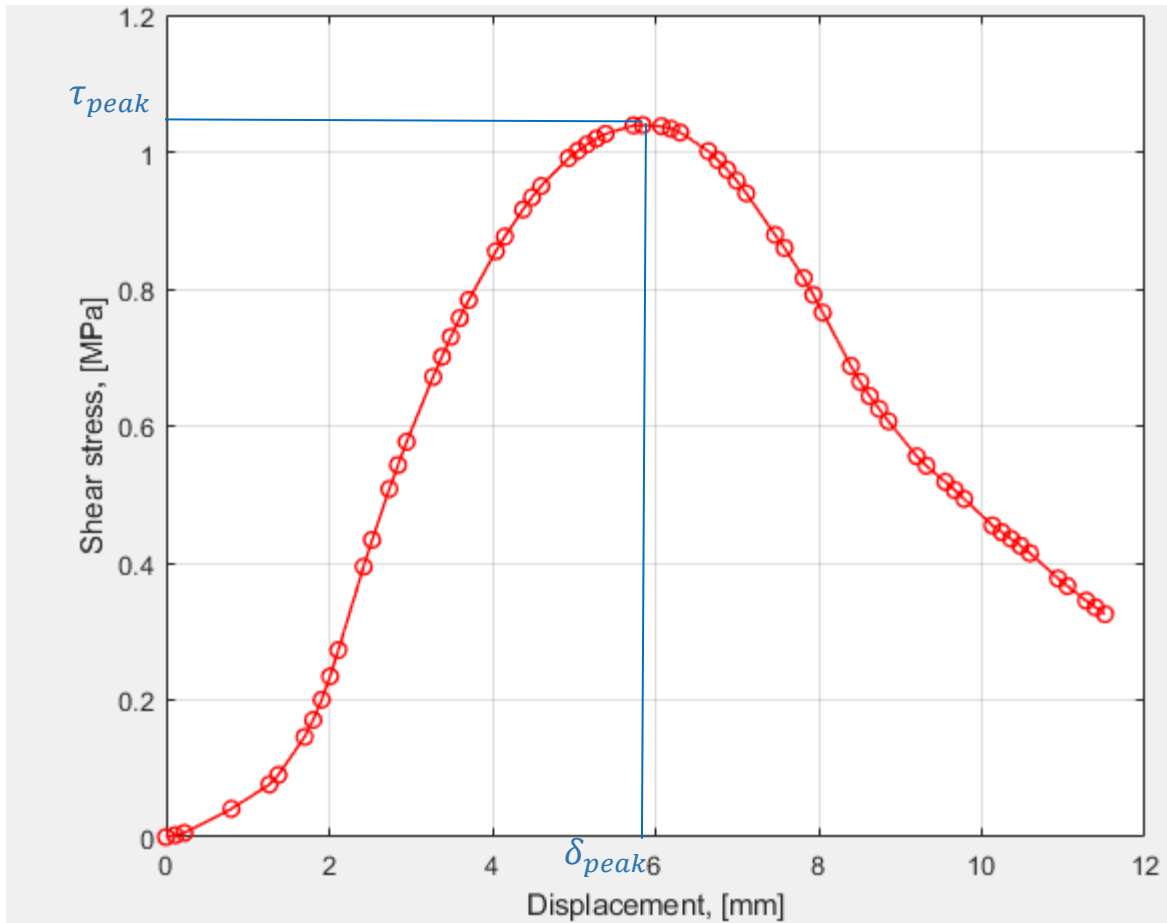


Figure 3.2: Example of shear stress versus displacement plot, obtained from a Leutner test.

As mentioned in Chapter 2, some authors have characterized this plot in various sections, which describe the observed behavior during these tests. A detailed characterization, based on the information previously recollected, will be given in this segment, to provide a better understanding on the results of the tests that study the interlayers' behavior solely under shear loading. In order to do so, the previous stress – displacement curve will be divided into two main stages: the bonded segment and the debonded segment.

The dividing point of these segments is located at the point of maximum peak shear stress ( $\tau_{peak}$ ) and its corresponding displacement ( $\delta_{peak}$ ). The segment prior to this point, is defined as the *bonded segment of the curve*, whereas, past this point, it is defined as the *debonded segment of the curve*. The following sections of the document will describe these two segments.

### 3.2.1. Bonded segment of the curve.

As just mentioned, this first segment of the curve is comprised by all the values that are located

between the beginning of the test (0,0) and the peak shear stress and corresponding displacement ( $\tau_{peak}, \delta_{peak}$ ). Figure 3.3 shows just the bonded segment of the curve presented in the previous figure:

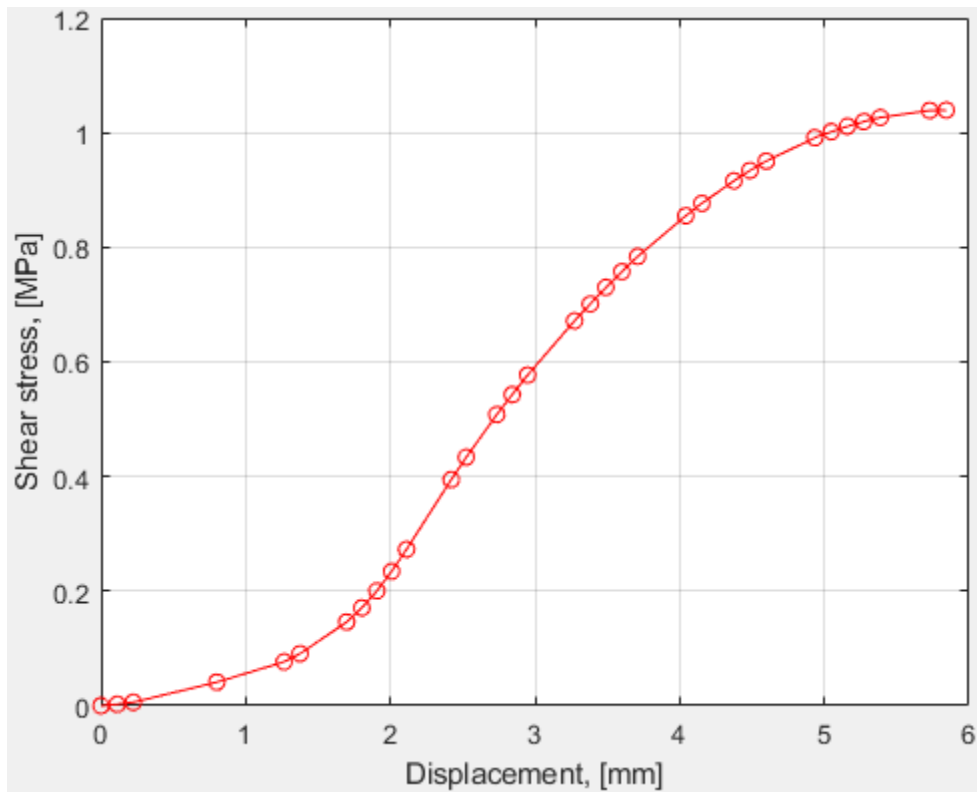


Figure 3.3: Bonded segment of the shear – displacement curve.

At the same time the bonded segment itself can be divided in sub – segments. Initially, it can be observed that there is a marked increment on the measured displacement, while the shear stress increases slowly. This sub-segment has been mentioned in Chapter 2, and has been identified as an initial stage which, is associated to the adjustment of the sample into the testing apparatus (Szydło and Malicki, 2016). As mentioned by this author, and from the processing of data instructions given by the standard on shear bond testing, this portion is not considered to characterize the interlayer’s response under shear loading.

Following this initial sub-segment, the specimen enters in a second sub-segment, characterized by a linear increase of the stress with respect to the displacement. The linear relation between these two variables shows a steady response of the material to the applied shear stress. The constitutive equation that is used to describe the interlayer’s shear response under shear loading alone, focuses mainly on this sub-segment.

In order to describe the behavior in this segment of the plot, linear elastic theory has been employed in the past (Canestrari *et al.*, 2013). This linear elastic theory considers the interlayer as a thin material, characterized by a shear modulus ( $G$ ) and a thickness ( $h$ ). As observed previously, the shear action generates a relative displacement between ( $\Delta\epsilon$ ) the two main layers of the specimens. As mentioned by Canestrari *et al.*, the equation that relates the shear stress, the relative displacement and the two previous characteristic values of the interlayers ( $G, h$ ) is shown in

Equation (3.1):

$$\tau = G \cdot \frac{\Delta\varepsilon}{h} = G \cdot \gamma \quad (3.1)$$

In the previous equation,  $\gamma$  is the shear strain of the interlayer (thin material), and it represents the ratio between the relative displacement and the thickness of the material. Consequently, this first segment of the shear load versus displacement, can be described through Goodman's constitutive equation, and is shown in Equation (3.2):

$$\tau = K \cdot \Delta\varepsilon \quad (3.2)$$

As previously mentioned, in these kinds of tests, the relative displacement ( $\Delta\varepsilon$ ) can be substituted with the measured displacement ( $\delta$ ), and therefore Goodman's constitutive equation can be rewritten according to Equation (3.3)

$$\tau = K \cdot \delta \quad (3.3)$$

Goodman's constitutive equation has been used to describe multi-layered elastic systems, and it describes a linear relation between the applied shear load and the relative displacement between the layers. Both these quantities are related through the variable  $K$ , which is defined as the *Interlayer shear stiffness*, or in some other cases it can be found in the literature as *Interlayer reaction modulus* and is usually measured in [MPa/mm].

Once this the specimen exits the lineal sub-segment of the bonded segment, it enters into a curved stage, where once again, the displacement begins to increase rapidly while the shear stress increases more slowly. It continues like this until the separating point, where the specimen reaches its peak shear stress ( $\tau_{peak}$ ), accompanied by the displacement at peak shear stress ( $\delta_{peak}$ ).

At this precise point, the interlayer reaches its failure state, and once this value is reached, the bond is damaged and will no longer sustain the applied stresses, thus, entering the second segment of the curve; the *debonded segment of the curve*.

### 3.2.2. Debonded segment of the curve.

Once the peak shear stress is reached, the plot enters into debonded segment, in which, the interlayer's bonding is damaged. As the peak shear stress is exceeded, the interlayer no longer resists the shear load. In the moment just after passing the peak shear stress, there is a rapid decrease in the measured shear load for a slow increase of the displacement. After a while, the measured shear load remains almost constant, while the displacement keeps increasing. Due to the speed at which the test is performed, somewhere along this part of the curve, the test is stopped, and no further information is collected.

It is worth mentioning that, after the debonding occurs, the device still measures a reduced value of shear stress, rather than rapidly decreasing to zero. This is due to the fact that, at this point, there is still friction occurring between the upper and lower layer, which produces a reduced value of the shear stress. However, it is expected that, if the displacement keeps increasing during the debonding, eventually, the shear stress will reach zero, since at some point, the friction will no

longer be able to withstand the induced displacement.

Although the whole shear behavior is described by both the bonded and debonded segment of the curve, the interlayer's performance characterization is mainly focused on the bonded segment and on the peak shear stress value. This is given the fact that, in design or modelling applications, the focus is always centered in the situation before the failure of the material occurs.

More specifically, when studying the flexible pavement's interlayer, the main values to describe its performance are the interlayer reaction modulus, as well as the peak shear stress, and its corresponding displacement. For such reason, although this chapter focuses on the constitutive models that reign the interlayer's mechanical behavior, it is important to discuss these values, in order to properly understand the objective of performing Leutner shear tests.

### 3.2.3. The interlayer reaction modulus, $K$ .

As it was just discussed, when describing the bonded segment of the curve, in Goodman's constitutive equation, the variable that links the shear stress and the shear displacement is the *interlayer reaction modulus* or *interlayer shear stiffness*, denoted by the letter  $K$ . As observed in Equation (3.1) and (3.2), it is defined as the ratio between the interlayer's shear modulus ( $G$ ) and its thickness ( $h$ ).

The interlayer shear stiffness is a parameter that has been used to characterize the interlayer bonding. Various authors have focused on studying the variation of such parameter and how it affects the stress-strain distribution along pavements (some of which have been already discussed in Chapter 2). Among such studies, some have found some boundary values for this parameter, used to define the interlayer bonding condition (Canestrari *et al.*, 2013). Such limiting values are shown in Table 3.1:

Table 3.1: Interlayer stiffness boundary values to describe the interlayer bonding condition

Value	Description
$K \leq 10^{-2}$ MPa/mm	Complete debonding
$10$ MPa/mm $< K < 10$ MPa/mm	Partial bonding
$K \geq 10^2$ MPa/mm	Full bonding

It was found that when the interlayer reaction modulus has a value lower than  $10^{-2}$  MPa/mm, the stress and strain distribution in the pavement resembles the completely debonded condition, in which the perfect slippage occurs. On the other hand, when it assumes a value higher  $10^2$  MPa/mm, the interlayer is under full bonding condition, which means that there is no differential displacement between the upper and lower layers. However, in reality, the interlayer condition is always found within these limits, which means, in the partial bonding condition (Canestrari *et al.*, 2013).

Given the difficulty of measuring the thickness of such a thin material, it is possible to obtain the interlayer's reaction modulus from the stress – displacement curves, which can be obtained from any testing device that measures both the shear load and shear displacement.

In order to determine the interlayer's reaction modulus, the standard on shear bond testing for hot-

mix asphalt pavements, states that, by plotting the stress – displacement curves, it is possible to obtain the modulus' value, as shown in Figure 3.4, which depicts the example of stress – displacement curve provided by the standard:

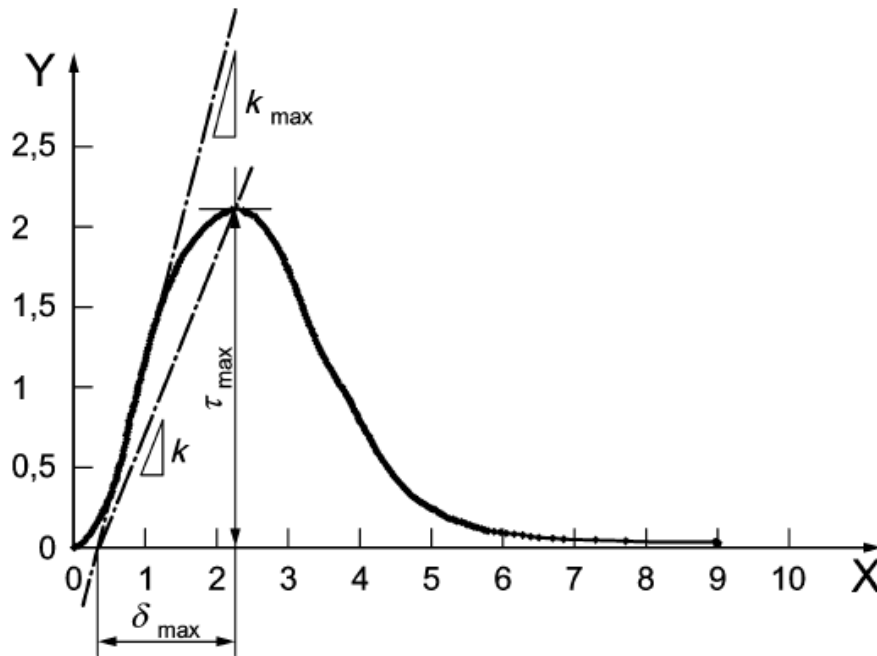


Figure 3.4: Stress – displacement curve (bsi group, 2019).

It can be observed that the standard depicts that there are two possible values for the interlayer reaction modulus,  $K$  and  $K_{max}$ . The maximum interlayer shear stiffness,  $K_{max}$ , can be obtained by performing a linear regression in the linear sub-segment of the curve. This will yield as a result, a linear equation, in which, the slope will represent  $K_{max}$ . By extending the resulting line to the x-axis, it is possible to eliminate the displacement produced by the initial stage of the test, which is disregarded in the interlayer's shear characterization. Additionally, it is expected that this line intercepts the y-axis at a negative value of the shear stress.

The intercept of the  $K_{max}$  line, with the x-axis will be defined as the corrected initial displacement, and will be denoted as  $\delta_0$ . It is important to determine this value, as it is needed in order to determine other values that will be described shortly.

On the other hand,  $K$ , is defined just as the interlayer shear stiffness, and once again, can be determined as the slope of another line. In the case of  $K$ , a lined that passes through the corrected initial displacement  $(\delta_0, 0)$  and through the point at which the peak shear stress occurs  $(\delta_{peak}, \tau_{peak})$ .

All in all, the interlayer reaction modulus/ shear stiffness is the main parameter used to characterize the bonding condition of the interface, when subjected only to shear loads. As previously mentioned, various authors have found that by varying this parameter, the stress – strain distribution along the pavement can change significantly (from the results obtained by considering a perfectly bonded interface versus a fully debonded interface). Therefore, to ensure a proper pavement design, it is important to calibrate an adequate value for the interlayer reaction modulus.

### 3.2.4. Peak shear stress and corrected displacement at peak shear stress.

Apart from the previously discussed interlayer reaction modulus, there are also a pair of variables that are very useful to describe the interlayer's shear characterization. Such variables, are the peak shear stress,  $\tau_{peak}$  and the displacement that occurs at this value,  $\delta_{peak}$ . Firstly, it is important to determine the peak shear stress, as it is the maximum value of shear stress withstood by the interlayer before the debonding occurs, and consequently,  $\delta_{peak}$  is the displacement at which the failure occurs. In order to determine  $\tau_{peak}$ , simply the maximum shear stress obtained from the measured data during the test must be found, and  $\delta_{peak}$  will simply be the displacement measured at that point.

However, due to the fact that the initial stage of the curve is disregarded, and by performing the linear regression needed to determine the  $K_{max}$  line,  $\delta_0$  is obtained, a corrected value of the displacement at the peak shear stress is defined, denoted by  $\delta_{max}$ . It can be easily calculated, from the values of  $\delta_0$  and  $\delta_{peak}$ , as shown by Equation **Error! Reference source not found.:**

$$\delta_{max} = \delta_{peak} - \delta_0 \quad (3.4)$$

The previously described values, constitute the most important values that can be obtained by performing a shear test in which no normal load is applied, and will be used to analyze the experimental data obtained, as well as to elaborate a method to calibrate the interlayer condition in asphalt pavement design software in following chapters.

However, as it is well known, the real situation in asphalt pavements is more complex, since the traffic loads actually induce normal stresses, strains and displacements in the pavement (that are accompanied by shear stresses, strains and displacements). The following segment will describe the influence of the presence of normal loads on the interlayers.

### 3.3. Models considering shear and normal stresses.

As it is known, the stresses, strains and displacements that occur in pavements are a result of the traffic loads acting on them. As the interlayer's main objective is to avoid the slippage between two layers to occur, the main focus while studying them regards mainly its response to the shear action, as it is the shear action itself that causes the layers to slip.

However, previous studies, as detailed in Chapter 2, have found that the normal stress acting on the interlayer has an effect on its shear response. For such reason, there are some laboratory tests that allow the application of a fixed normal load, whilst applying the shear load at constant rate. Not only these tests allow to measure the shear and normal load applied, but they also measure the displacements both in the direction of the shear load and of the normal load. An example of such tests is the ASTRA device, the Romanoschi device, among others.

To give a better understanding of this situation, Figure 3.5 shows a scheme of what occurs to the specimens during the tests that involve both shear and normal quantities and displacements:

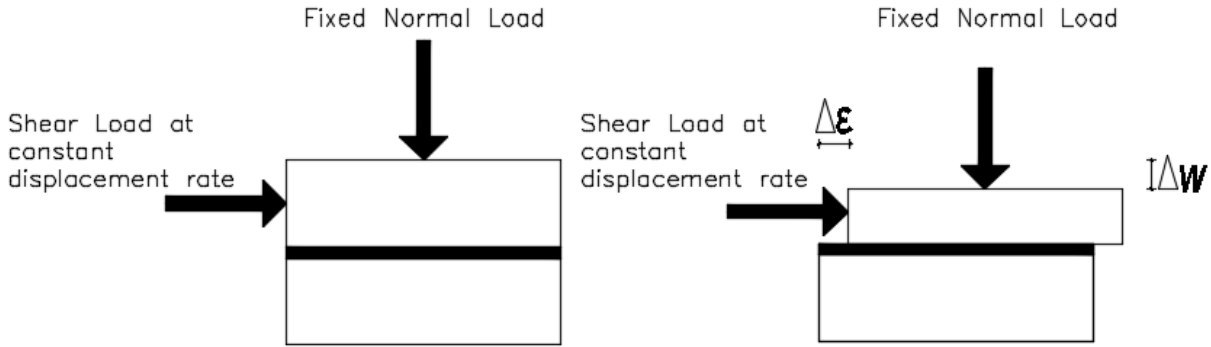


Figure 3.5: (a) Undeformed state of the double-layered specimens. (b) Deformed state of the double-layered specimens under shear load and normal load.

In Figure 3.3 (b), it can be observed that, due to the effect of the shear load, there's a displacement in the horizontal direction, depicted as  $\Delta \epsilon$ , whilst, the vertical deformation, result of the applied normal load is depicted as  $\Delta w$ . These types of tests, allow to test various fixed normal loads, while the shear displacement is increased at a constant rate for each of the fixed normal loads. Consequentially, the results from these tests may be plotted in the Mohr-Coulomb plane.

By plotting the peak shear stress versus the normal stresses, the failure criterion of the interlayers can be individuated by using Coulomb's Failure law (Canestrari *et al.*, 2005), described by Equation (3.5):

$$\tau_{peak} = c_0 + \sigma \tan \varphi_p \quad (3.5)$$

This equation is widely known and used in soil mechanics, and it expresses the peak shear resistance as the sum of the contributions of the material's pure shear resistance ( $c_0$ ) plus the normal stress times the peak friction angle of the material ( $\varphi_p$ ). As this equation is obtained by performing a linear regression between all measured pair of points of the peak shear stress at the corresponding applied normal stress,  $c_0$  is the intercept with the y-axis. This means that  $c_0$  is the value of the peak shea stress when no normal load is applied, similar to the peak shear stress measured in tests where only shear load is applied.

In addition to this, it has been shown that the peak shear resistance provided by the whole system at the interlayer level, is the total sum of four contributions (Canestrari *et al.*, 2005), for a given value of the normal stress, the peak shear stress is described by Equation (3.6):

$$\tau_{peak} = \tau_{res} + \tau_{ic} + \tau_d + \tau_a \quad (3.6)$$

As this equation describes, there are four main contributions to the maximum shear resistance at the interlayer level. The first contribution,  $\tau_{res}$ , is the shear resistance that is measured after failure.  $\tau_{ic}$  represents the shear resistance provided by the inner cohesion of each of the main layers' materials. Then,  $\tau_d$  is the shear resistance provided by the dilatancy phenomenon that occurs between the layers' surfaces which are in contact at the interlayer level. Finally,  $\tau_a$  represent the shear resistance given by the adhesion of a tack coat (in the absence of a tack coat, this component becomes zero).

From the previous contributions, it is important to mention the fact that, the resistance provided by  $\tau_{ic}$ , is a contribution that depends on the materials' properties, as well as  $\tau_a$  (which depends on the tack coat's properties). However, the resistance provided by  $\tau_d$  is of a different nature.

### 3.3.1. Contribution of $\tau_d$ .

Dilatancy is a phenomenon of a geometric nature, which occurs when the surfaces of both layers that are in contact at the interlayer, interlock between them, which means that the asperities of one surface climb over the asperities of the other surface. Such phenomenon has been defined in the past, according to Taylor's model.

To get a better understanding of Taylor's model, Figure 3.6 provides with a scheme of the interlocking that occurs when a double-layered specimen is under shear and normal load at the interlayer level:

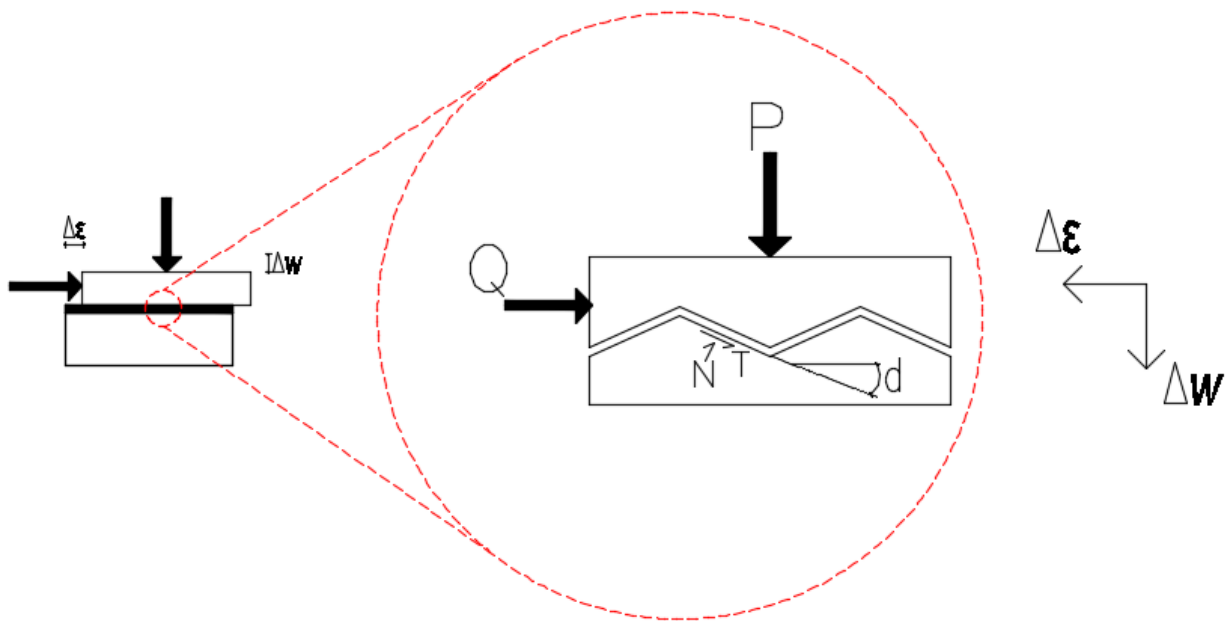


Figure 3.6: Detail of the interlocking between surfaces at the interlayer level.

In the close-up, it can be observed that there is a shear load applied ( $Q$ ) along with a normal load ( $P$ ). As a consequence of both of this, there are two increments in the displacements, one in the horizontal direction ( $\Delta\varepsilon$ ) and one in the vertical direction ( $\Delta w$ ). The tangent of the angle of dilatancy ( $d$ ), can be defined as the ratio between the incremental in the vertical displacement according to Equation (3.7):

$$\tan(d) = -\frac{\Delta w}{\Delta\varepsilon} \quad (3.7)$$

According to Taylor's model, it is possible to determine the shear stress that occurs due to the dilatancy phenomenon, by determining the vertical and horizontal translational equilibrium,

expressed by Equations (3.8) and (3.9) and then combining it with the condition of displacement along the inclined plane, which is given by Equation (3.10):

$$\sigma = P \cos(d) + Q \sin(d) \quad (3.8)$$

$$\tau = -P \sin(d) + Q \cos(d) \quad (3.9)$$

$$\tau = \sigma \tan \varphi_b \quad (3.10)$$

In Equation (3.10),  $\varphi_b$  is the friction angle in stationary state ( $\Delta V = 0$ ), and is referred to, as the base friction angle. By combining the previous equations, Taylor's model states that, the shear stress generated by the dilatancy can be determined in accordance to Equation (3.11):

$$\tau_d = \sigma \frac{\tan(d) + \tan(\varphi_b)}{1 - \tan(d) \tan(\varphi_b)} = \sigma \cdot \tan(\varphi_b + d) \quad (3.11)$$

It can be observed that, the dilatancy's contribution to the shear stress, depends on the displacement in both vertical and horizontal direction. It is worth mentioning that, previous studies have demonstrated that the peak shear stress occurs at the interlayer at the same point as the maximum dilatancy.

### 3.3.2. Contribution of $\tau_{res}$

At this point, it has been commented that  $\tau_{ic}$  and  $\tau_a$  are contributions to the peak shear stress whose nature depends on the material of the layers and on the applied tack coat (if any is applied) and there is also a contribution due to the effect of the dilatancy on the peak shear stress, when both shear and normal loads are applied. The final contribution left to discuss is  $\tau_{res}$ .

During these type of shear tests, after the specimen's peak shear stress is reached, and failure occurs, the measured shear load drops rapidly while the displacement continues to increase. Then, the load tends to become constant around a given value. Such value will be characterized as the residual shear stress,  $\tau_{res}$  [MPa], which can also be determined through the Coulomb failure law, by plotting the measured value of  $\tau_{res}$  versus its correspondent normal stress in Mohr's plane. The residual shear stress can be determined according to Equation **Error! Reference source not found.** in a similar way to how the peak shear stress is calculated in Equation (3.12).

$$\tau_{res} = \sigma \tan \varphi_{res} \quad (3.12)$$

Where  $\sigma$  represents the normal stress [MPa] and  $\varphi_{res}$  is the residual friction angle. This last value, is obtained by performing a linear regression on the measured pair of values of residual shear stress and applied normal stress. This residual shear stress occurs because, after the specimen reaches failure, there is still friction occurring between the upper and lower layer since there is the presence of a perpendicular load to the direction of movement.

Finally, the constitutive equations that rule the interlayer's shear behavior, are summarized in Table 3.2, along with their respective resistance parameters. The purely under shear behavior is obtained

from the stress – displacement curves, and its characterized by the interlayer reaction modulus  $K$ . On the other hand, when under shear and normal load, the constitutive equation that describes the interlayer behavior is given by the Mohr – Coulomb failure envelope, obtained from the Mohr’s plane. The peak shear stress under normal and shear loads is a combination of various contribution, as just previously described.

Table 3.2: Constitutive equations that rule the interlayer shear behavior.

	Constitutive Equation	Parameters
Shear	$\tau = K \cdot \Delta\varepsilon$	Interlayer reaction modulus ( $K$ )
Normal + Shear	$\tau_{peak} = c_0 + \sigma \tan \varphi_p$	Pure shear resistance ( $c_0$ ), peak friction angle ( $\varphi_p$ )

As the current study focuses on the Leutner test, which only evaluates the shear behavior, the parameters that will be used to characterize the interlayer shear behavior are the calculated peak shear stress ( $\tau_{peak}$ ), along with the maximum interlayer reaction modulus ( $K_{max}$ ), the interlayer reaction modulus ( $K$ ).

# **4. Chapter 4 – Analysis of measured data.**

## 4.1. Introduction to chapter

In order to set up and calibrate the model representing the interlayers' shear behavior as well as to validate it, a set of experimental data was used. This data, was collected in Stefano Cutica's thesis dissertation by using a Leutner Shear test device. This device, as it has been mentioned earlier, measures the applied shear load, as well as its consequent displacement. The first section of this chapter will focus on giving a description about the test, so to have a better understanding of what the model is trying to represent.

As one of the specific objectives of this research is to provide with a database of input values for software, calibrated from results of Leutner shear tests, an analysis on experimental data obtained from such test must be done. This chapter focuses on this experimental part of the research, where firstly, the nature of the tests performed will be presented. Then, such data will be used to obtain the values that characterize the tested configurations of the specimens in terms of the interlayer mechanical response solely under shear load. Such results will be also analyzed and discussed.

## 4.2. Experimental program and data obtention.

Regarding the experimental program data and obtention, it is important to mention that part of this study was done during the lockdown period in Italy, in which it was impossible to perform laboratory tests just for this study. Therefore, the Leutner test results that was used during this research was taken from previous studies. This section is dedicated to summarizing the experimental programs used in order to obtain the data.

The main data source for the modelling and analysis of the interlayer shear response, comes from a previous study called *Indagine sperimentale sul comportamento a taglio delle interfacce bituminose*. During such study, an actual pavement section composed of a binder layer in the inferior part (thickness – 5 cm.) and then, a surface course (thickness – 5 cm) placed over it. The mixes used for both binder and surface course were the same along the whole section.

The construction of the pavement section used by Cutica in his studies, was performed, firstly, by laying a thin layer (made of binder mix) over an existing pavement surface, in order to obtain a regular surface (defined as *regularization paving*). After such layer was constructed, the binder layer (lower portion of specimens) was laid with the use of a wheeled paver, and then compacted with help of a roller compactor in order to achieve the desired thickness (5 cm).

Then, the sub-sections were divided and marked, from I to VI, to identify the different interlayer treatments that were used, with a length of 4 m each one. Subsequently, the different treatments were applied in each sub-section, by weighing the amount of emulsion related to each application rate and then pouring such quantities over the binder surface and spreading it with brooms and brushes.

Finally, after an hour of application of the interlayer treatments, the surface layer was laid and compacted with the help of a paver. Then, a roller compactor was once again used to compact to reach the desired thickness of the surface layer (5 cm). Figure 4.1 shows the final setup of the pavement test section that was constructed:

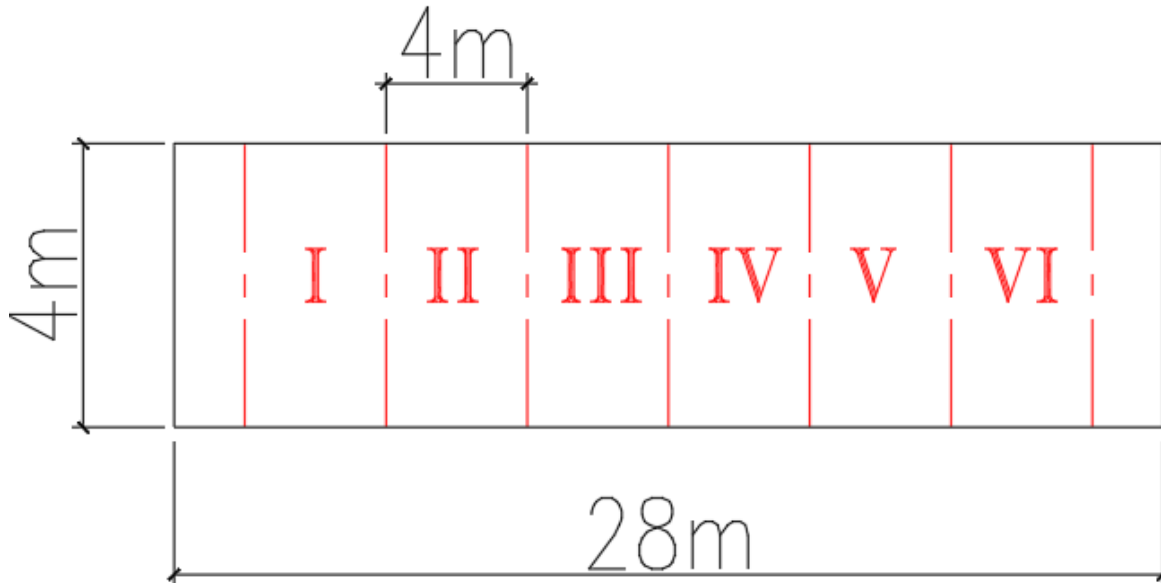


Figure 4.1 Setup of the pavement test section and sub-sections.

As one of the main objectives of the study was to analyze different tack coats (applied between the binder and the surface course layers) and different application rates, each sub-section was characterized by the following interlayer treatments/ application rates:

- **I:** No tack coat was used.
- **II:** Cationic emulsion – 0.15 kg/m<sup>2</sup> residual.
- **III:** Cationic emulsion – 0.30 kg/m<sup>2</sup> residual.
- **IV:** Thermoplastic membrane.
- **V:** Modified emulsion – 0.15 kg/m<sup>2</sup> residual
- **VI:** Modified emulsion – 0.30 kg/m<sup>2</sup>.

As observed, two different types of emulsion at two different application rates (which are measured through the residual application rate) were used, along with the case of no tack coat applied as well as the use of a thermoplastic membrane. As the current study focuses mainly on the application of tack coats (or no application at all), the results obtained for the thermoplastic membrane will not be considered here.

It is important to remark the fact that such study focused on testing double-layered specimens in two different types of device (ASTRA and ATREL), which can measure the shear stress and displacements, along with a fixed normal stress, in order to obtain the Mohr – Coulomb failure criterion. However, in order to compare and validate the results obtained from such devices, some specimens were tested with the Leutner shear device, from which, the data that is used in the current study was obtained from.

The cores that were used for testing, were extracted from the different sub-sections within the whole pavement structure, by using a coring machine, which was able to extract specimens of 100 mm and 150 mm of diameter. The bigger specimens were used in order to control the scale effect on the interlayer response, and therefore, will not be considered here, as the Leutner test was only performed in those with 100 mm of diameter. As the cores were extracted from the previously described pavement section, the total thickness was of 100 mm, with the interlayer placed exactly

in the middle. Figure 4.2 shows the schematic of the cores that were considered for this study:

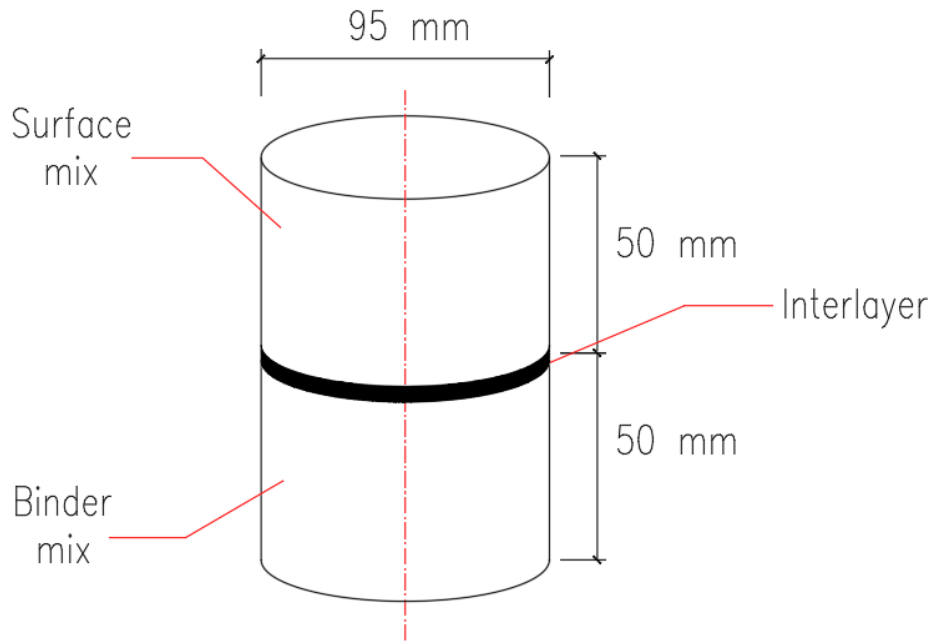


Figure 4.2: Schematics of the double – layered cores obtained from the pavement test section.

Although the coring configuration was set at 100 mm of diameter, the actual measured diameter in the specimens was of 95 mm. From the total of samples recollected from the test section, some were allocated for being tested in the Leutner device. As mentioned before, the results from those specimens taken from the sub-section in which the thermoplastic was used in the interlayer, will not be used in the current study. From the five remaining sub-sections' cores, three Leutner tests were performed per each, for a total of 15 sets of results.

From these results, the shear stress [MPa] was calculated in order to obtain the stress – displacement curves, from which, the previously described characteristic values are obtained. The results from such process will be presented in the following chapter of this document.

### 4.3. Experimental results analysis

As mentioned earlier, three Leutner tests were performed on each of the sub-section's cores, in order to assess the shear behavior of each of the used interlayers treatments. Five sub-sections will be used during this study, which correspond to the Modified Emulsion treatment and Traditional Emulsion (both with residual application rates of 0.15 kg/m<sup>2</sup> and 0.30 kg/m<sup>2</sup>), and the interface without any type of treatment. For the current analysis, the results will be categorized according to the type of treatment, the application rate and finally on the test number, as follows:

[Type of treatment] \_ [Residual application rate] \_ [Test number]

Regarding the type of treatment used, the possible options are:

- **ME:** Refers to those cores in which a modified emulsion was applied as interlayer treatment.

- **TE:** Refers to those cores in which a traditional emulsion was applied as interlayer treatment.
- **NT:** No treatment applied at the interface of the specimens.

Then, regarding the residual application rate, the identification is:

- **1:** The residual application rate for the selected type of treatment is equal to 0.15 kg/m<sup>2</sup>.
- **2:** The residual application rate for the selected type of treatment is equal to 0.30 kg/m<sup>2</sup>.
- In case the case where no treatment was used, only test number will be specified.

Finally, regarding the test number:

- **1:** Test number 1.
- **2:** Test number 2.
- **3:** Test number 3.

Therefore, to refer to the third test, performed in a core taken from the sub-section in which a traditional emulsion was used with a residual application rate of 0.30 kg/m<sup>2</sup>, the code TE\_2\_3 shall be used.

Once the categorization of the data has been described, the following procedure was to begin processing and analyzing the data obtained from each of the performed Leutner tests, which yields data in terms of the measured shear load ( $P$ ) [kN] and displacements ( $\delta$ ) [mm]. Taking into account the shear load and the diameter ( $D$ ) [mm] of the specimens, it is possible to determine the shear stress [MPa], according to Equation (4.1):

$$\tau = \frac{F}{\frac{\pi D^2}{4}} \quad (4.1)$$

Once the shear stress has been calculated for each of the measured points, it is possible to obtain the stress – displacement curves, which will be the main tool to be used in order to characterize the shear behavior of all the specimens. Therefore, the obtained curves will be presented in the following section.

#### 4.4. Stress – displacement curves.

In order to understand the shear response of the tested specimens when only shear loading is applied, the stress – displacement curves of every test performed were obtained. Firstly, the results will be given for each type of treatment and for each of the residual application rates.

- **ME\_1:**

Figure 4.3 shows the stress – displacement curves for all of the three Leutner tests performed in the cores pertaining to the sub – section, where a modified emulsion was applied at a residual application rate of 0.15 kg/m<sup>2</sup>:

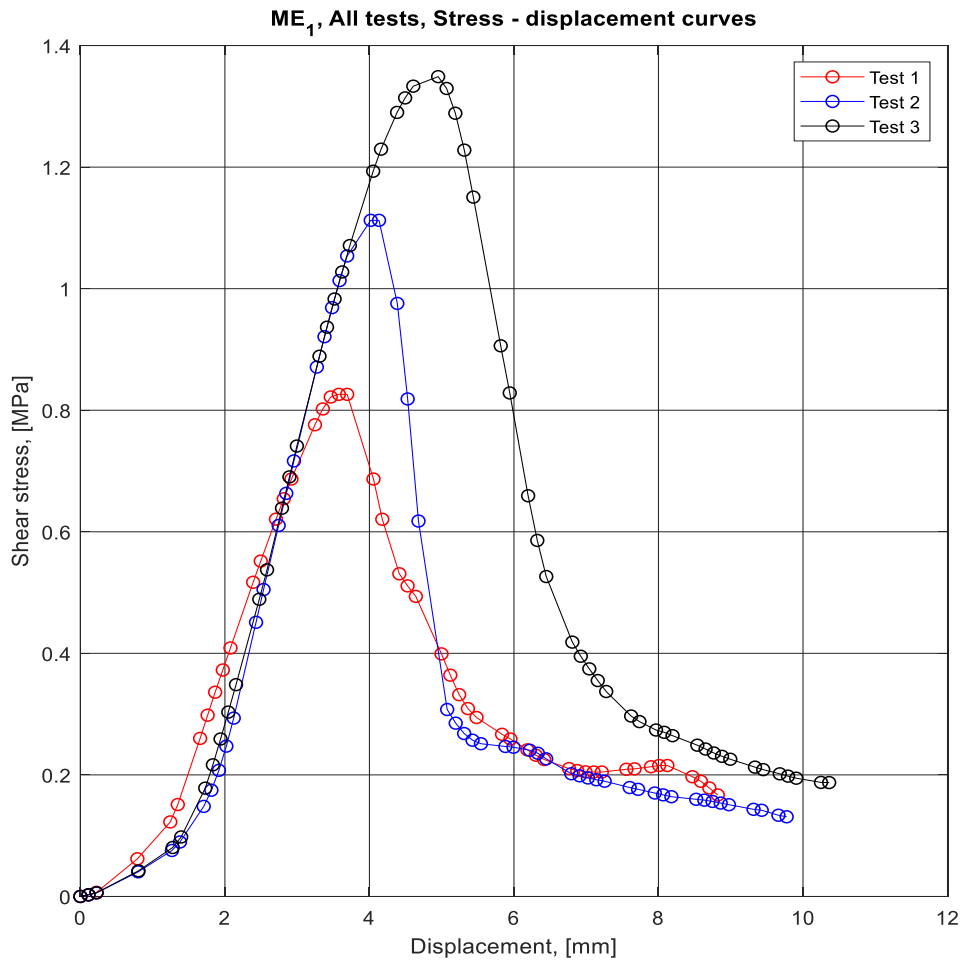


Figure 4.3: Stress – displacement curves for ME\_1 cores.

As it can be observed, the three tests performed in the ME\_1 cores, yield slightly different results in terms of the measured  $\tau_{peak}$  and  $\delta_{peak}$ . According to the previous figure, the calculated peak values are presented in Table 4.1:

Table 4.1: Peak values for ME\_1

	$\delta_{peak}$ [mm]	$\tau_{peak}$ [MPa]
<b>Test 1</b>	3.577	0.826
<b>Test 2</b>	4.018	1.112
<b>Test 3</b>	4.951	1.349

As shown, the highest value of both peak shear stress and corresponding displacement, are obtained for Test 3. However, in order to obtain a characteristic value of the peak shear stress for this particular interface treatment and residual application rate, the average between the three peak values is obtained, as well as the standard deviation, provided by Table 4.2:

Table 4.2: Average of  $T_{peak}$  for ME\_1

$\tau_{peak,avg}$ [MPa]	Std Deviation [MPa]
1.096	0.26

In this case, the characteristic value of peak shear stress for ME\_1 is equal to 1.096 MPa, with a corresponding standard deviation of 0.26 MPa. Given this standard deviation value, it can be observed that all of the measured peak values are found within,  $\pm 2$  Std Deviation from the mean, which indicates that the measured values are within an acceptable range to indicate the true value of the peak shear stress. Regarding the values of  $\delta_{peak}$ , the average was not computed, as  $\tau_{peak}$  will be the main value used to characterize the overall shear resistance of ME\_1.

- **ME\_2:**

Figure 4.4 shows the stress – displacement curves obtained for the same type of interlayer treatment, but with a higher residual application rate ( $0.30 \text{ kg/m}^2$ ), once again, for each of the three tests performed in this type of core:

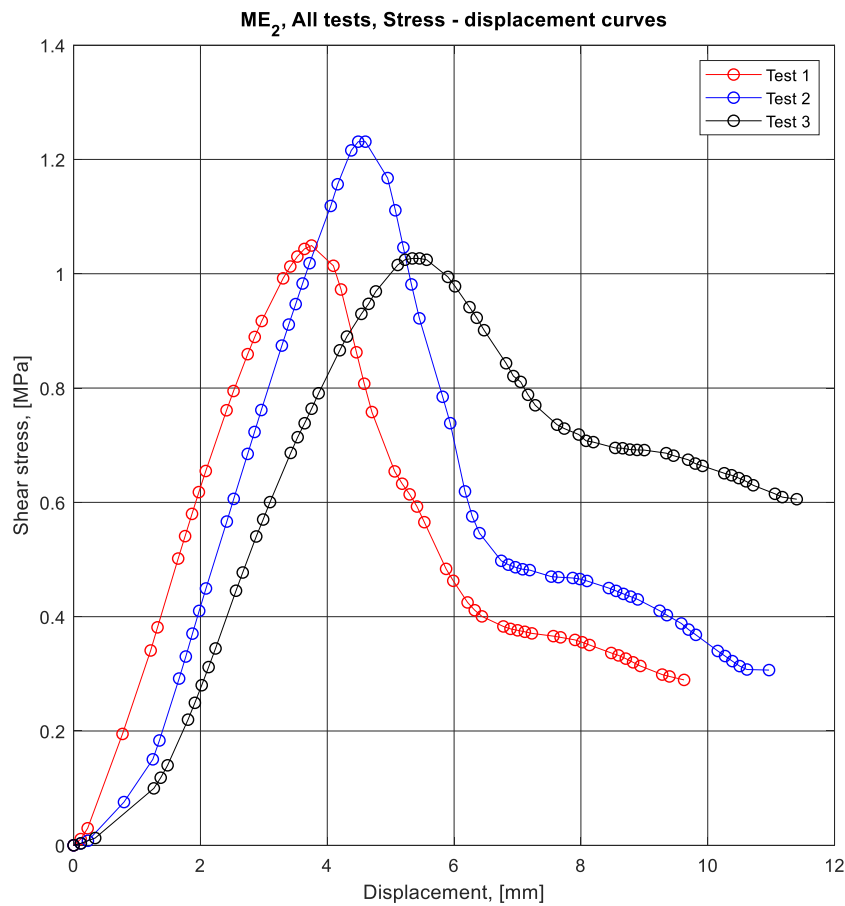


Figure 4.4: Stress – displacement curves for ME\_2 cores.

From this figure, it can be observed that, although in Test 1 and Test 3 the peak shear stress value of both curves is pretty close, there is a relatively big difference in the displacement corresponding to  $\tau_{peak}$ . As done previously, both  $\tau_{peak}$  and  $\delta_{peak}$  for each curve were obtained and presented in Table 4.3:

Table 4.3: Peak values for ME\_2.

	$\delta_{peak}$ [mm]	$\tau_{peak}$ [MPa]
<b>Test 1</b>	3.752	1.049
<b>Test 2</b>	4.488	1.231
<b>Test 3</b>	5.341	1.027

Additionally, the average for the peak shear stress and the standard deviation were determined, and the results are presented in Table 4.4:

Table 4.4: Average of  $T_{peak}$ , ME\_2

$\tau_{peak,avg}$ [MPa]	Std Deviation [MPa]
1.102	0.11

In this case, for the ME applied at a higher residual application rate, there was a slight increase in terms of the characteristic value of  $\tau_{peak}$ , in comparison to the value obtained when the ME was applied at 0.15 kg/m<sup>2</sup>. Regarding the standard deviation, it can be observed that the measured values are quite close to the computed mean.

- **TE\_1**

Now, moving onto the next type of interface treatment, Figure 4.5 shows the results obtained for the cores categorized as TE\_1:

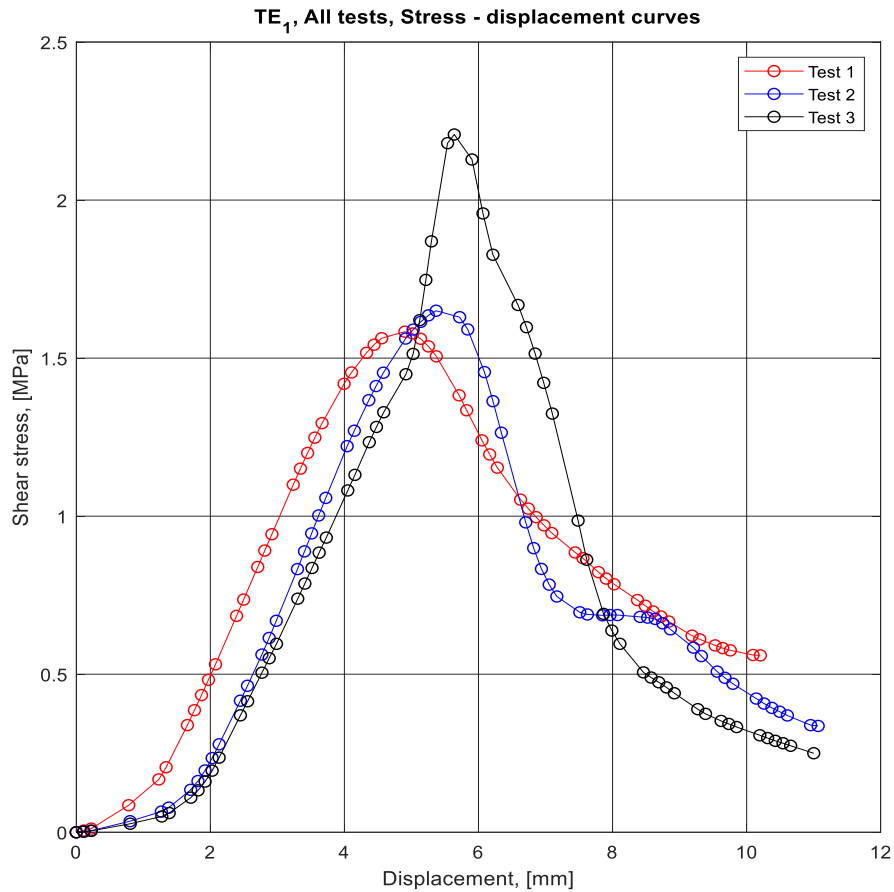


Figure 4.5: Stress – displacement curves for TE<sub>1</sub> cores.

In the case of the TE<sub>1</sub> cores, Test 1 and Test 2 resulted in quite similar curves, whereas the Test 3 yield a higher value of  $\tau_{peak}$  and differs slightly from the typical curves, as it presents a notable variation in its slope when approaching the peak value. Additionally, Table 4.5 presents the summarized peak values for this type of cores:

Table 4.5: Peak values for TE<sub>1</sub>.

	$\delta_{peak}$ [mm]	$\tau_{peak}$ [MPa]
<b>Test 1</b>	4.902	1.584
<b>Test 2</b>	5.368	1.650
<b>Test 3</b>	5.639	2.207

Subsequently, Table 4.6 shows the average values calculated for these types of cores and the standard deviation of the measured data:

Table 4.6: Average of  $\tau_{peak}$  for TE<sub>1</sub>.

$\tau_{peak,avg}$ [MPa]	Std Deviation [MPa]
1.814	0.34

The characteristic value for the peak shear stress for TE\_1 core is equal to 1.814 MPa, which is higher than the one measured in the previous two cases. Regarding the standard deviation, it can be observed that in this case, the results obtained are a little further from the computed mean value, however all of them fall within a range of  $\pm 2$  Standard Deviation.

- **TE\_2**

Figure 4.6 shows the curves obtained for the TE with a higher application rate than the previous case:

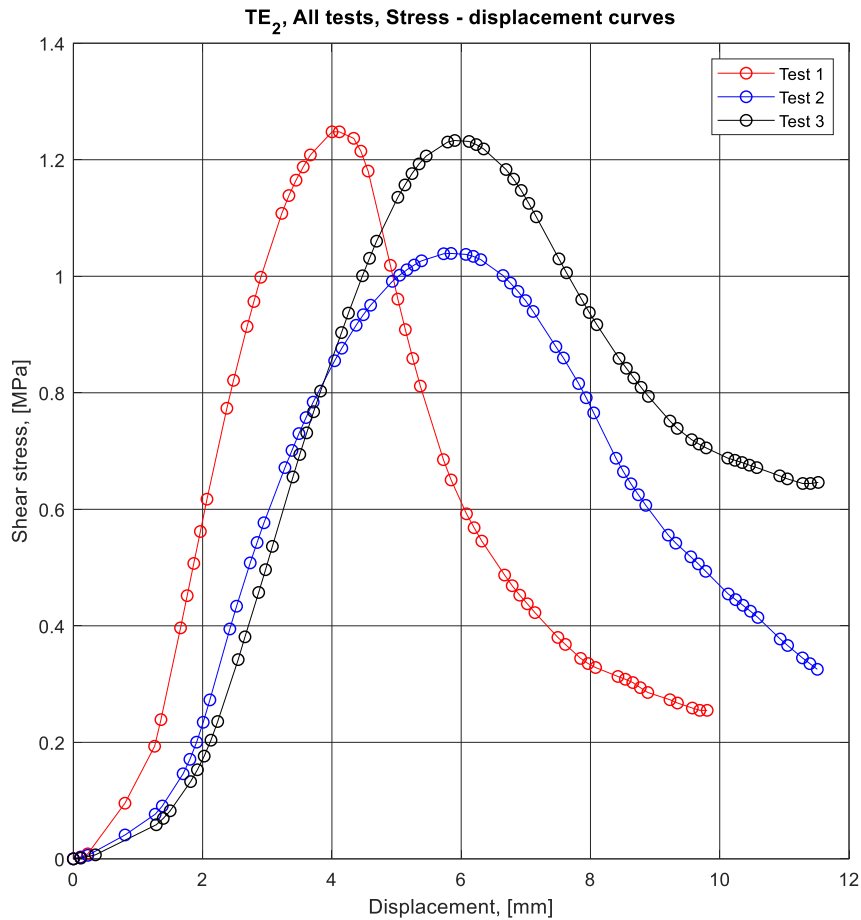


Figure 4.6: Stress – displacement curves for TE\_2 cores.

In this case, the curves obtained for each of the performed tests have the typical curve shapes expected for these types of tests. The computed peak values for each test are presented in Table 4.7:

Table 4.7: Peak values for TE\_2.

	$\delta_{\text{peak}}$ [mm]	$\tau_{\text{peak}}$ [MPa]
<b>Test 1</b>	4.002	1.248
<b>Test 2</b>	5.843	1.039
<b>Test 3</b>	5.901	1.233

And in order to characterize a peak shear stress for this type of cores, the mean value and the standard deviation are computed, and the results are presented in Table 4.8:

Table 4.8: Average Peak values for TE\_2.

$\tau_{\text{peak,avg}}$ [MPa]	Std Deviation [MPa]
1.173	0.12

As compared with the TE\_1 cores, it can be observed that for this particular type of emulsion, the characteristic peak value is lower at a higher application rate.

- **NT:**

Finally, Figure 4.7 shows the curves obtained for the cores in which no treatment was applied at the interface. The results obtained from this dataset will help to establish comparisons between the cases where there is a treatment applied in comparison to when it is not applied.

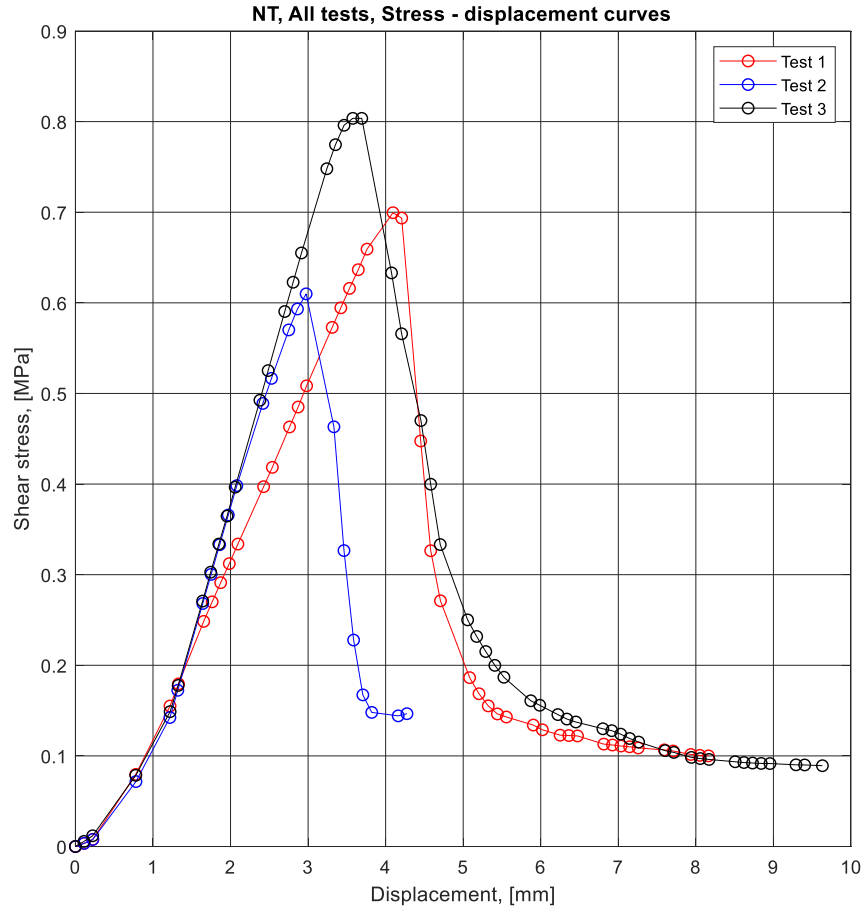


Figure 4.7: Stress displacement curves for NT cores.

From this Figure, it can be observed at a first glance that the peak shear stress values for these types of cores are quite lower than those measured in the previous cases. To have a clearer insight into this, Table 4.9 shows the peak values for each test, whereas

Table 4.10 shows the characteristic peak shear stress, computed by finding the average of all three tests, as well as the standard deviation of the data:

Table 4.9: Peak values for NT cores.

	$\delta_{peak}$ [mm]	$\tau_{peak}$ [MPa]
<b>Test 1</b>	4.095	0.699
<b>Test 2</b>	2.975	0.610
<b>Test 3</b>	3.577	0.804

Table 4.10: Average Peak value for NT cores.

$\tau_{peak,avg}$ [MPa]	Std Deviation [MPa]
0.704	0.10

Clearly, the highest value of peak shear stress is found in Test 3, although, this value does not necessary correspond to the highest measured peak displacement. As it has been already discussed over in this document, this effect is due to the value of the interlayer reaction modulus ( $K$ ). Regarding the characteristic value of the peak shear stress, it is the lowest of all of the sub-sections that were analyzed.

In order to obtain a broader look into the analyzed specimen’s shear resistance, the characteristic peak shear stress, obtained for all the sub-section’s cores, are summarized in Table 4.11:

Table 4.11: Summary of the results obtained in terms of  $T_{peak}$  for all cores

		$T_{peak}$ [MPa]	$T_{peak,avg}$ [MPa]
<b>ME_1</b>	<b>Test 1</b>	0.826	1.096
	<b>Test 2</b>	1.112	
	<b>Test 3</b>	1.349	
<b>ME_2</b>	<b>Test 1</b>	1.049	1.102
	<b>Test 2</b>	1.231	
	<b>Test 3</b>	1.027	
<b>TE_1</b>	<b>Test 1</b>	1.584	1.814
	<b>Test 2</b>	1.650	
	<b>Test 3</b>	2.207	
<b>TE_2</b>	<b>Test 1</b>	1.248	1.173
	<b>Test 2</b>	1.039	
	<b>Test 3</b>	1.233	
<b>NT</b>	<b>Test 1</b>	0.699	0.704
	<b>Test 2</b>	0.610	
	<b>Test 3</b>	0.804	

Additionally, this information can be better observed by plotting the previous values into a graphic, as shown in Figure 4.8:

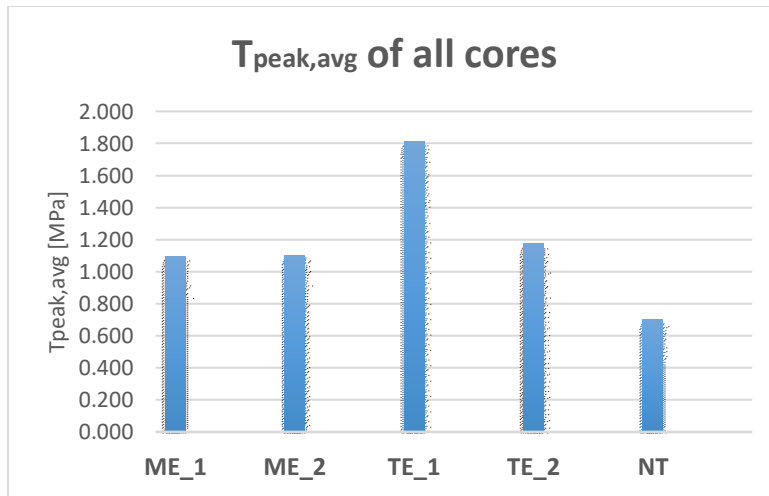


Figure 4.8:  $T_{peak,avg}$  for all of the analyzed cores.

Firstly, it can be observed that, the characteristic peak shear stress for the sampled cores, ranges between the 0.704 MPa and 1.81 MPa, where the lowest value corresponds to the cores in which no interface treatment (NT) was applied. This result is coherent with the findings of previous authors in this field, regarding the fact that, the presence of a tack coat in the form of emulsion improves the shear resistance in asphalt pavements.

The second interesting fact that can be observed both from the previous table and the previous figure, is that, in this particular case, the shear resistance in the specimens characterized by the application of a traditional emulsion (TE) at any residual application rate, is higher than the shear resistance offered by the specimens of the modified emulsion (ME).

Finally, the last appreciation to give regarding this information, concerns the residual application rates used in the ME and TE cores. Regarding the TE cores, it can be clearly observed that, at residual application rate of  $0.15 \text{ kg/m}^2$ , a higher characteristic peak shear stress is obtained than for those cores where the residual application rate was  $0.30 \text{ kg/m}^2$ .

On the other hand, for the ME cores, although the obtained values for the characteristic peak shear stress are quite similar, in this particular case, when the emulsion was applied at an application rate of  $0.30 \text{ kg/m}^2$  was slightly higher than the results obtained for the  $0.15 \text{ kg/m}^2$  cores.

The reason behind this, is what has been defined as the optimal application rate. Among the Literature Review presented in Chapter 2, some studies focused on characterizing how the application rates affect the peak shear stress. These studies have defined the optimal application rate of a given tack coat, as the application rate at which the highest peak shear stress is obtained.

Additionally, such studies have found that the optimal application rate varies depending on various factors, such as the type of tack coat applied or the type of mixes used for the layers both above and below the interface among others. In this particular case, although the optimal application rate cannot be determined, since it requires more application rates to be tested, it shows that the type of emulsion used does generate a difference in the optimal application rate. For instance, in this particular case of study, the traditional emulsion works more effectively when applied at  $0.15 \text{ kg/m}^2$  than at  $0.30 \text{ kg/m}^2$ . On the other hand, the inverse situation can be observed, as it works better at a residual application rate of  $0.30 \text{ kg/m}^2$  than of  $0.15 \text{ kg/m}^2$ . Despite this observation, no conclusion regarding the optimal application rate of any of the used tack coats will be made, given the fact that this value may be found at other rates different from those tested during this study.

#### **4.5. Interlayer reaction modulus ( $K$ ) analysis.**

Once the initial analysis of the data was performed, in terms of the peak shear resistance and correspondent displacement, the next step consists on determining and analyzing the results for the interlayer reaction modulus for each of the cores analyzed in the previous point. For this particular scope, it is important to recall the definition of the interlayer reaction modulus,  $K$ , which has been previously discussed in Chapter 3.

The definition of the *interlayer reaction modulus* or, as it is also known, the *interlayer shear stiffness*, measured typically in  $[\text{MPa}/\text{mm}]$ , is the variable that links the shear displacement and the shear stress, according to Goodman's constitutive model. The proper definition of this variable can be observed in Equation (3.1) and (3.2), as the ratio between the shear modulus,  $G$ , and the thickness of the interlayer,  $h$ .

However, while performing a Leutner test, neither of these parameters are known, and therefore, a different way of determining the interlayer reaction modulus is necessary. As it has been also discussed in Chapter 3, it is possible to obtain this value from the stress – displacement curves. As mentioned by the standard, from the stress – displacement plot, two values of  $K$  can be determined ( $K_{max}$  and  $K$ ) along with a corrected value of the displacement, denoted as  $\delta_{max}$ .

Therefore, the current analysis was performed, relying on this definition given by the standard, along with what was discussed in Chapter 3, regarding on the methodology used to obtain these two values from the plot. Additionally, is worth mentioning that  $K_{max}$  is the slope of the linear part within the stress – displacement curves, whereas  $K$  is the slope of the line that passes through the point in which the  $K_{max}$  intercepts the x-axis and the point of peak shear stress (and its corresponding displacement). Also,  $\delta_{max}$  is the corrected peak displacement, which goes from the intercept of the x-axis and the  $K_{max}$  line, until the original value of  $\delta_{peak}$ .

Once again, these calculations were performed in all of the previously mentioned datasets, in order to perform an analysis on the results obtained. The first dataset that was analyzed, was the one referring to the ME\_1 sub-section’s specimens.

- **ME\_1**

Figure 4.9 shows the bonded portion of the stress – displacement curve, as well as the lines from which it is possible to obtain  $K_{max}$  and  $K$ , by finding the lines’ slope, for every specimen of the ME\_1 tests:

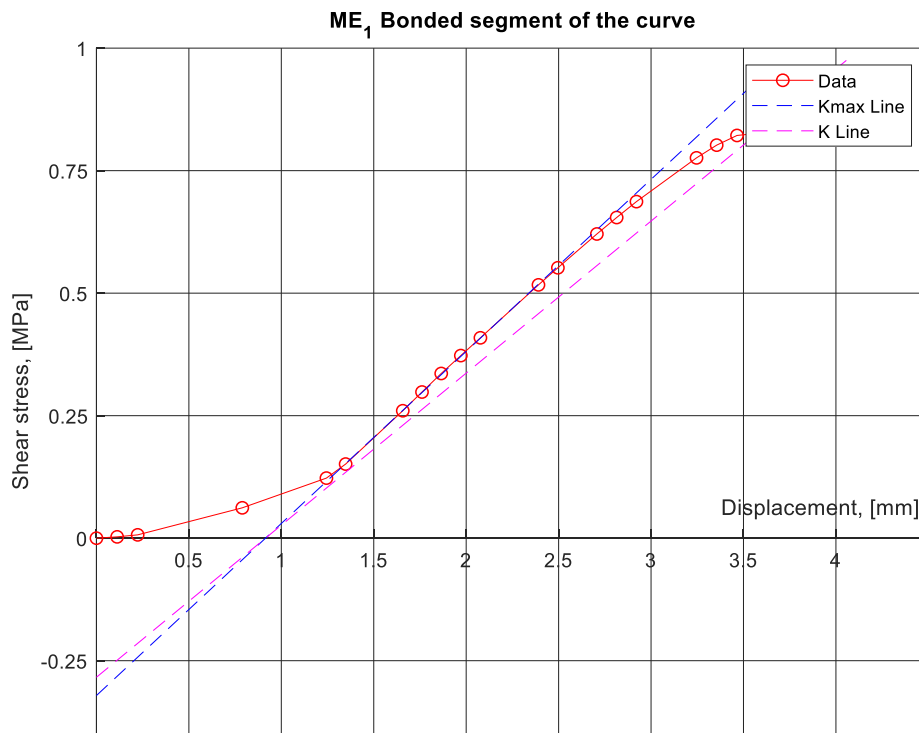


Figure 4.9 (a): Lines used to find  $K_{max}$  and  $K$  in ME\_1\_1.

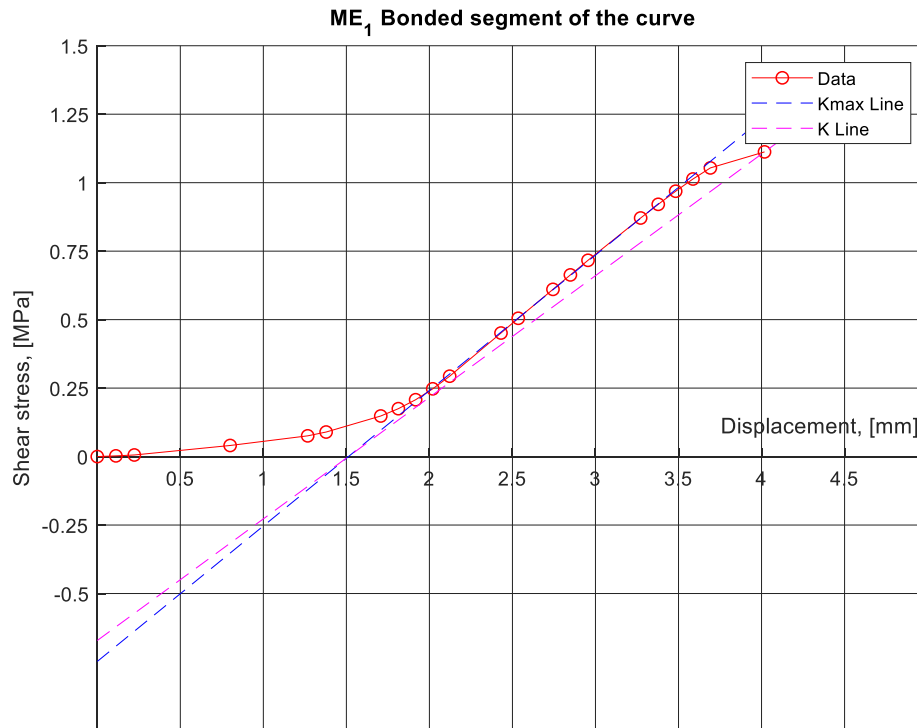


Figure 4.9 (b): Lines used to find  $K_{max}$  and  $K$  in  $ME_{1\_2}$ .

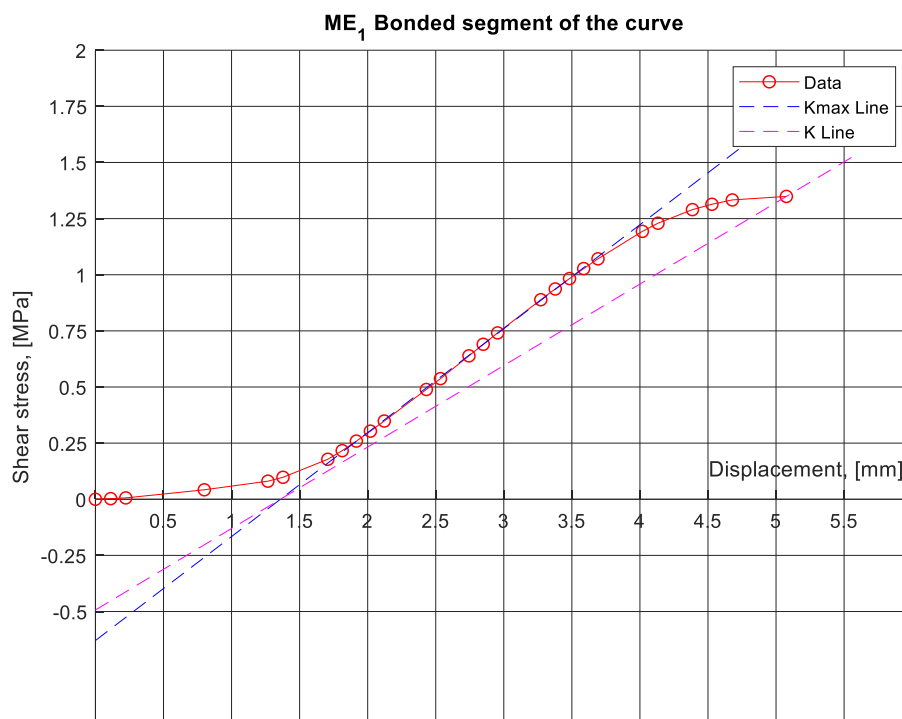


Figure 4.9 (c): Lines used to find  $K_{max}$  and  $K$  in  $ME_{1\_2}$ .

It can be observed that in test 1 and test 2, both lines have a similar slope, whereas in test 3 there

is a more pronounced difference between the two. Table 4.12 shows the calculated slopes for the three tests performed on these types of specimens:

Table 4.12:  $K_{max}$ ,  $K$  and corrected peak displacement, all tests in ME\_1 specimens.

	$K_{max}$ [MPa/mm]	$K$ [MPa/mm]	$\delta_{max}$ [mm]
<b>Test 1</b>	0.351	0.310	2.662
<b>Test 2</b>	0.495	0.444	2.505
<b>Test 3</b>	0.463	0.363	3.717
<b>Average</b>	0.436	0.372	
<b>Std deviation</b>	0.075	0.067	

In general terms, from these values it can be observed that, test 2 was the case with higher values for both  $K_{max}$  and  $K$ , whereas  $\epsilon_{max}$  was the lowest from all three tests. The calculated average will be used to be compared with the values obtained from the analysis of the other types of specimens.

- **ME\_2**

The plot from which the results of  $K_{max}$ ,  $K$  and  $\epsilon_{max}$  were obtained, for this type of specimen can be found in Appendix A. Table 4.13 shows the numerical values calculated for these variables, as well as the average and standard deviation for all tests:

Table 4.13: Results for  $K_{max}$ ,  $K$  and  $\epsilon_{max}$  for all tests of ME\_2.

	$K_{max}$ [MPa/mm]	$K$ [MPa/mm]	$\delta_{max}$ [mm]
<b>Test 1</b>	0.353	0.298	3.525
<b>Test 2</b>	0.363	0.339	3.630
<b>Test 3</b>	0.298	0.240	4.270
<b>Average</b>	0.338	0.292	
<b>Std deviation</b>	0.035	0.050	

In this case, it can be appreciated that the difference between  $K_{max}$  and  $K$  is equal to 0.046 MPa/mm and the highest value for both terms of the interlayer reaction modulus was obtained during Test 2. Comparing these results with the previous ones, it can be observed that in ME\_2, the average values were lower than for ME\_1.

- **TE\_1:**

The plots used for the estimation of the values presented in Table 4.14 can be found within Appendix A. This table, as in the previous cases, show the summarized data obtained for the specimens classified as TE\_1:

Table 4.14: Results for  $K_{max}$ ,  $K$  and  $\epsilon_{max}$  for all tests of TE\_1.

	$K_{max}$ [MPa/mm]	$K$ [MPa/mm]	$\delta_{max}$ [mm]
<b>Test 1</b>	0.466	0.398	3.983
<b>Test 2</b>	0.508	0.443	3.721
<b>Test 3</b>	0.447	0.525	4.207
<b>Average</b>	0.474	0.455	
<b>Std deviation</b>	0.031	0.064	

Regarding the TE\_1 cores, it can be observed that in this case, both the maximum and the normal interlayer reaction modulus have higher values than both of the previous types of cores analyzed (ME\_1 and ME\_2). Additionally, by looking at the average values of  $K_{max}$  and  $K$  it can be observed that for this type of cores, there is a smaller variation between these values than in the previous cases.

Also, it is worth mentioning that, in Test 3 there is an abnormality in the calculated values of the interlayer reaction modulus, since in this case, the value of  $K$  is higher than the obtained value of  $K_{max}$ . The reason behind this can be observed by taking a look at Figure 4.10, which shows the plot of the stress – displacement curves obtained from the data measured during TE\_1\_3 tests.

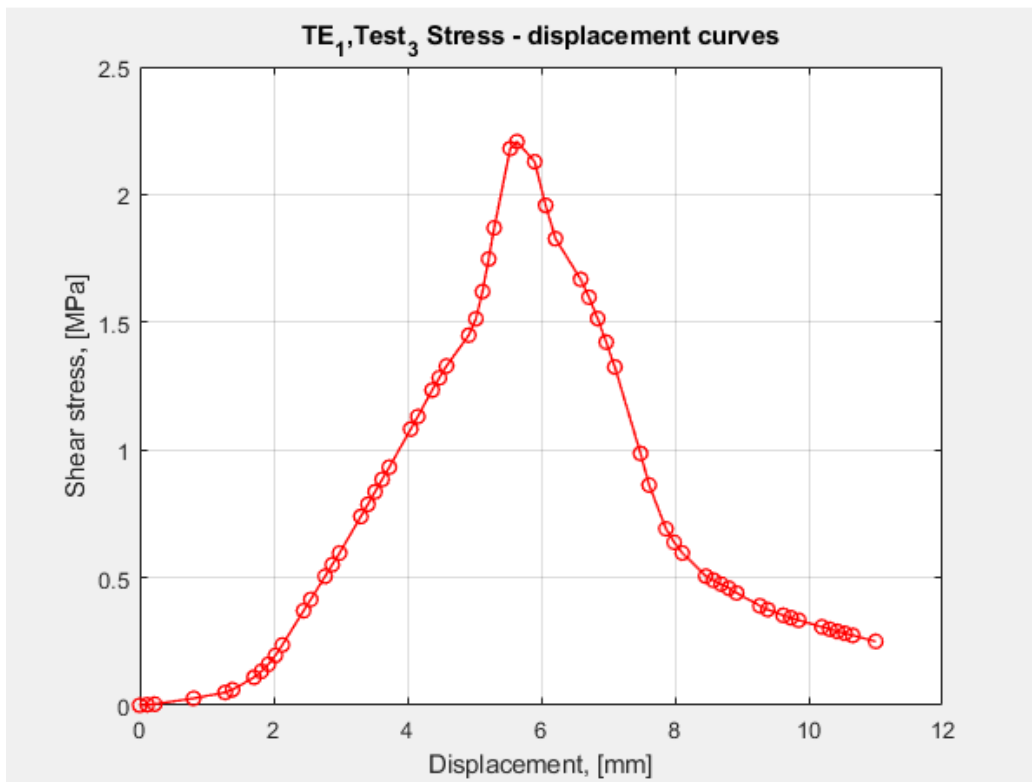


Figure 4.10: Stress – displacement curves, TE\_1\_3.

As it can be observed, the stress – displacement curves obtained for TE\_1\_3, do not have the typical behavior of the curves obtained from Leutner tests. It can be easily identified that, after the lineal sub-segment of the bonded segment of the curve, there is another lineal segment with a higher

slope than the second. Usually, what is expected after the lineal sub-segment, is a curved sub-segment which will have a decreasing slope as it reaches  $\tau_{peak}$ . This difference with the typical curves is what causes the unexpected case in which the calculated  $K$  is higher than  $K_{max}$ .

- **TE\_2:**

The plots used for the estimation of the values presented in Table 4.15 can be found within Appendix A. This table, as in the previous cases, show the summarized data obtained for the specimens classified as TE\_:

Table 4.15: Results for  $K_{max}$ ,  $K$  and  $\epsilon_{max}$  for all tests of TE\_2.

	$K_{max}$ [MPa/mm]	$K$ [MPa/mm]	$\delta_{max}$ [mm]
<b>Test 1</b>	0.526	0.402	3.103
<b>Test 2</b>	0.375	0.233	4.464
<b>Test 3</b>	0.362	0.282	4.376
<b>Average</b>	0.421	0.306	
<b>Std deviation</b>	0.091	0.087	

In this case, it is possible to observe that, in terms of both  $K_{max}$  and  $K$ , there is a reduced value to that obtained by using the same type of emulsion as interface treatment in a lower dosage. Also, it can be observed that so far, this type of cores shows the highest difference between the two values of interlayer reaction modulus, at 0.116 MPa/mm of difference.

- **NT:**

The plots used for the estimation of the values presented in Table 4.16 can be found within Appendix A. This table, as in the previous cases, show the summarized data obtained for the specimens classified as NT:

Table 4.16 Results for  $K_{max}$ ,  $K$  and  $\epsilon_{max}$  for all tests of NT.:

	$K_{max}$ [MPa/mm]	$K$ [MPa/mm]	$\delta_{max}$ [mm]
<b>Test 1</b>	0.199	0.190	3.675
<b>Test 2</b>	0.290	0.270	2.255
<b>Test 3</b>	0.287	0.267	3.007
<b>Average</b>	0.259	0.243	
<b>Std deviation</b>	0.052	0.045	

Finally, in the cores that did not had any type of interlayer treatment, as expected the values of the interlayer reaction modulus are the lowest from all of the data recorded. On the other hand, this case shows the lowest difference between both values of the modulus, at 0.016 MPa/mm.

In order to make further observations regarding these results, Table 4.17 shows the average values for  $K_{max}$  and  $K$  in all of the analyzed sub -sections, while Figure 4.11 shows the results in form of a column chart:

Table 4.17: Summarized results of the interlayer reaction modulus for all categories of specimens.

	$K_{max}$ [MPa/mm]	$K$ [MPa/mm]	$\Delta K$ [MPa/mm]
ME_1	0.436	0.372	0.064
ME_2	0.338	0.292	0.046
TE_1	0.474	0.455	0.019
TE_2	0.421	0.306	0.115
NT	0.259	0.243	0.016

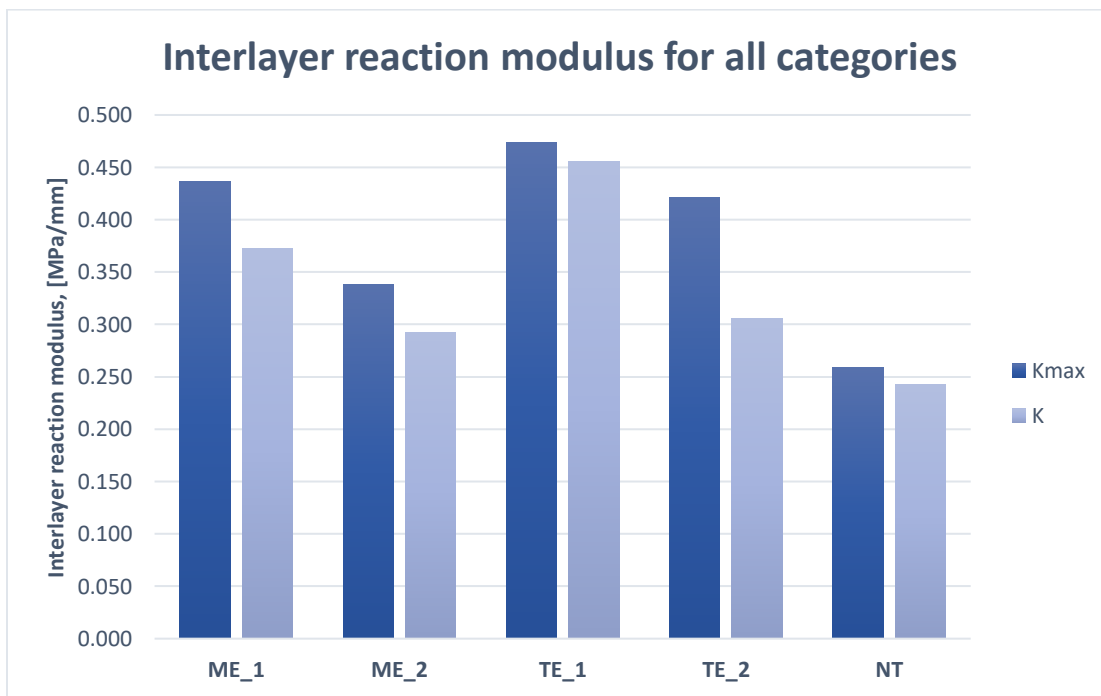


Figure 4.11: Interlayer reaction modulus results for all categories.

In the previous table, it is possible to get a broader look on how the interlayer reaction modulus varies from one type of specimen to another. Firstly, by observing the results for the specimens with no interface treatment, it is possible to appreciate that these kinds of specimens had the lowest values of the modulus, for both of them.

This was expected, since the reaction modulus is directly linked with the results obtained for the peak shear stress analysis, in which, also the NT cores yielded the lowest results of in terms of the peak stress.

On the other hand, the highest value in terms of  $K_{max}$  was obtained for the TE\_1 cores, which also yielded the highest value in terms of  $K$ , followed by the ME\_1 specimens, then the TE\_2 and then by the ME\_2. Therefore, it can be clearly stated that the presence of a tack coat of either traditional emulsion and modified emulsion increases the effectiveness of the interlayer’s response when

subjected to shear loading.

Then, by comparing the specimens that did had some type of interface treatment, as already mentioned, TE\_1 cores obtained the best results in terms of the interlayer reaction modulus. However, it is not possible to say that one emulsion behaves more effectively than the other, since the results are once again influenced by the residual application rate. Despite the fact that TE\_1 has higher values, ME\_1 results are higher than those from TE\_2.

From this statement, it can be observed that although no conclusion can be drawn regarding the type of emulsion used, the obtained data does show that the results obtained for the specimens in which the emulsion was applied at a higher residual application rate are lower than when it was applied at a lower rate.

This apparent decrease in the interlayer reaction modulus when increasing the residual application rate, for this situation is called as apparent because in order to define a proper relationship between the application rate and the modulus, it would be necessary to test more specimens at different application rates in order to draw a clear conclusion, that relates the optimal application rate with the interlayer reaction modulus.

However, these particular results show that in the case of the traditional emulsion (TE), the reaction modulus is higher for the lowest application rate, which concord with the results of the peak shear stress. In this case, it seems to be a relationship between the optimal application rate and the modulus.

On the other hand, in the case of the modified emulsion (ME), there is a mismatch between the results of the peak shear stress analysis and the reaction modulus analysis. In the first one, it was observed that for the higher residual application rate, higher values were obtained for the peak shear stress, whereas, in terms of the modulus, the higher values were obtained for the lowest application rate.

Finally, it is worth mentioning that the previously described mismatch between the optimal application rate and the reaction modulus, can be explained by the definition and the procedure that has been used to calculate such application rate. Previous studies have focused mainly in characterizing the optimal application rate, depending on the results of peak shear stress obtained at certain application rates. However, this procedure does not take into account the deformations measured, whereas, in the interlayer reaction modulus analysis, both the shear stress and deformation are taken into account.



# **5. Chapter 5 - Software analysis.**

## 5.1. Introduction to chapter.

As the main objective of this work is focused on the calibration of the interlayer condition, parting from raw data obtained from Leutner tests, to input into various flexible pavement design software, this chapter focuses, firstly, on reviewing such software, both by interacting with them and by reviewing their User's guide. The objective of this, is because, in order to calibrate any value from the measured data, the knowledge on how these software allow to define the interlayer condition is needed.

Consecutively, once the review on the software is done, and the parameter that must be calibrated for each one of them (some of them only allow to define the condition of fully bonded/partially bonded/debonded) is clear, the following part of this chapter focuses on the discussing which value of the interlayer reaction modulus (as it has been described in previous chapters, the standard proposes that two values of the modulus are obtained from the Leutner test results) must be used.

Then, once the most adequate value of the modulus is defined from the previous analysis, a method on how to perform the full analysis on raw data obtained from Leutner tests, which will result in obtaining the interlayer reaction modulus' value. This last segment, is accompanied by a proposed MATLAB script that will help the user to perform such analysis in an automatic way.

Finally, taking into account the previous information, two models will be developed in BISAR 3.0 and EVERSTRESS in order to assess the influence of the selecting the value of the interlayer reaction modulus, by comparing the results obtained by evaluating both  $K_{max}$  and  $K$ , while confronting these results with those obtained by also evaluating the fully bonded and the completely debonded condition.

## 5.2. Assessment of the bonding conditions in pavement analysis software.

One of the main objectives of this research, is to review and analyze how different software specialized in the flexible pavement analysis and design, take into consideration the bonding condition at the interlayers and its influence in the calculation of stresses and strains. In order to do so, the following software have been reviewed:

- BISAR (Bitumen Structures Analysis in Roads).
- EVERSTRESS.
- KENPAVE.
- EVERSTRESSFE.

This segment focuses on giving a brief description on each of these software, and how each one of them takes into account the bonding/debonding between layers in order to calculate the stresses and strains.

### 5.2.1. BISAR (Bitumen Structures Analysis in Roads).

The Bitumen Structures Analysis in Roads is a software property of Shell International Oil Products, and it was developed during the early 1970s, and was used initially to draw the design the charts of the Shell Pavement Design Manual. At this moment, BISAR was developed as a

mainframe computer program. The following versions developed by Shell, allowed BISAR to be used in any personal computer, and to be used by pavement designers, researchers, among others.

The version BISAR 3.0 allows to calculate stresses, strains, deflections under various loading configurations and patterns. This version, allows the user also to account for the presence of horizontal forces and the slippage between the pavement’s layers (Bitumen Business group, 1998).

It is important to mention that BISAR 3.0 calculates the stress, strains and deflections based on an elastic theory, applied on multi-layered systems, based on some considerations, which are better described in the User’s Manual.

According to the BISAR 3.0 user manual, this version of the program allows to account for horizontal forces and the slippage (either full or partial), which is directly related with the bonding condition in the interlayers of the pavement that is under analysis. This software allows to make these considerations based on the concept of shear spring compliance. Prior to providing detail on this concept, the way these values are input into the software is shown. Figure 5.1 shows the screen in which the slippage degree between layers can be configured:

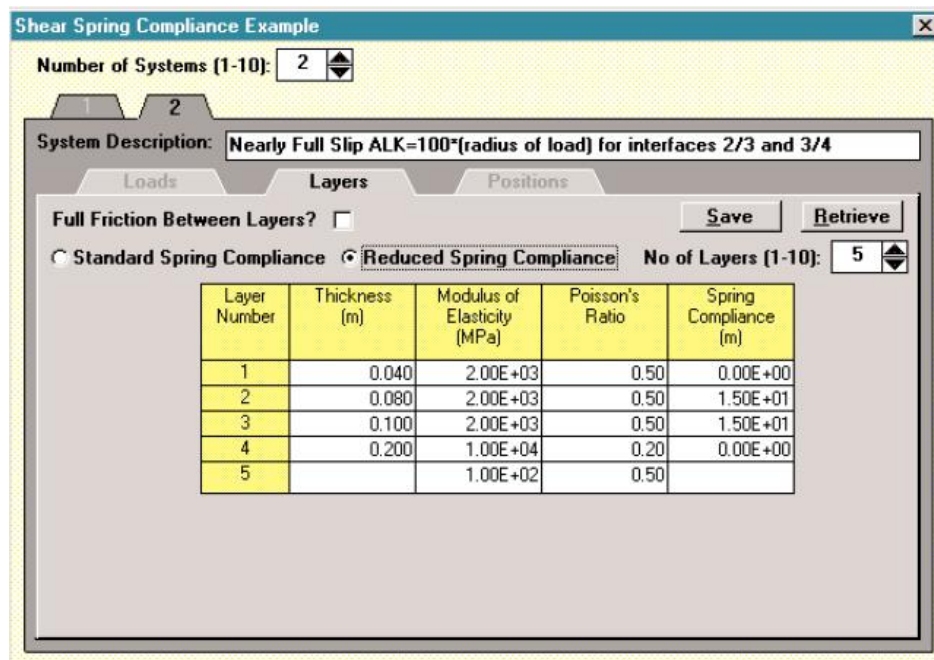


Figure 5.1: Input screen to define slippage between layers in BISAR 3.0 (Bitumen Business group, 1998).

As it can be observed in the previous figure, this example shows how it is possible to define the degree of slippage between any couple of layers. Firstly, right below the tab “Layers”, there is a check box, to define if whether there is full friction between layers. In this case, full friction between layers means full adhesion (the two layers under analysis are completely bonded).

If a couple of layers is to be considered as not having full friction, the check box must not be checked but rather, the user must select between inputting either the Standard Spring Compliance or the Reduced Spring Compliance.

According to the User Manual, that provides the theoretical background behind the slippage analysis, which, as it has been already mentioned, is based on the concept of the shear spring

compliance. The first factor to take into account is that the interlayers is represented as an infinite thin membrane, which strength is defined by the spring compliance. This parameter, denominated as  $AK$ , is defined in Equation (5.1):

$$AK = \frac{\Delta\varepsilon}{\tau} \quad (5.1)$$

As it can be observed, the shear spring compliance is defined as the ratio between the relative displacement between the layers and the applied shear stress. Clearly, this parameter is the inverse of the interlayer's stiffness  $K$ , and from it, it can be said that BISAR assumes that the displacement is proportional to the applied stress at the interlayers, which has been already expressed several times by Equation (5.2):

$$\tau = K \cdot \Delta\varepsilon \quad (5.2)$$

It can be remarked, from this equation, that the interlayer stiffness  $K$  can be easily defined as the applied shear stress, divided by the relative displacement between layers. The spring shear compliance, as it just has been said is the inverse of this value, and in BISAR is input in [ $\text{m}^3/\text{N}$ ]. Nevertheless, the shear spring compliance,  $AK$ , does not provide any insight into the actual situation of slippage between layer, (if there's partial or full slippage). In order to define the degree of slippage, the designers of BISAR introduce the friction parameter,  $\alpha$ , and is defined in Equation (5.3):

$$\alpha = \frac{AK}{AK + \frac{1+\nu}{E} \cdot a} \quad (5.3)$$

Where:

- $a$ : Radius of the load [m].
- $E$ : Modulus of the layer right above the interlayer [Pa].
- $\nu$ : Poisson's ratio of the layer above the interlayer.

The friction parameter  $\alpha$ , is comprised between zero and one. When  $\alpha = 0$ , it means that there is full friction, whilst when  $\alpha = 1$  it means there is complete slippage. From the previous Equation, it can be easily observed that the friction parameter is nothing like the classical friction coefficients and is not purely a material property, but rather, is also affected by the radius of the applied load.

Finally, the BISAR 3.0 User Manual, defines the reduced shear spring compliance,  $ALK$  [m], through the relation presented in Equation (5.4), which relates the Shear spring compliance,  $AK$ , with the reduced shear spring compliance, through the modulus and Poisson's ratio of the layers in the structure, as:

$$AK = ALK \cdot \frac{1+\nu}{E} \quad (5.4)$$

Additionally, it is possible to obtain the reduced spring shear compliance,  $ALK$ , through another relationship with the previously defined friction parameter,  $\alpha$ , and the radius of the load,  $a$  [m], as it is presented in Equation (5.5):

$$ALK = \frac{\alpha}{1 - \alpha} \cdot a \quad (5.5)$$

Now, taking into consideration Equations (5.1), (5.3), (5.4) and (5.5), the BISAR software is capable to determine the friction parameter, from the input values of the layers characteristics, the loading characteristics and the shear spring compliance (or reduced spring shear compliance), which defines the mechanical response at the interlayers. Additionally, if the value of for example, spring shear compliance is input manually and the checkbox of input value is changed from the spring shear compliance to the reduced shear compliance option, the software will automatically calculate the  $ALK$  related to the  $AK$  that was input (and vice versa).

It is important to mention that in the BISAR 3.0 User Manual states the fact that it is difficult to assign a given value and for this reason, the recommended method to assign a given value of either  $AK$  or  $ALK$ , is to perform a sensibility analysis with various values of either of them. In the case of  $ALK$ , it is recommended to perform calculations by varying this value from 0 to 100 times the radius of the load, such that the analysis covers the whole range of slippage (from  $\alpha = 0$  to  $\alpha = 0.99$ ).

However, doing such kind of sensitivity analysis could be very time consuming, as it would mean performing several calculations, just in order to calibrate one value (or set of values if analyzing more than two layers). For such reason, in this study, a more effective way of calibrating these parameters, parting from Leutner test data is proposed.

### 5.2.2. EVERSTRESS

This software is part of a package of software, designed by the Washington State Department of Transportation and called *Everseries Pavement Analysis Program*. *Everstress* is based on the multi-layered elastic theory, to analyze the response of Hot-mix asphalt pavement under circular loading (Washington State Department of Transportation, 2005).

It allows to configure a wide range of parameters to make a model and among them, it is possible to define the frictional contact between layers (Washington State Department of Transportation, 2005), through the parameter called *Interface Contact*. Figure 5.2 shows where this value can be defined in Everstress:

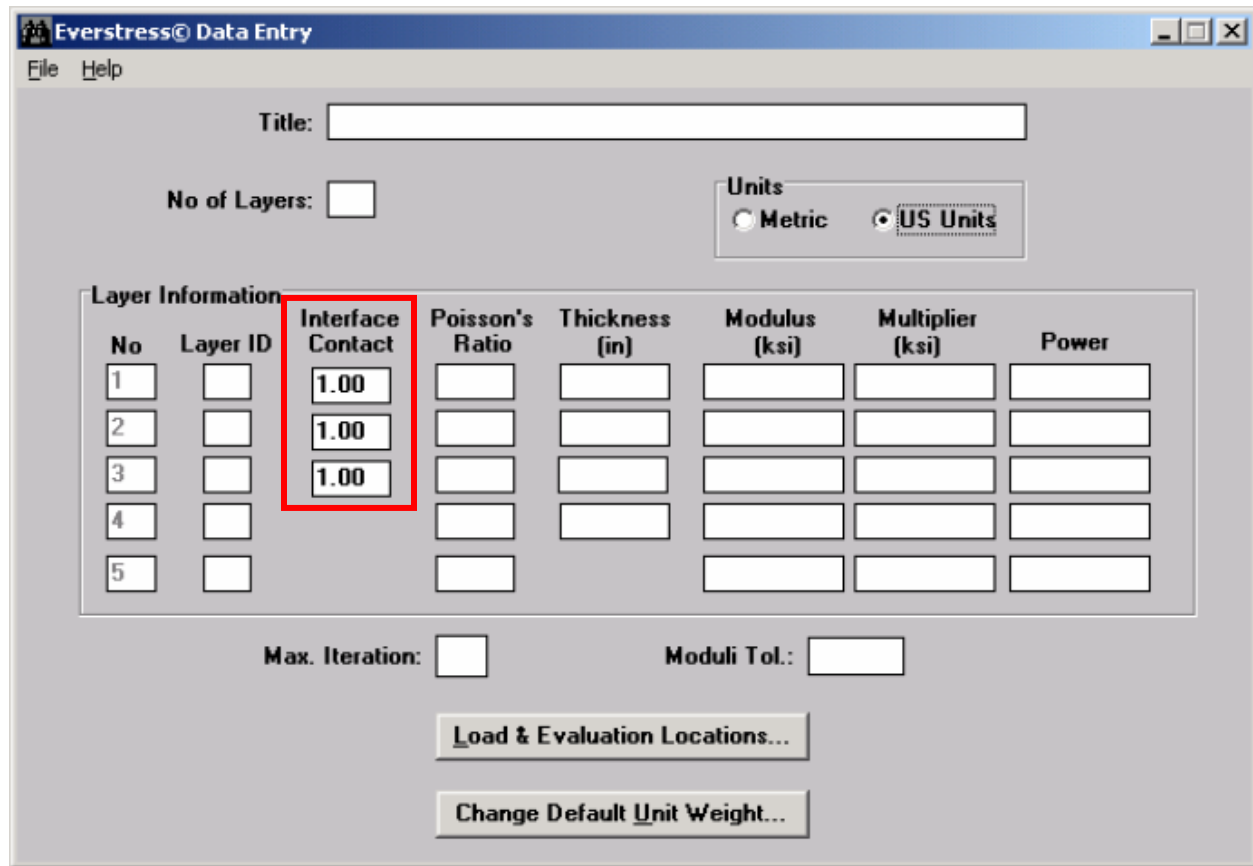


Figure 5.2: Location of the interface contact configuration screen in Everstress.

As shown in the previous example, Everstress allows to configure what within the software is called *Interface contact*, between any pair of layers in which, the superior one a bituminous layer. This term is related to the frictional contact within layers, and it allows the following options to be input:

- [0]: When this value is selected, the software assumes full slippage at the interlayer.
- [1]: This value indicates that there is full adhesion between layers.
- [2 – 1000]: This value indicates that there is a partial slip between the indicated layer.

### 5.2.3. EVERSTRESSFE

This software, created by the University of Michigan (with funding of the Washington State D.O.T.), allows to analyze the response of flexible pavements under wheel loads by means of 3D Finite Element Analysis.

Similar to the previous software, this one allows to define certain conditions at the interlayer. Such configuration can be performed in the software's tab labeled as *Meshing*. More specifically, under the title of *Vertical Meshing Parameters*. Figure 5.3 shows where the *Interface Condition* can be defined in EverStressFE:

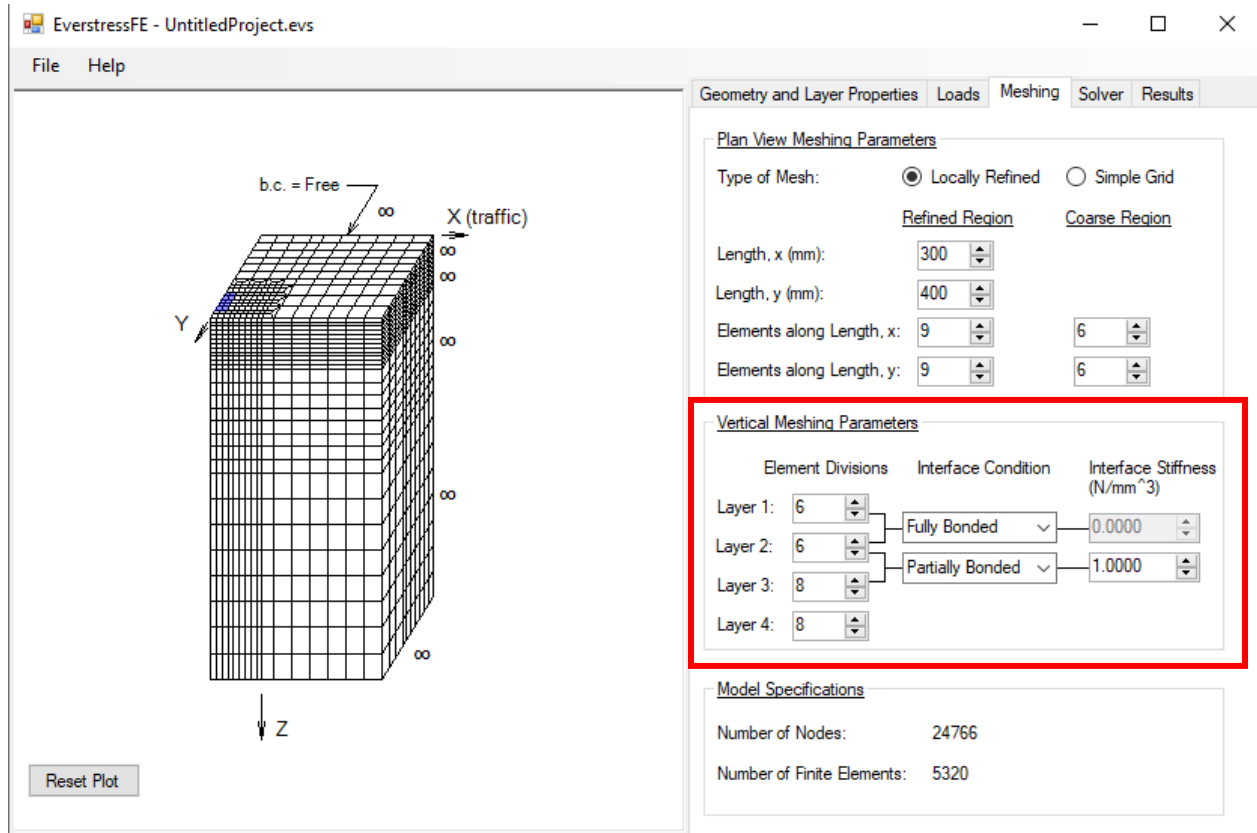


Figure 5.3: Interface condition configuration in EverStressFE.

As it can be observed in this example, where a system composed of four layers was selected, it is possible to define an Interface Condition between the upper layers of the asphalt pavement (composed of bituminous mixtures). Two possible options can be selected in this case:

- Fully bonded.
- Partially bonded.

If *Partially bonded* is selected, it is possible to input a value of *Interface Stiffness* [N/mm<sup>3</sup>]. The units of this value are force over volume, which is the same as the [MPa/mm] that has been used to characterize the Interlayer Stiffness Modulus, *K* in this document. Additionally, if the value input is zero, the software assumes that there is complete slippage/complete debonding between the specified layers. On the other hand, if the *Fully Bonded* condition is selected, the interface stiffness value is blocked.

### 5.2.4. KENPAVE

*KENPAVE* is another software package that is used for both analysis and design for both rigid and flexible pavements, developed by Yang H. Huang. As the other software previously described, it allows to calculate the response in terms of strains, deformations and stresses. It is constituted of two main software, *KENLAYER* and *KENSLABS*, the first one focuses on analyzing flexible pavements and the second focuses in rigid pavements.

As the focus of this work is on flexible pavements, the software that will be described is *KENLAYER*. However, to use this software, characteristics of the layered system are input in the *LAYERINP* screen. Figure 5.4 shows *KENPAVE*'s main screen:

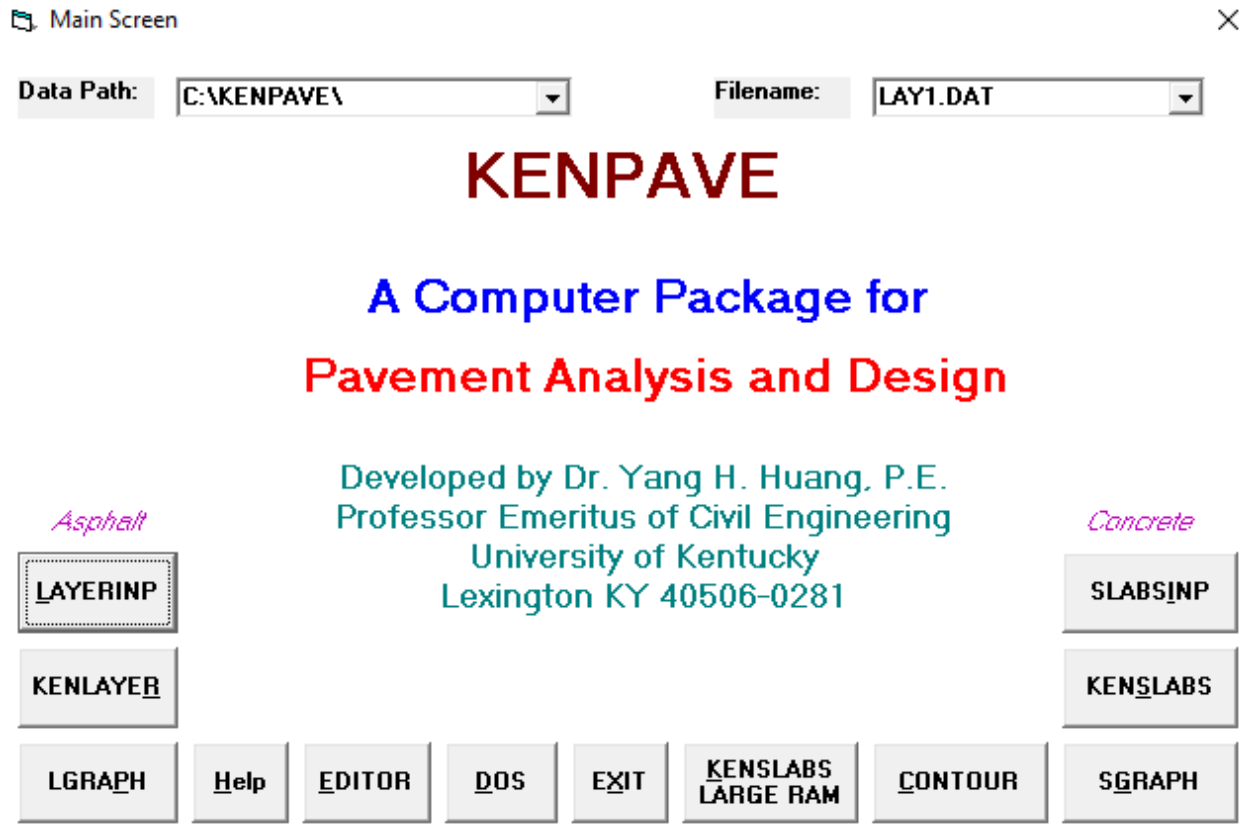


Figure 5.4: *KENPAVE* main screen.

By opening the *LAYERINP* screen, it is possible to define various parameters of the system that is being defined. Along the general parameters to be configured, this software allows to define the types of interface between two layers, via the parameter called *NBOND*. This parameter defines whether all the interfaces are fully bonded or not.

By setting  $NBOND = 1$ , the software assumes that all the layers in the system are bonded and by setting  $NBOND = 0$ , it indicates that some layers are frictionless/unbonded, which is stated in the software's instructions. If the input of *NBOND* is set to zero, it is possible to define which layers are bonded and which are frictionless (again by selecting either 0 or 1 in the *INT* parameter) to specify which are bonded and which not), as shown in Figure 5.5:

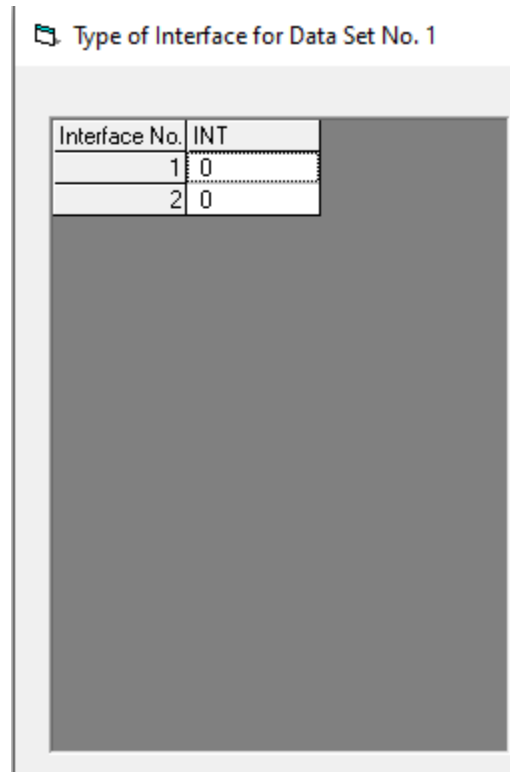


Figure 5.5: Type of Interface screen in KENPAVE.

Although this software does allow to configure the interlayer condition in the layered system, it has a binary configuration, where it either allows to set the condition to either bonded or unbonded, it does not allow to introduce any additional values. For such reason, this software does not take into account the value of the Interlayer Stiffness or any other parameter related to it that allows to characterize more precisely the interface.

However, since it is not possible to directly see how the software treats the interface condition, it is possible to review what are the differences in the results when selecting one bonding condition or the other.

### 5.3. Proposed method to calibrate the *Interlayer Stiffness K* and input in different pavement analysis software.

Once a review on the previous software was done, it was observed that, each one of them has a different procedure to calibrate the interlayer condition, ranging from binary configurations, up to some in which the interlayer reaction modulus could be directly input into the model. However, in any of them there is an indication of how this value should be calibrated or input.

For such reason, one of the scopes of this study is to provide a method on how to calibrate and input this value in various software. More specifically, how to calibrate it from results obtained by performing Leutner shear tests, in double-layered asphalt pavement specimens. The first step in such process, is derived from the study of the constitutive models and the description given in previous chapters, regarding the shear characterization purely under shear action.

Before discussing the method, it is important to remark that it focuses in the software in which a specific value can be input to characterize the bonding condition, rather than those which merely provide a binary option to define either the bonding or partial bonding in the interlayer. Said this, the software for which the method is developed, and their corresponding value to calibrate are presented in Table 5.1:

Table 5.1: Software and parameters to calibrate.

	Parameter	Units
<b>BISAR</b>	Shear Spring Compliance (AK)	m <sup>3</sup> /N
<b>EVERSTRESSFE</b>	Interface Stiffness	N/mm <sup>3</sup>

As previously discussed, BISAR treats the interlayer condition through the friction coefficient ( $\alpha$ ), and from either the shear spring compliance (AK) or the reduced shear spring compliance (ALK). In this particular case, the shear spring compliance, which is the inverse, by definition, of the interface reaction modulus, and therefore, can be also estimated by calculating the modulus and finding its inverse.

Regarding the Interface stiffness, which is the parameter used in EVERSTRESSFE, it can be observed in the previous table that it is measured in N/mm<sup>3</sup>, which is equivalent to MPa/mm, which is the unit in which the interlayer reaction modulus is calculated from the stress – displacement curves.

Now that the previous clarifications have been made, it is time to focus on the method that will be used to calibrate either of these parameters to be used in the correspondent software. In order to do so, based on the results obtained from Leutner tests, it is necessary to recall, once again, all the information that has been discussed in previous chapters, regarding the interlayer stiffness modulus.

Additionally, for the current study, a MATLAB script was written, which synthesizes the method itself and allows to perform the calculations in an automatic way, based in the whole theory here described. Such script will be also described along this section of the document, in order to provide a clearer view into the method and the written code can be found within Appendix B.

The first aspect to mention regarding the method, are the input values. From the Leutner tests, as it has been already mentioned, the raw data that it is obtained is both the measured shear load [kN], as well as the shear displacement [mm]. Another important variable that is known prior to doing any calculations, is the diameter of the specimens [mm]. Therefore, these three sets of values are the parting point for the whole process, and within the MATLAB script, are the main input values.

The other input values that are used for the script, which are introduced manually when indicated by the script, in order to initialize the calculations, are presented in Table 5.2:

Table 5.2: Prompts in the MATLAB script to initialize the calculations.

Input	Description
'Enter name of output file'	This will be the name of the output excel file
'Select a dataset to analyze'	The dataset contains the raw data obtained from the Leutner test.
'Diameter of specimen'	Measured diameter of the tested specimens.
'Which dataset to analyze'	The number of test within a category of specimen, or all tests at once.

Regarding the name of the output file, this command will name the excel file which will contain all the results that will be described later on. Regarding the prompt 'Select a dataset to analyze', the user has to choose between the options presented on screen, and the options are the categories of the subsections used in the experimental data analysis [ME\_1, ME\_2, TE\_1, TE\_2 and NT]. By selecting one of these options, the script will load the information from an Excel file in which the results for all of the three Leutner tests carried for each category are presented, both in terms of shear load [kN] and displacement [mm].

Finally, the prompt 'Which dataset to analyze', allows the user to choose between performing the analysis focusing only on the results of an individual test within a category (e.g. ME\_1\_1) or carrying the analysis in the in all of the three tests simultaneously, by selecting one of the options provided in screen. The MATLAB script will load the respective data by launching the function defined as *Load\_Dataset*, whose code is provided in Appendix B

Once that the input values have been entered, meaning the shear load [kN], the displacement [mm] and the diameter of the specimen [mm], the next step, consists in what will be defined as the first data analysis. It consists on calculating the peak shear stress [kN] by dividing the applied shear load by the area, as it has been already mentioned in previous chapters. Consequently, this will yield the data points necessary to obtain the stress – displacement curves, that will be the main tool used to calibrate the interlayer reaction modulus.

This is what precisely the function denominated as *Analyze\_Dataset* within the MATLAB script does (also presented in Appendix B). It takes the raw data obtained dataset, calculates the shear stresses related to each of the measured points, and returns the stress – displacement curves plot, alongside with the peak shear stress [MPa] and its corresponding peak displacement [mm]. As it has been observed in Chapter 4, the peak shear stress is one of the main variables that has been used to measure the effectiveness of an applied interlayer treatment. Figure 5.6 shows an example of the plots obtained by the MATLAB script, for both a single test analysis or a simultaneous analysis.

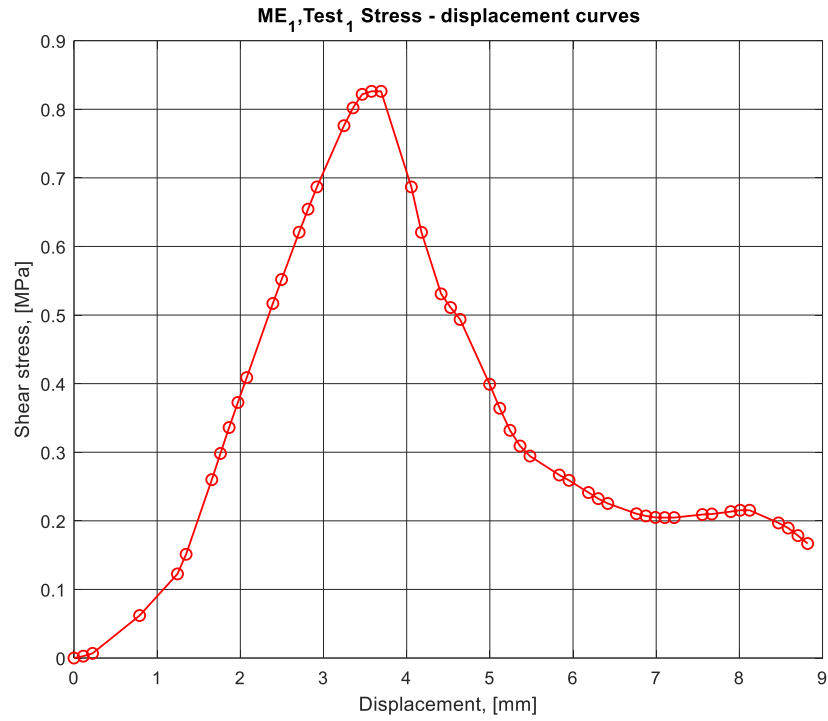


Figure 5.6(a): Stress – displacement curve plot obtained from the MATLAB script, ME\_1\_1.

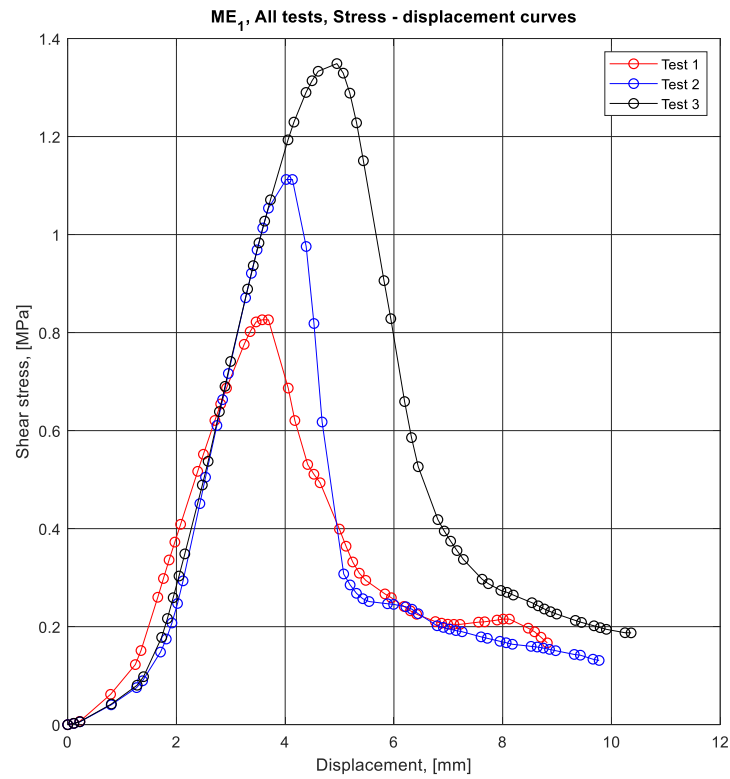


Figure 5.6(b): Stress – displacement curves plot obtained from MATLAB script, ME\_1, All tests.

These plots, alongside with the peak shear stress and its corresponding peak displacement,

calculated from the input data, will be exported into ‘Sheet 1’, of the output Excel file, which will be named according to the name given by the user into the first prompt. If a single test is selected to be analyzed, in Sheet 1 the calculated shear stress for every point measured in the Leutner test, the displacements, and the peak values can be found (alongside the stress – displacement curve).

On the other hand, if the option to analyze all tests simultaneously is selected, Sheet 1 will have the results obtained for all three tests, alongside with the computed average of the peak shear stress, which will be useful to characterize each type of specimen in terms of the shear resistance. Additionally, the three stress – displacement curves are plotted within a single figure (like in the example above).

Once this first part of the data analysis has been performed, a new prompt is given by the MATLAB script, which indicates if the user wishes to continue and perform the second analysis (user must write yes/no when prompted by the script), otherwise, the script finishes and the output will solely be comprised of the shear stress data previously described.

This second analysis, consists on processing the information obtained from the first analysis (the stress – displacement curves), in order to calculate the values of the interlayer reaction modulus. As described in Chapter 3, and also mentioned in the standard on shear bond testing the values to be calculated during this process are  $K_{max}$  and  $K$ .

By definition  $K_{max}$  is the slope of the linear portion of the stress – displacement curves, whereas  $K$  is the slope of the line that passes through the interception point of the line used to determine  $K_{max}$  with the x – axis and the point of  $\tau_{peak}$ ,  $\delta_{peak}$ .

Therefore, following this order of ideas, the first step within this second analysis, is to determine the linear portion of the curve and perform a linear regression with the data points that fall within this segment of the plot. Such linear regression, will allow to determine the equation and to draw the line in order to determine its interception with the horizontal axis, which will be the base point to determining the second line, which corresponds to  $K$ .

Once the  $K_{max}$  line’s equation has been determined, alongside with its interception with the horizontal axis, a second line must be determined. As already mentioned, this line will pass from such interception and then through  $\tau_{peak}$ ,  $\delta_{peak}$ . By determining this second line’s equation, the value of  $K$  is also determined, as the slope of this line.

The third variable that it is obtained by performing such analysis, will be the value of  $\delta_{max}$ , which is the corrected value of the maximum displacement, which will be measured between the interception of the  $K_{max}$  line with the x-axis and the  $\delta_{peak}$ , calculated during the first analysis by the MATLAB script.

In the MATLAB script, this second analysis is performed once the user types the answer ‘Yes’ to the prompt ‘Proceed to find  $K$ ’. Doing such action will launch the function defined as *Find\_K* (whose code is provided in Appendix B), which takes the results from *Analyze\_Dataset*, as well as the some of the prompts input by the user, and returns, as output, the values of  $K_{max}$ ,  $K$  and  $\delta_{max}$  alongside with the plot of the bonded segment of the curve and the two regression lines used to determine  $K_{max}$  and  $K$ .

The function *Find\_K* follows the methodology just described for the second analysis, and therefore, the first thing it does, is selecting the shear stress and displacement points that are comprised in the

bonded segment of the stress – displacement curves, in other words, it selects the points that go from  $(0,0)$  up to  $(\tau_{peak}, \delta_{peak})$ . Once the bonded segment of the curve has been defined, it is plotted by the script, which will allow to determine the linear part of the plot. In order to do so, the script allows the user to manually select the points for which the linear regression will be performed, by placing the cross in the plot shown by MATLAB and clicking over the point.

Figure 5.7 shows an example of the ME\_1\_1 bonded segment of the curve, alongside with the cross that is used to select the points, that will be used in the linear regression to find the value of  $K_{max}$ :

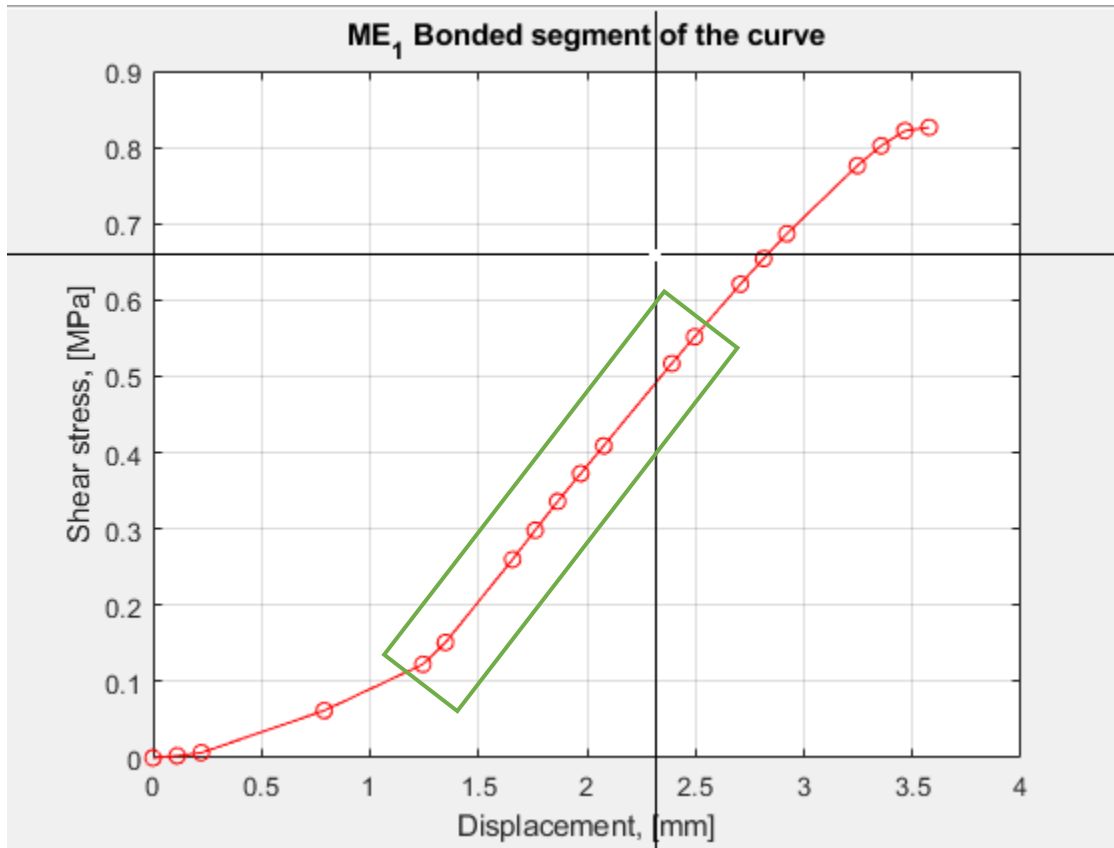


Figure 5.7: ME<sub>1</sub>\_1 bonded segment of the curve plotted by MATLAB script to select points.

As it can be observed in this figure, by plotting the bonded segment of the curve, it is possible to visually identify at least five points (as highlighted by the green box in the figure) that fall within the linear portion of the bonded segment. From this plot, the script requires the user to select five points, and the suggestion is to do so by distributing the five selections as evenly as possible through the linear segment, in order to obtain an accurate linear regression of such portion.

It is important to mention that, in order to avoid errors while selecting the points, the script automatically approximates the values clicked by the user (what the script does is extract the cartesian coordinates in which the user clicked), to the closest point of the measured data. This ensures that when the linear regression is performed, it does it with the measured points that fall in the linear segment.

Once the user has selected the five points in the linear part of the bonded segment of the curve, the script proceeds to perform a linear regression with such data. The linear regression, considers the

displacement as the dependent value whereas the shear stress is considered as the independent value. Therefore, it will yield the typical linear equation shown in Equation (5.6), which can be interpreted in the terms of this analysis as shown in Equation (5.7):

$$y(x) = ax + b \quad (5.6)$$

$$\tau(\delta) = K_{max} \cdot \delta + b \quad (5.7)$$

As it can be observed, the dependent variable of the linear equation will be accompanied by its coefficient (slope), that will be  $K_{max}$ , whereas  $b$  represents the interception of this line with the y-axis. Additionally, by calculating this line's equation, it is possible to plot it in the same figure of the bonded segment of the curve. Figure 5.8 shows the  $K_{max}$  regression line plotted along with the bonded segment of the curve for ME\_1\_1, whereas Table 5.3 shows the results of the linear regression performed to the five, evenly-distributed points selected by the user:

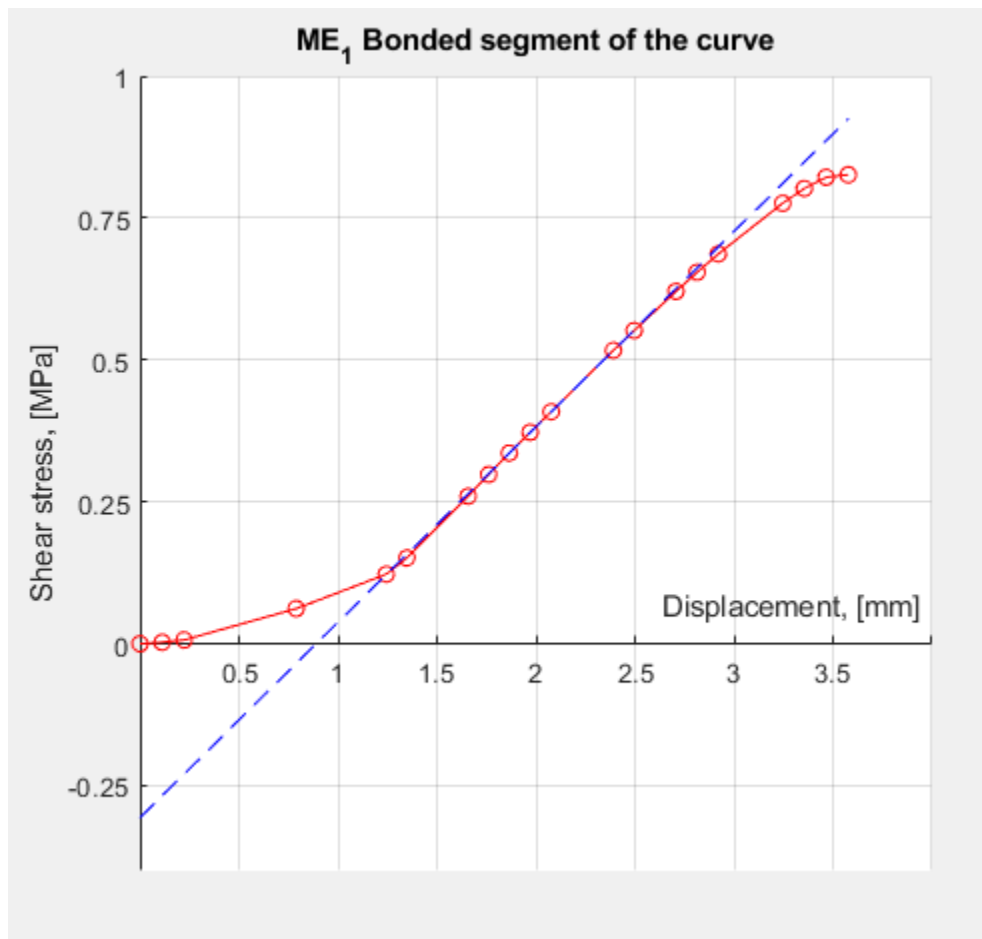


Figure 5.8:  $K_{max}$  line plotted over the bonded segment of the curve.

Table 5.3: Results of the linear regression on the selected points.

	Estimate
Intercept [MPa]	-0.30614
$K_{max}$ [Mpa/mm]	0.34412
$R^2$	1

In the previous figure, it can be observed that, visually, the five selected points, evenly-distributed along the linear part of the curve, generate an accurate result, as the  $K_{max}$  line seems to perfectly fit this linear segment. This can be further corroborated by observing the results of the linear regression performed by the MATLAB script, where the value of the coefficient of determination ( $R^2$ ) is equal to 1, which is an indicator of a good fit of the regression line with the measured data.

In the analysis performed for the other sets of data, similar results in terms of the coefficient of determination are obtained, which shows that the method of manually selecting the points to perform the regression of the linear part of the curve yields accurate results.

Once  $K_{max}$  has been determined by following this procedure, and the correspondent linear equation is found, in order to make the plot, the next steps are focused on finding the value of  $K$  and  $\delta_{max}$ . To determine both of these values, it is necessary to obtain the coordinates at which the  $K_{max}$  line intercepts with the x-axis. The MATLAB script determines this value by solving Equation (5.8) for  $\delta$ :

$$0 = K_{max}\delta + b \quad (5.8)$$

The solution for this equation, in terms of the displacement, will yield the displacement value for the line when the shear stress is equal to zero. For this purpose, this value will be defined as  $\delta_0$ . Then, once this value has been determined, the other two main output values of the *Find\_K* function can be calculated. Firstly,  $\delta_{max}$  is calculated, according to its definition as shown by Equation (5.9):

$$\delta_{max} = \delta_{peak} - \delta_0 \quad (5.9)$$

At the same time, it is possible to define a line, that passes through two points of coordinates; the first is  $(\delta_0, 0)$  while the second will be  $(\tau_{peak}, \delta_{peak})$ . The lineal equation is calculated, in order to determine  $K$  (will be the slope of this line), and also to plot this line within the same graphic as the bonded segment of the curve and the  $K_{max}$  line. Figure 5.9 shows the previously described plot, which is also one of the outputs of the *Find\_K* function:

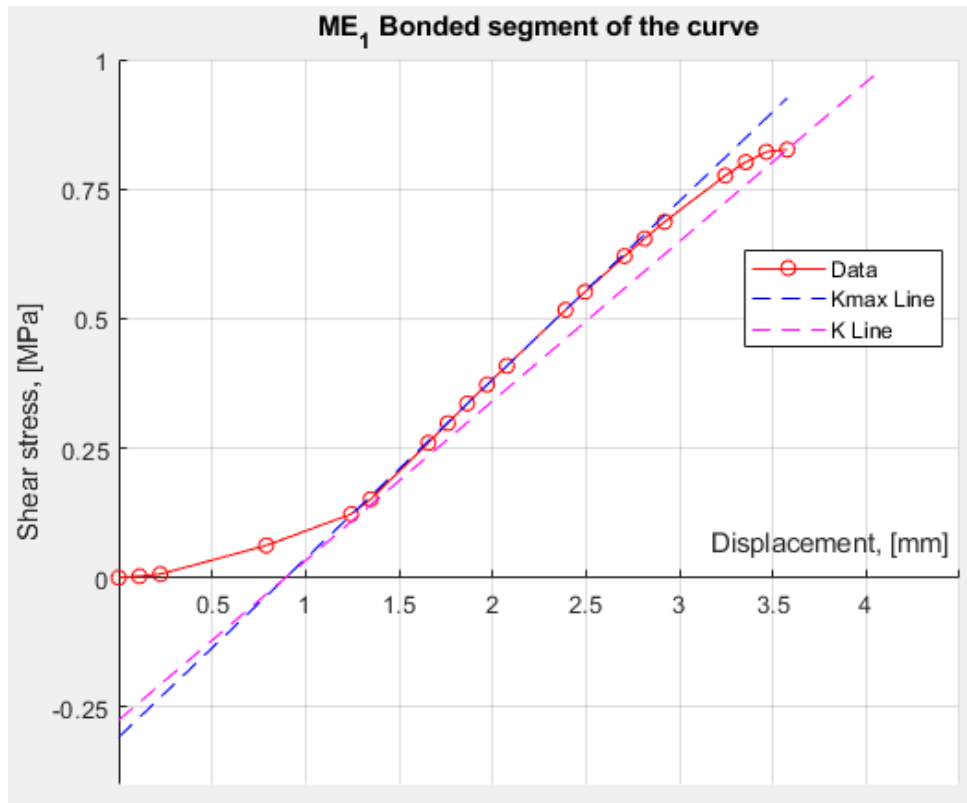


Figure 5.9: Bonded segment of the curve, Kmax and K lines, ME\_1\_1.

Once these calculations have been performed by the MATLAB script, the values of  $K_{max}$ ,  $K$  and  $\delta_{max}$  will be reported in ‘Sheet 2’ of the output Excel file, alongside with the plot of both lines and the bonded segment of the curve. It is important to remark that if in previous steps the user prompts the option ‘All\_Tests’, to perform the analysis on all three tests simultaneously, the whole process done by the function *Find\_K*, will be done for the results of each test, one by one, first for Test\_1, then for Test\_2 and finally for Test\_3. The output file will contain the three different plots, alongside with the values of  $K_{max}$ ,  $K$  and  $\delta_{max}$  for each one. Additionally, in the output file, an average value for both of the calculated values of the interlayer reaction modulus is given, to provide a characteristic value for the analyzed category of specimens.

As it can be observed, the provided MATLAB script allows, not only two values for the interlayer reaction modulus, but also it provides a tool that allows to analyze results obtained from the Leutner test, in terms of the plots obtained and in terms of the peak shear stress and corresponding displacement. As an additional comment, it is worth mentioning that, although such script was developed specifically for results obtained from Leutner test, it can analyze datasets obtained by other tests designed to test the bonding or the shear response of the interlayer, that yield measurements in terms of shear stress (or shear load) versus shear displacement.

This whole process, as mentioned before, is based on the information provided by the constitutive models, as well as what is stated in the standard regarding the shear bond testing. Within the output of the MATLAB script, the values that are required to be calculated by such standard are determined, up to this point, a definite value for the interlayer shear stiffness to select and input into the asphalt pavement design/modelling software has not been defined yet. The next sub-section

of this document will discuss which of the interlayer reaction modulus determined by the script should be used in software.

### 5.3.1. Difference between considering $K_{max}$ and $K$ .

In the beginning of the previous segment, the parameters that must be introduced in the software were summarized. In one case, the value is the same interlayer reaction modulus (EVERSTRESSFE), whereas in the other case, the inverse value of the modulus must be introduced in order to allow BISAR to make the respective calculations. The script previously describes yields two values for the modulus, as it was developed following what has been established by the shear bond testing standard, however, a unique value between these two must be chosen to be input.

As already commented in Chapter 3, the constitutive equation that rules the interlayer shear behavior, when analyzed solely under shear loading, proposes a linear relationship between the shear stress and the shear displacement. To recall, Equation (5.10) shows Goodman's constitutive equation, which is the base of the following analysis:

$$\tau = K\delta \quad (5.10)$$

In order to do so, an analysis on the  $K_{max}$ , and  $K$  was done. Firstly,  $K_{max}$  is the slope of the line that passes through the linear portion of the stress – displacement curve. As mentioned in previous studies, the initial stage of the curve (before the lineal segment), of variable length happens at the beginning of the test and it is associated with an adjustment of the sample to the testing apparatus and should not be taken into account in the characterization of the interlayer (Szydło and Malicki, 2016).

The same study additionally mentions that, by performing the linear regression of the points located within the linear segment of the curve and extending such line to the x-axis, this initial stage, which should not be taken into account is eliminated (and for such reason  $\delta_{max}$  is also calculated).

By calculating the interlayer reaction modulus as the slope of the linear part of the displacement curves, it is ensured that the behavior along such segment is stable and as it can be observed in the results of performing the analysis to find the  $K$  values, the linear segment covers a majority of the measured points. Take for example Figure 5.10, which refers to the results obtained for ME\_1\_1, and by selecting  $K_{max}$  as the modulus:

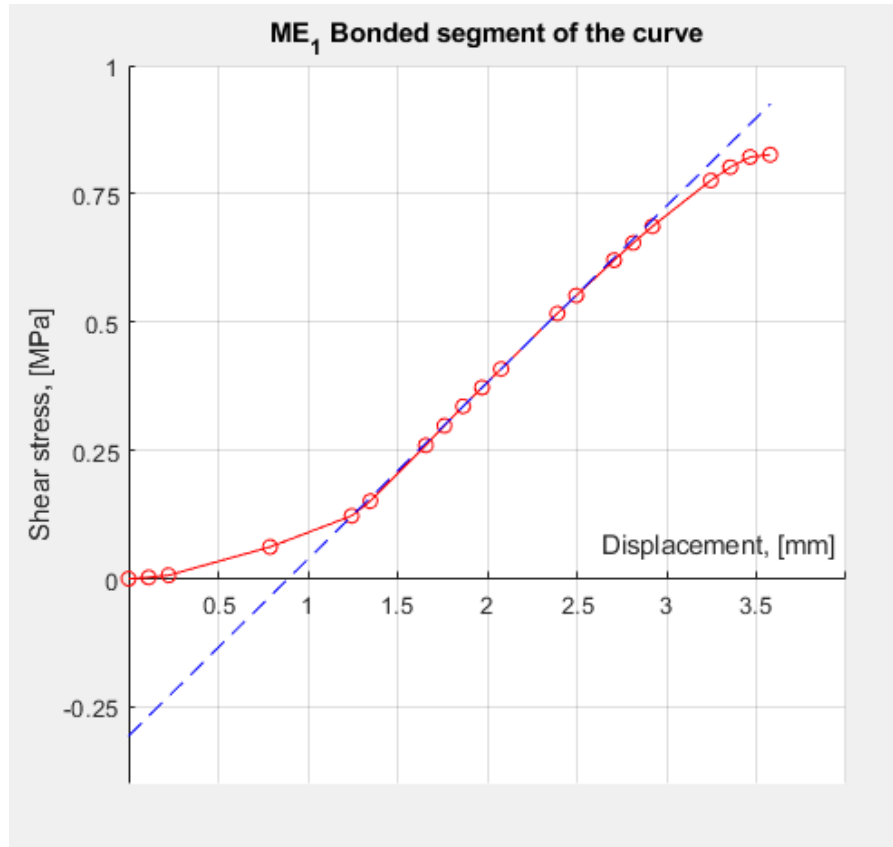


Figure 5.10: Bonded segment of the curve,  $K_{max}$  line, ME\_1\_1.

In this case, it can be observed that the linear segment of the plot goes from the fifth measured point, up to the fourteenth point. In terms of the shear stress range, which goes from zero up to the value of peak shear stress (0.826 MPa/mm), the linear part of this graph constitutes around 65% of the total range of shear stress values. In most of the cases, it occurs that the linear segment covers a majority of the shear stress range values. This percentage increases, since by doing the linear regression, the initial stage is eliminated, and therefore it covers values from 0 MPa, up to the last point in the lineal segment.

Another observation to make is that, due to the previous commented fact, this linear regression simulates more closely the stress – displacement curve that the line that goes from  $\delta_0$  to  $\tau_{peak}$ . By selecting  $K_{max}$ , the shear stress will be calculated according to Equation (5.11) (according to Goodman's constitutive law:

$$\tau = K_{max}\delta \quad (5.11)$$

From this equation, it can be noted that,  $\tau = 0$  when  $\delta = \delta_0$ , and for such reason  $\delta_{max}$  must be calculated, and thus it must be taken into account that the displacement related to the initial stage of the test has not been considered. When the evaluated  $\delta$  is within the lineal segment of the curve, the results of Equation **Error! Reference source not found.** converge to the calculated stress – displacement curve, result of the Leutner test measurements.

However, as  $\delta$  is evaluated after the lineal segment is passed, the results from Equation **Error!**

**Reference source not found.** begin to diverge from the stress – displacement curve, and as  $\delta$  is increased, this difference will also increase. Finally, for such reason when Equation (5.11) is evaluated at  $\delta = \delta_{peak}$ , the highest difference between the curve and the computed results is reached.

On the other hand, there is the possibility to select  $K$  as the value to input into the software. An example of such situation can be observed in Figure 5.11 **Error! Reference source not found.**, where the  $K$  line and the bonded segment of the curve of ME\_1\_1 is shown:

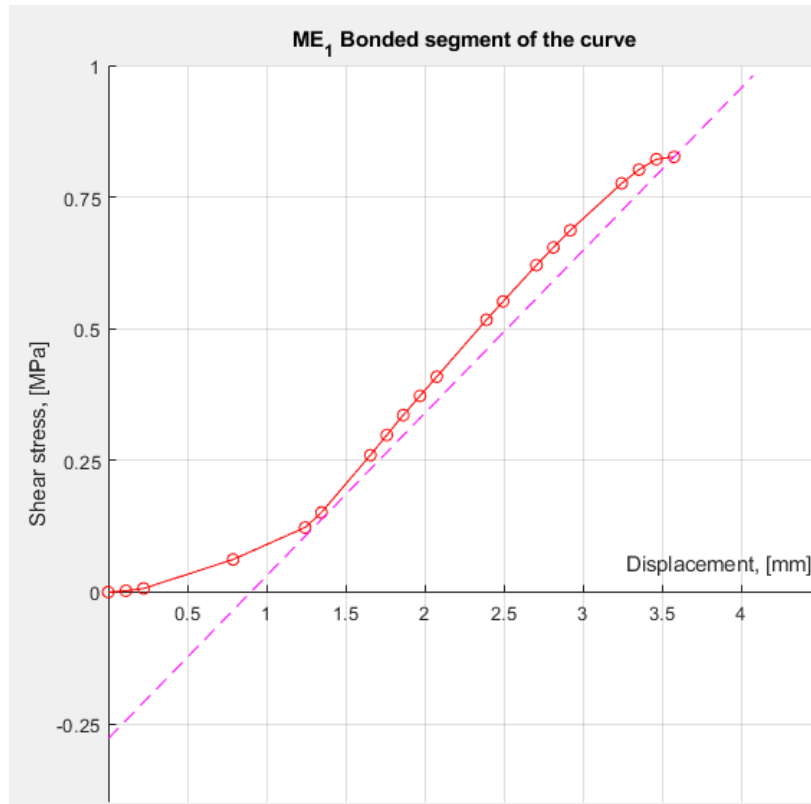


Figure 5.11: ME\_1\_1 Bonded segment of the curve and K line.

From the previous figure, it can be visually observed that the percentage of values of the shear stress for which the results of the Equation **Error! Reference source not found.** converge to those of the curves, along the total range are lower than in the case of Figure 5.10.

By selecting  $K$  as the modulus, Goodman’s constitutive equation will be as described by Equation (5.12)

$$\tau = K\delta \tag{5.12}$$

Once again, when  $\delta = \delta_0$ ,  $\tau = 0$ , since, by definition,  $K$  is the slope of the line that passes through  $(\delta_0, 0)$  and  $(\tau_{peak}, \delta_{peak})$ . As  $\delta$  increases, the results of Equation (5.12) diverge from the calculated stress – displacement curve, until the equation is evaluated at  $\delta = \delta_{peak}$ . At this point, the results from Equation (5.12) converge with the last point of the bonded segment of the curve.

Following this analysis of the two possible options to select/input into software, it is possible to

state that,  $K_{max}$  is the most adequate of them to describe the bonding condition of a given type of specimen. By selecting this value, the results of Goodman's constitutive equation approximate more closely to the stress – displacement curve than the  $K$  line does.

For such reason, when calibrating the input value for the software that allow to define the interlayer shear stiffness (taking into account also BISAR that uses  $AK$ , which is the inverse of the modulus), based on the results obtained from a Leutner shear test, the value that should be used is  $K_{max}$ .

Given the fact that, usually more than one test is carried out on every type of specimen's configuration, a characteristic value of  $K_{max}$  should be calculated, as this will be the value that will represent the bonding condition for a given type of specimen. This characteristic value, will be defined as  $K_{max,avg}$ , as it will be the mean value of the  $K_{max}$  calculated for each test performed on a given type of specimen.

Therefore, to summarize up to this point, the value that will be input into the software, is found by calculating the  $K_{max}$  for every single Leutner test performed on a given type of specimen, and then, calculating the mean value for the total of tests. By doing so, the characteristic interlayer reaction modulus is found for a given type of specimen, and this value can be input into the software. In the case of the software analyzed during this study, the input values are summarized by Table 5.4:

Table 5.4: Input values in the analyzed software.

	Parameter	Input value	Units
<b>BISAR</b>	Shear Spring Compliance (AK)	$\frac{1}{K_{max,avg}}$	mm/MPa
<b>EVERSTRESSFE</b>	Interface Stiffness	$K_{max,avg}$	N/mm <sup>3</sup>

It is important to take into account that, for a general or first approach, the suggested value to use is  $K_{max,avg}$ , as this is the value that, for most of the values (of shear stress/displacement), approximates more closely to the measured stress – displacement curve. However, as it was previously mentioned during the analysis, after the lineal segment of the curve, the results of Goodman's constitutive equation start to diverge from those of the curve. This difference increases as the evaluated  $\delta$  approaches  $\delta_{peak}$ , and at this final value, this difference reaches its highest value.

#### 5.4. Interlayer reaction modulus effect on asphalt pavement modelling.

In order to observe the real impact of the proper calibration of the parameters that define the interlayer bonding condition on the modelling and design of asphalt pavements, the previously discussed results were used to develop and analyze a model in both BISAR 3.0 and EVERSTRESSFE.

Before entering into the details regarding the models, it is important to make some comments on both of the software. Although in both of them it is possible to define vertical loads, only BISAR 3.0 allows to define horizontal loads. This generates a big impact when analyzing the interlayers

through modelling, given the fact that the shear stresses that mostly affect them, come mostly from the acceleration/braking of vehicles.

Additionally, the Leutner test consists simply in the measurement of the shear load and displacement. While in EVERSTRESS only vertical loads can be defined, which means that the situation differs from that of the Leutner test, the ability of BISAR to input horizontal loads allows to make a better connection with the test. For such reason, the first model was performed in BISAR 3.0.

#### 5.4.1. Modelling in BISAR 3.0

The model defined in BISAR consists of a two-layered system, in order to approach as much as possible the test conditions, as it can be observed in Figure 5.12, where the geometric and layer characteristics used in BISAR are shown:

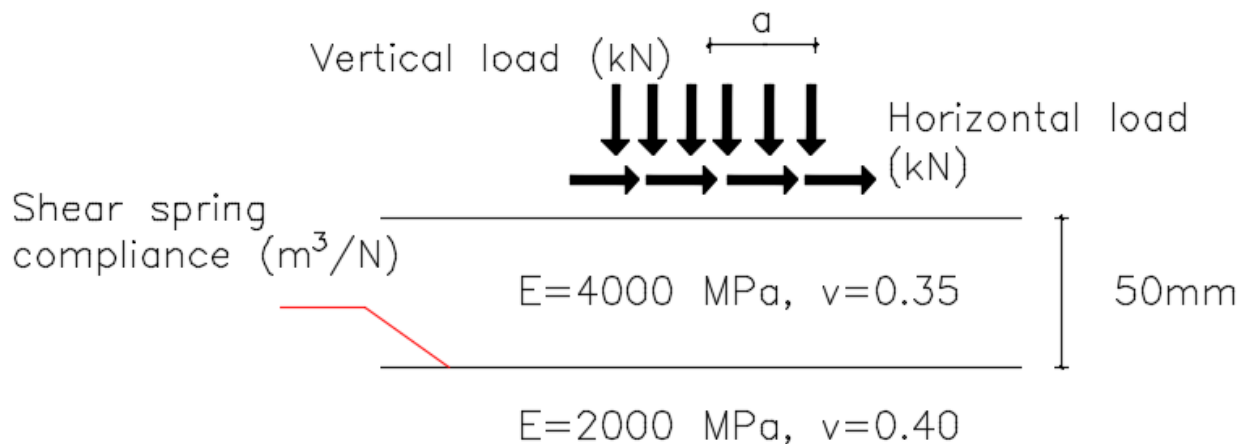


Figure 5.12: Scheme of the modelled pavement section in BISAR 3.0

Where  $a$  is the radius of the contact area, which was set equal to the radius of a single tire of the standard axle configuration, equal to (0.107 m). The values of the elasticity modulus of the layers corresponds to the modulus of the measured cores.

For the previous model, various scenarios were run, in order to assess the impact of the interlayer reaction modulus on the asphalt pavement modelling and design. The parameters that were studied were: Shear load, the shear spring compliance (used to characterize the interlayer bonding condition) and finally, some scenarios with the presence of vertical loads were run, in order to make some comparisons with the model of EVERSTRESSFE that will be discussed later.

In the case of the shear load, two values were defined: 1kN and 20kN. Firstly, the value of 1 kN was selected, as it is in the order of magnitude of the measured shear loads in the experimental part. On the other hand, the load of a single tire configuration of a standard axle is equal to 40kN (Kim *et al.*, 2015). However, various authors have stated that the magnitude of the horizontal load is determined as the vertical load multiplied by the friction coefficient between tire – pavement. In this case, the friction coefficient was set as 0.5, and therefore, the horizontal load corresponding to this configuration is of 20 kN. The value of 40 kN of the vertical load will be also used to study

the effects in terms of vertical loading.

In the case of the shear spring compliance, the values that were analyzed were those obtained for all the types of cores that were measured through the Leutner test plus the fully bonded and the fully debonded interlayer conditions. By recalling the interlayer reaction modulus (MPa/mm) from the measured data obtained in Chapter 4, it is possible to find the corresponding input values in terms of the shear spring compliance ( $\text{m}^3/\text{N}$ ) for both  $K_{max}$  and  $K$ , which are shown in Table 5.5: Interlayer reaction modulus (MPa/mm) to shear spring compliance ( $\text{m}^3/\text{N}$ ) conversion.

Table 5.5: Interlayer reaction modulus (MPa/mm) to shear spring compliance ( $\text{m}^3/\text{N}$ ) conversion.

	$K_{max}$ [MPa/mm]	BISAR [ $\text{m}^3/\text{N}$ ]	$K$ [MPa/mm]	BISAR [ $\text{m}^3/\text{N}$ ]
ME_1	0.436	2.29E-09	0.372	2.69E-09
ME_2	0.338	2.96E-09	0.292	3.42E-09
TE_1	0.474	2.11E-09	0.455	2.20E-09
TE_2	0.421	2.38E-09	0.306	3.27E-09
NT	0.259	3.86E-09	0.243	4.12E-09

Given the fact that the shear spring compliance  $AK$  is defined as the inverse value of the interlayer reaction modulus, and the measuring units are of a different order of magnitude, the resulting shear spring compliance is of the order of magnitude of  $1 \times 10^{-9} \text{ m}^3/\text{N}$  for all the types of cores. By recalling the limits proposed by previous authors for the interlayer reaction modulus (Canestrari *et al.*, 2013), discussed in Chapter 3 it is possible to define the same boundaries in terms of the shear spring compliance. Table 5.6 shows the boundary values of the shear spring compliance that defines the three possible bonding conditions:

Table 5.6: Interlayer bonding condition boundary limits in terms of the shear spring compliance

Interlayer bonding condition	
Shear spring compliance	Description
$AK \leq 10^{-11} \text{ m}^3/\text{N}$	Full bonding
$10^{-11} \text{ m}^3/\text{N} < AK < 10^{-7} \text{ m}^3/\text{N}$	Partial bonding
$AK \geq 10^{-7} \text{ m}^3/\text{N}$	Complete debonding

By taking a look at the limiting values, and those obtained from the measured data, it can be observed that the shear spring compliance of all the types of cores are in the partial bonding condition, just as expected.

The fully bonded condition can be defined directly in the software, as already discussed earlier in this chapter, simply by selecting the option to consider ‘Full friction between layers’ and finally, to evaluate the fully debonded condition, the shear spring compliance is defined as  $1 \text{ m}^3/\text{N}$ , as this value falls within the range of complete debonding defined in the previous table.

Since BISAR allows to run at once multiple scenarios, which within the program are defined as ‘Systems’, the first set of scenarios that were run, were those in which there is the presence of an horizontal load equal to 1 kN, while the vertical load was defined equal to 0.001 kN (the software

does not allow to set the vertical load equal to zero), in order to study the response of the modelled pavement in loading conditions as close as possible to those found while performing the Leutner test. The results, shown in Table 5.7 were evaluated in terms of displacement at the interlayer, for all core types and in the fully bonded/ fully debonded condition.

Table 5.7: BISAR results for a horizontal load equal to 1 kN.

T= 1 kN					
Core type	Interlayer condition	Position	$\delta(\text{mm})$	$\Delta\delta$ (mm)	$\tau_{\text{calc}}$ (MPa)
ME_1	K <sub>max</sub>	Upper	2.761E-03	2.300E-03	1.003E-03
		Lower	4.614E-04		
	K	Upper	2.852E-03	2.418E-03	9.006E-04
		Lower	4.337E-04		
ME_2	K <sub>max</sub>	Upper	2.906E-03	2.488E-03	8.413E-04
		Lower	4.178E-04		
	K	Upper	2.990E-03	2.596E-03	7.590E-04
		Lower	3.945E-04		
TE_1	K <sub>max</sub>	Upper	2.716E-03	2.240E-03	1.061E-03
		Lower	4.760E-04		
	K	Upper	2.739E-03	2.271E-03	1.034E-03
		Lower	4.685E-04		
TE_2	K <sub>max</sub>	Upper	2.783E-03	2.328E-03	9.801E-04
		Lower	4.547E-04		
	K	Upper	2.964E-03	2.562E-03	7.830E-04
		Lower	4.016E-04		
NT	K <sub>max</sub>	Upper	3.061E-03	2.685E-03	6.948E-04
		Lower	3.758E-04		
	K	Upper	3.100E-03	2.734E-03	6.635E-04
		Lower	3.660E-04		
Fully bonded		Upper	1.290E-03	0.000E+00	
		Lower	1.290E-03		
Fully debonded		Upper	6.027E-03	5.972E-03	
		Lower	5.454E-05		

As it can be observed, the results were calculated at the depth of the interlayer, and by measuring the displacement just before and right after the interlayer, in order to determine the relative displacement between layers. Additionally, the shear stress was calculated by using Goodman's constitutive equation.

Firstly, it can be observed that in all cases, the upper layer has greater displacements than the lower layers (except for the fully bonded situation). This is due to the effect of slippage, as the partial bonding between layers generates a discontinuity at the interlayer level. On the other hand, in the fully bonded situation not only the relative displacement is zero, as expected, but also, the measured

displacement was smaller than in the other cases.

By comparing the use of either  $K_{max}$  or  $K$ , it can be observed, for all cores, that the relative displacements obtained in the case of the maximum interlayer reaction modulus were smaller than those obtained by using just  $K$ . This has a direct connection with the definition of the shear spring compliance (defined as the inverse of the reaction modulus). As  $K_{max}$  are always higher values than  $K$ , it is expected that the shear spring compliance for  $K_{max}$  is smaller than that of  $K$ . Finally, a smaller shear spring compliance, means smaller deformations for the same applied load.

Although the characteristics of the modelled system are as close as possible as those found in the Leutner test, it can be observed that the calculated shear stress in the interlayer are of the order of  $10^{-4}$  -  $10^{-3}$  MPa. By comparing these values with those obtained from the Leutner tests in Chapter 4, it can be observed that these values are located in the very initial part of the bonded segment of the curve and do not even get close to the peak shear stresses from the measured data. However, this was expected, as in the case of the Leutner test, the shear load is applied at the interlayer, while in the modelling case, the shear load is applied at the surface, and the depth of the interlayer affect the shear stresses obtained.

Then, the second set of systems that were analyzed in BISAR consisted once again in the same interlayer bonding conditions that were defined in the previous case, but with the presence of a higher horizontal load (20 kN). Table 5.8 shows the results of the displacements at the interlayer, calculated by BISAR and the shear stress calculated by using Goodman's constitutive equation.

Table 5.8: BISAR results for a horizontal load equal to 20 kN.

T= 20 kN					
Core type	Interlayer condition	Position	$\delta$ (mm)	$\Delta\delta$ (mm)	$\tau_{calc}$ (MPa)
ME_1	$K_{max}$	Upper	5.514E-02	4.588E-02	2.002E-02
		Lower	9.256E-03		
	K	Upper	5.695E-02	4.825E-02	1.797E-02
		Lower	8.701E-03		
ME_2	$K_{max}$	Upper	5.804E-02	4.966E-02	1.679E-02
		Lower	8.383E-03		
	K	Upper	5.971E-02	5.179E-02	1.514E-02
		Lower	7.918E-03		
TE_1	$K_{max}$	Upper	5.423E-02	4.468E-02	2.117E-02
		Lower	9.547E-03		
	K	Upper	5.469E-02	4.529E-02	2.062E-02
		Lower	9.398E-03		
TE_2	$K_{max}$	Upper	5.557E-02	4.645E-02	1.955E-02
		Lower	9.121E-03		
	K	Upper	5.919E-02	5.113E-02	1.562E-02
		Lower	8.060E-03		
NT	$K_{max}$	Upper	6.113E-02	5.359E-02	1.387E-02
		Lower	7.543E-03		
	K	Upper	6.191E-02	5.456E-02	1.324E-02

		Lower	7.347E-03		
<b>Fully bonded</b>		Upper	2.567E-02	0.000E+00	
		Lower	2.567E-02		
<b>Fully debonded</b>		Upper	1.205E-01	1.194E-01	
		Lower	1.121E-03		

When increasing the horizontal load, it can be observed that the observations done for the case of the horizontal load equal to 1 kN still hold. For the maximum interlayer reaction modulus, the relative displacements are lower than for *K*, and in terms of the shear stress, the opposite relation is obtained. It can be observed that, as expected there is a linear increase between the data obtained for both values of the horizontal load. Additionally, it can be observed that, although the magnitude of the horizontal load was twenty times that of the first case, both the relative displacements and the shear stresses are far from reaching the peak values obtained from the experimental data. For such reason, these values keep falling on the very beginning of the bonded segment of the curve.

Finally, for comparing purposes with EVERSTRESSFE, which only allows the configuration of vertical loads, a set of systems characterized by the same interlayer bonding conditions as the previous two but only in the presence of vertical load, equal to 40 kN was also modeled. Table 5.9 shows the results obtained, once again, in terms of the relative displacements and shear stress.

Table 5.9: BISAR results for a vertical load equal to 40 kN

<b>P= 40 kN</b>					
<b>Core type</b>	<b>Interlayer condition</b>	<b>Position</b>	<b>δ(mm)</b>	<b>Δδ (mm)</b>	<b>τ<sub>calc</sub> (MPa)</b>
<b>ME_1</b>	<b>K<sub>max</sub></b>	Upper	1.783E-02	2.351E-02	1.025E-02
		Lower	-5.679E-03		
	<b>K</b>	Upper	1.792E-02	2.370E-02	8.825E-03
		Lower	-5.778E-03		
<b>ME_2</b>	<b>K<sub>max</sub></b>	Upper	1.796E-02	2.379E-02	8.044E-03
		Lower	-5.830E-03		
	<b>K</b>	Upper	1.803E-02	2.393E-02	6.998E-03
		Lower	-5.901E-03		
<b>TE_1</b>	<b>K<sub>max</sub></b>	Upper	1.778E-02	2.340E-02	1.109E-02
		Lower	-5.624E-03		
	<b>K</b>	Upper	1.781E-02	2.346E-02	1.068E-02
		Lower	-5.653E-03		
<b>TE_2</b>	<b>K<sub>max</sub></b>	Upper	1.785E-02	2.355E-02	9.915E-03
		Lower	-5.704E-03		
	<b>K</b>	Upper	1.801E-02	2.389E-02	7.300E-03
		Lower	-5.880E-03		
<b>NT</b>	<b>K<sub>max</sub></b>	Upper	1.807E-02	2.402E-02	6.217E-03
		Lower	-5.954E-03		
	<b>K</b>	Upper	1.810E-02	2.408E-02	5.844E-03

		Lower	-5.981E-03		
<b>Fully bonded</b>		Upper	7.930E-03	0.000E+00	
		Lower	7.930E-03		
<b>Fully debonded</b>		Upper	1.851E-02	1.211E-02	
		Lower	6.398E-03		

Even with just the presence of a vertical load and no horizontal load, the previously commented relations hold within the results. The relative displacements were higher when using  $K$  instead of  $K_{max}$  while the opposite relation is observed in the calculated value of the shear stress. For this value of vertical load, the order of magnitude of the results is higher than that of when just using a horizontal load of 1 kN, but still, are located within the very initial part of the bonded segment of the curve. Additionally, it can be observed that when studying only the presence of a normal load, the difference between the obtained results is only significant when passing from the partially bonded condition to the fully bonded and fully debonded conditions.

From this BISAR analysis, it is possible to observe the importance of selecting a proper value of the interlayer reaction modulus (to calculate the shear spring compliance). Firstly, the partial bonding condition range goes from  $10^{-11}$  to  $10^{-7}$  m<sup>3</sup>/N, which indicates that the values of the shear spring compliance may vary along four orders of magnitude. However, from the experimental data analyzed, for all types of cores, the calculated reaction modulus (and therefore shear spring compliance) were all of the same order of magnitude. With these measured values of shear spring compliance, it can be observed that the results are sensitive to small differences between the defined values to input in the software. Therefore, it shows the importance of selecting a proper value, within the right order of magnitude in order to properly model the interface, rather than just selecting an arbitrary value within the given range of values of the partially bonded condition.

Secondly, once again, it is important to discuss the difference between the values obtained when selecting  $K_{max}$  or  $K$  while characterizing a given type of interlayer. When using  $K_{max}$ , lower displacements were found, whereas the shear stresses were higher than when using  $K$ . Therefore, by selecting  $K_{max}$ , it is assured that the design/modelling stays on the conservative side.

#### 5.4.2. Modelling in EVERSTRESSFE

As mentioned before, EVERSTRESSFE has the disadvantage, in this case, that it only allows the definition of vertical loads. However, to analyze how the selection of the proper value of the interlayer reaction modulus, a model, with similar specifications to the one performed in BISAR was done. The number of layers and their characteristics were kept the same as before, but EVERSTRESSFE allows to define a finite domain, and in an attempt to resemble the Leutner test situation, the dimensions of the studied pavement were set at the minimum length possible. Table 5.10 shows the layers specifications defined for the model in EVERSTRESSFE, while Figure 5.13 shows the modelled pavement section:

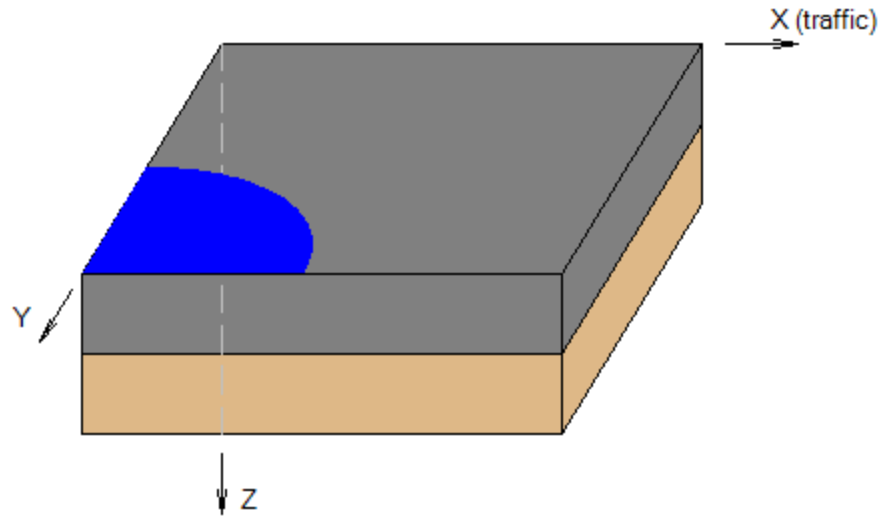


Figure 5.13: Modelled pavement section on EVERSTRESSFE.

Table 5.10: Layer specifications for model in EVERSTRESSFE

Surface course		Binder course	
Thickness (mm)	50	Thickness (mm)	50
E (MPa)	4000	E (MPa)	2000
$\nu$	0.35	$\nu$	0.4
Geometric properties		Boundaries	
Length x (mm)	300	Minimum value	Model Finite Domain
Length y (mm)	300	Minimum value	

The boundaries were defined as ‘Model Finite Domain’, given the fact that, within the software’s help guide, the authors suggested this value in order to simulate lab conditions. On the other hand, the loads were defined with the same parameters, a vertical load of 40 kN, loading in a circular area, on a single tire configuration of the single axle. In order to assess the results, the evaluating point was set at the edge of the loaded area, as previous studies have shown that at this point, is where the shear effect is more critical.

In this case, the parameter that varied was the interlayer condition and consecutively, the interlayer stiffness ( $N/mm^3$ ), which is the parameter used by EVERSTRESSFE to define the bonding condition. For this software, as it allows only the definition of vertical load, only the  $K_{max}$  value and  $K$  value for the ME\_1 cores was studied. Additionally, to define the boundary values that define the three different conditions was assessed, by performing a sensitivity analysis regarding the interlayer stiffness value. It is important to comment that this software, is a finite element analysis software, that only yields results in terms of graphs.

By comparing the results obtained by configuring the interlayer stiffness equal to  $K_{max}$  and  $K$ , in terms of the relative displacement and shear strains, shown by Figure 5.14, it is possible to observe that both in terms of displacements and strain the results are very similar.

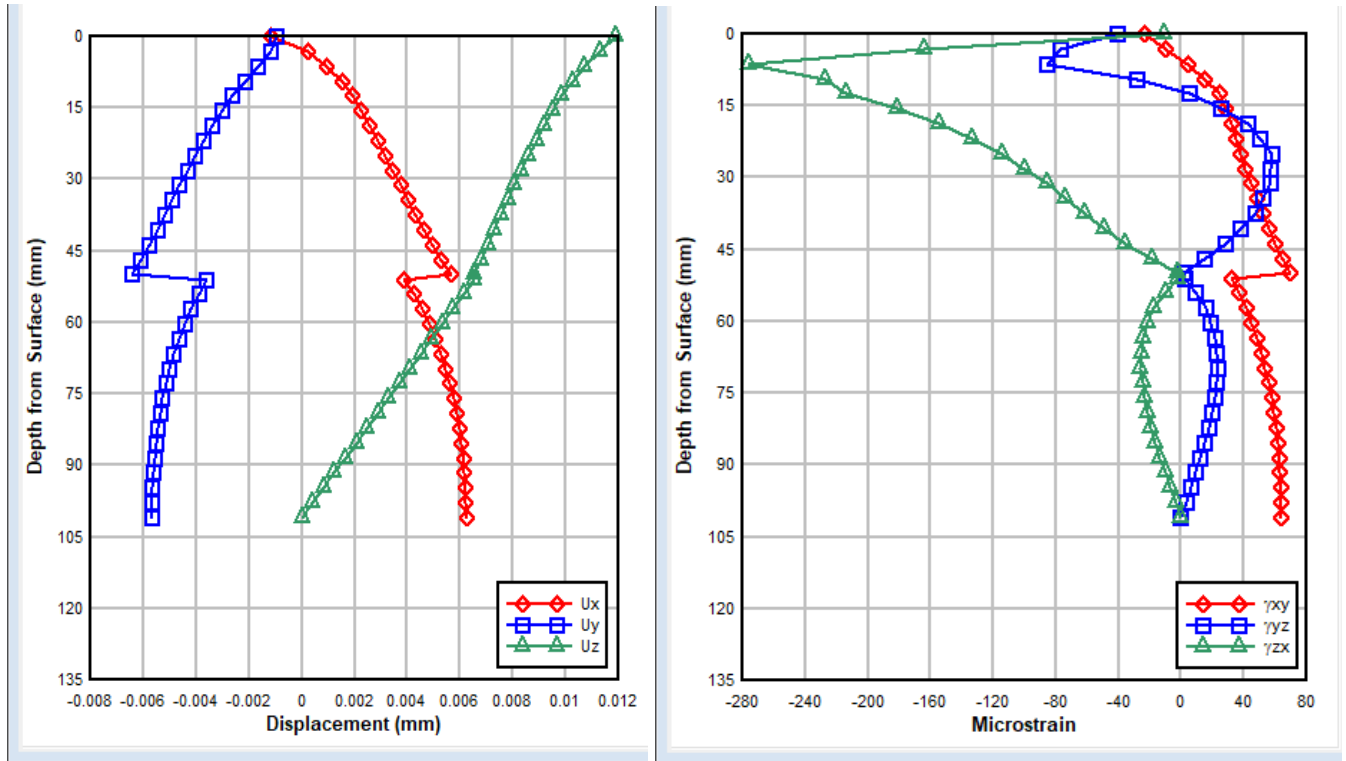


Figure 5.14 (a): Displacements and strains obtained for  $K_{max}$

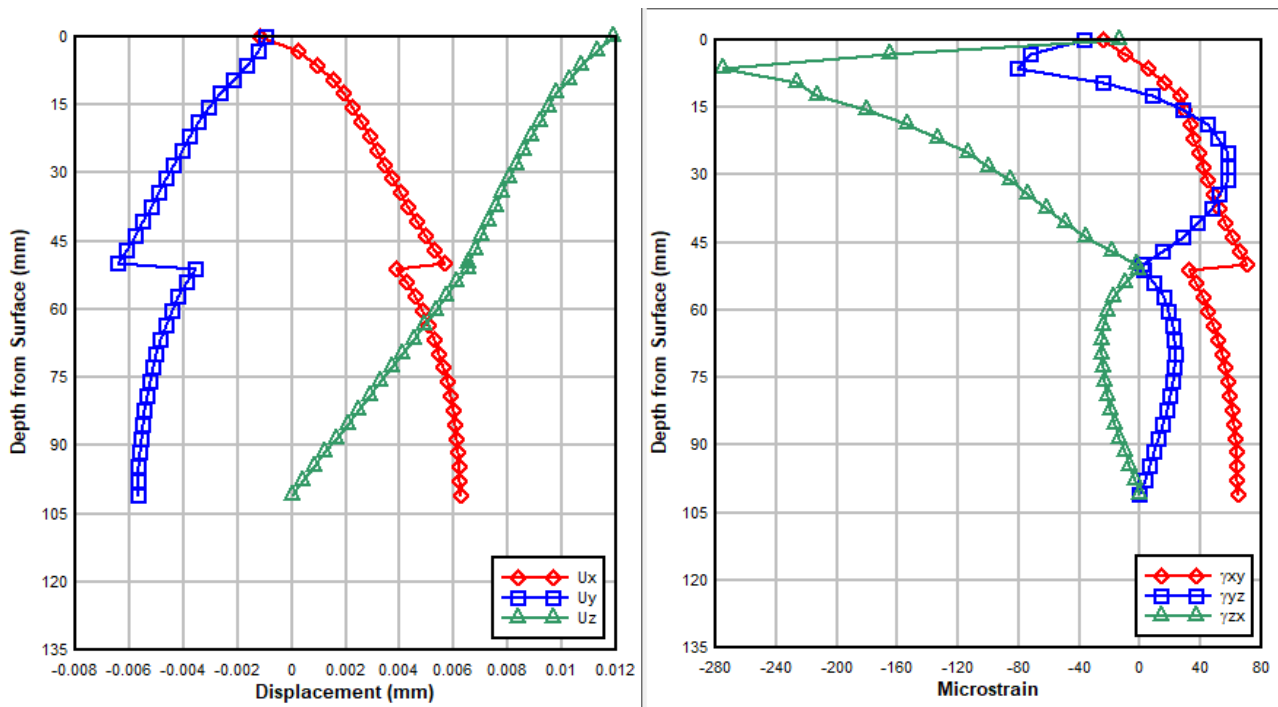


Figure 5.14 (b): Displacements and strain obtained for  $K$ .

To further understand the effects of the variation of the interlayer reaction modulus, Figure 5.15

shows the results obtained for the cases when the interlayer bonding condition was defined as fully bonded and fully debonded, respectively.

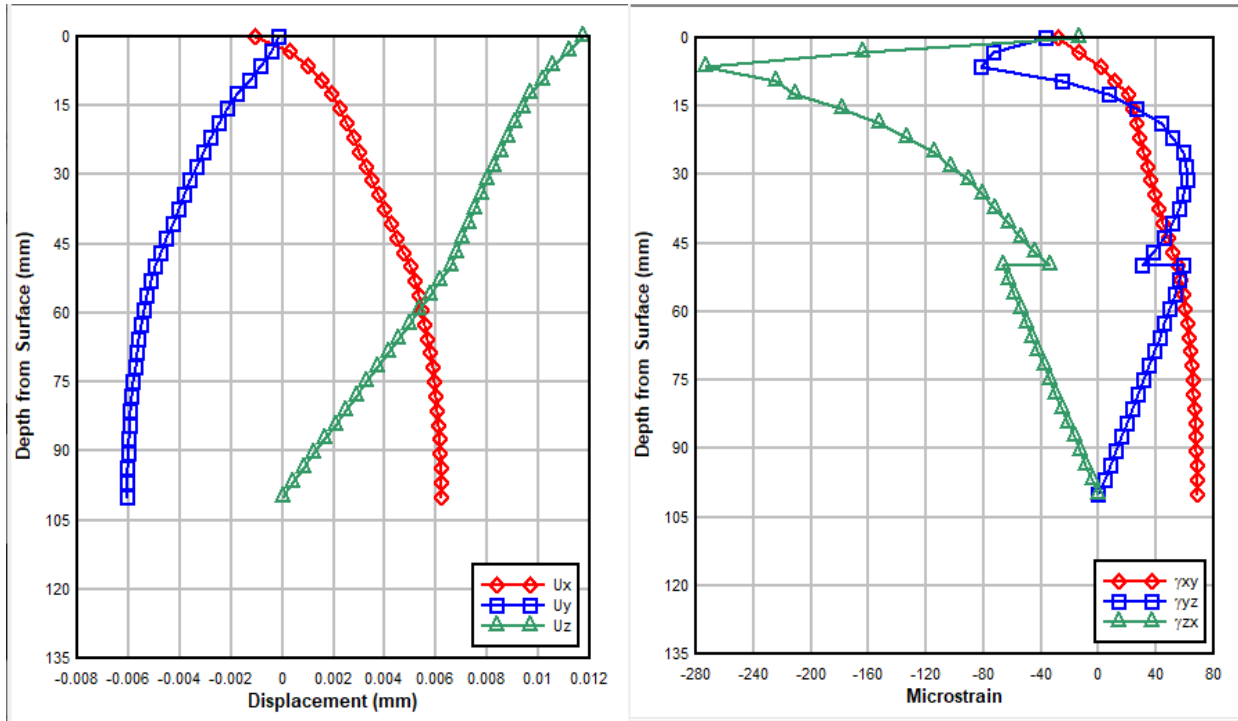


Figure 5.15 (a): Displacements and strain for fully bonded condition.

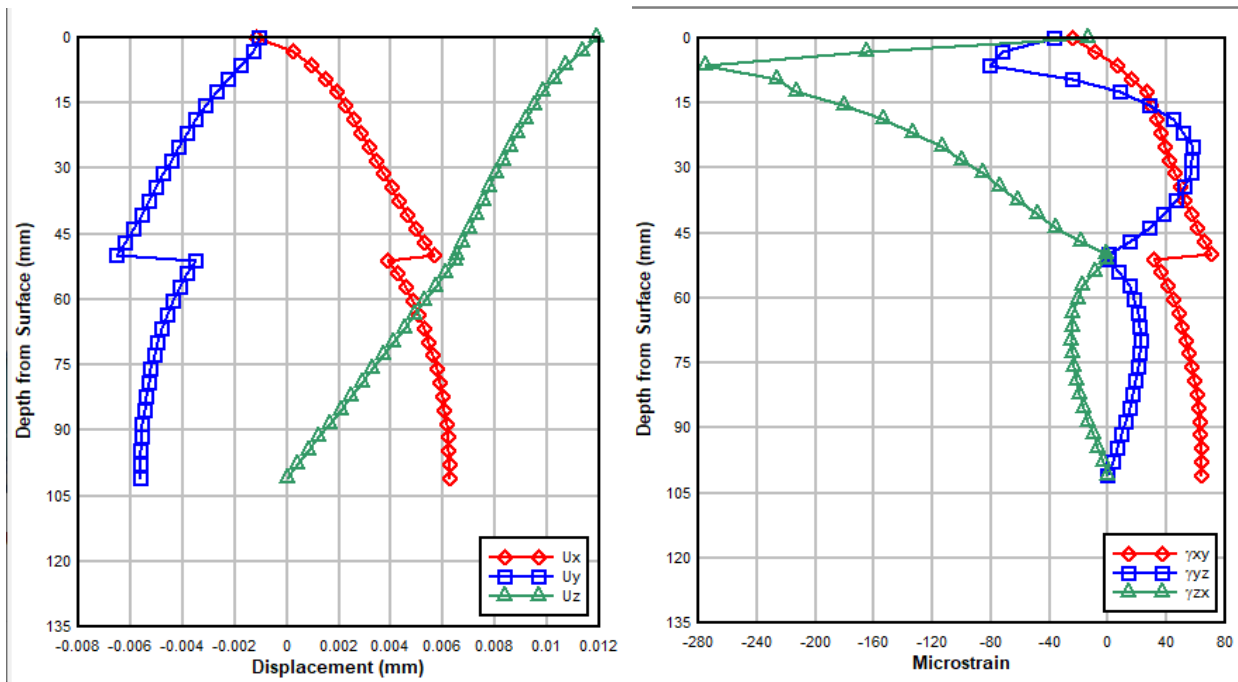


Figure 5.15 (b): Displacements and strains for fully debonded condition.

By comparing these results, with those obtained when the interlayer condition was defined as

partially bonded, with an interlayer stiffness equal to  $K_{max}$  and  $K$ , firstly it can be observed that the results of the debonded condition, at the depth of the interlayer are closer to the partially bonded condition with the experimental values of the interlayer reaction modulus. However, as expected, the relative displacement between layers is greater for the debonded case.

In terms of the generated strains, the debonded case, as well as the cases evaluated with  $K_{max}$  and  $K$ , a discontinuity can be observed at the depth of the interlayer for the shear strains in the xy direction ( $\gamma_{xy}$ ), which as expected, is larger in the debonded case. However, in terms of the shear strains in xz and yz directions ( $\gamma_{xz}$ ,  $\gamma_{yz}$ ) are equal to zero at the interlayer depth in the debonded case and in the partially bonded condition, these values are close to zero.

In the fully bonded condition, the results are the opposite; while there is no discontinuity in  $\gamma_{xy}$ , there is still presence of shear strains at the interlayer depth. In the case of  $\gamma_{xz}$  and  $\gamma_{yz}$ , these values are different from zero at the interlayer depth, and also present a discontinuity.

Finally, since when selecting the partially bonded condition, EVERSTRESSFE allows to configure the interlayer stiffness values in the range from 0 to 100000 N/mm<sup>3</sup>. In order to define the boundary values for the interlayer bonding condition in this software, a sensitivity analysis was performed by varying the interlayer stiffness along the allowed range by the software. By trying various values in this range, it was observed that the boundary values of the interlayer stiffness in EVERSTRESSFE are those presented in Table 5.11.

Table 5.11: Interlayer stiffness boundary values in EVERSTRESSFE.

Interlayer bonding condition	
Interlayer Stiffness	Description
$K \leq 10^{-2} \text{ N/mm}^3$	Complete debonding
$10^{-2} \text{ m}^3/\text{N} < K < 10^2 \text{ N/mm}^3$	Partial bonding
$K \geq 10^2 \text{ N/mm}^3$	Full bonding

By looking at these boundary values, as well as those defined for the shear spring compliance in BISAR and the values provided by previous authors (Canestrari *et al.*, 2013) it is possible to say that, the range of values for which the partial bonding condition has been defined extends around four orders of magnitude ( $10^4$  MPa/mm or  $\text{m}^3/\text{N}$  in the case of shear spring compliance).

### 5.4.3. Importance of calibrating adequately the interlayer bonding condition.

As seen in Chapter 2, various authors have remarked the importance of ensuring an appropriate bonding between the layers of asphalt pavements. By doing so, distresses like reflective cracking can be avoided and thus, the performance and the service life of the pavement are improved. It has been observed that, by supposing a fully bonded interlayer, the real effects of the loads are underestimated, as a fully bonded interface presents no slippage (relative displacements) between the layers.

On the other hand, if the interlayer condition is assumed as completely debonded, the effects of the applied loads would be overestimated, as the interlayer would no longer sustain the applied stresses, therefore leading to bigger displacements and strains. These overestimated values may lead to over

designing of the pavement sections.

It is clear, that the proper bonding condition to approximate the interlayer's real condition is the partial bonding condition, as it has been also mentioned in previous works. However, the ranges of values for which such condition has been defined in the analyzed software is extensive and the modelled data has shown that the results obtained from such software are sensitive to the variation of the given value to describe the interlayer condition. For such reason, it is important to calibrate adequately this value even within the partial bonding condition, rather than just picking an assumed value within this range.

As discussed previously, it is possible to obtain two different values of the interlayer reaction modulus ( $K_{max}$  and  $K$ ) from the Leutner test. However, given the analysis done in sub-chapter 5.3.1, the instructions given by standard on shear bonding tests, the work done by previous authors and finally, the modeled data in BISAR and EVERSTRESSFE, the definitive value that should be used is  $K_{max}$ .

To properly calibrate this value, the beforementioned method provides with a way to do so, parting from Leutner shear tests raw data in order to obtain the value of the characteristic value of the interlayer reaction modulus ( $K_{max,avg}$ ), which, as already has been defined, is the mean value of  $K_{max}$  for a given number of tests of a specific double-layered specimen type. Then, with such value, it can be directly used in EVERSTRESSFE, as the interlayer stiffness or in BISAR by converting it into terms of the shear spring compliance ( $AK$ ).

Finally, it is important to mention that due to the fact that the Leutner shear test is one of the most common laboratory methods to characterize the interlayer shear resistance and one of the most accessible ones, it proves an effective way to calibrate the interlayer condition. However, as discussed in Chapter 2, the shear resistance is not only affected by the shear loads, but also by the presence of normal loads. It was mentioned that the peak shear stress of the interlayer is function of the applied normal stress.

In fact, the presence of normal stress increases the value of the peak shear stress. For such reason, in reality, where traffic loads produce both normal and shear stresses, the actual peak shear stress is higher than the one calculated only in the presence of shear loads. Due to this, if the interlayer bonding condition is characterized from tests that only admit shear loads, this would result on overly designed pavement section, however the performance of the pavement is ensured, as it would be a conservative design.

#### **5.4.4. Input values from measured Leutner data**

Taking account all the previous considerations on the importance of calibrating properly the interlayer bonding condition some reference values will be given, in order to provide some guidelines on the proper characterization. In order to do so, the results obtained from the analysis of the raw data, which was performed in Chapter 4 are taken into account, along with the reasoning made in the previous segment of the current chapter.

Therefore, Table 5.12 provides the values that should be input into EVERSTRESSFE and BISAR, when modelling pavement structures composed by a given type of core.

Table 5.12: Obtained input values from experimental data.

	$K_{max,avg}$ [MPa/mm]	EVERSTRESSFE [N/mm <sup>3</sup> ]	BISAR [m <sup>3</sup> /N]
ME_1	0.436	0.436	2.29E-09
ME_2	0.338	0.338	2.96E-09
TE_1	0.474	0.474	2.11E-09
TE_2	0.421	0.421	2.38E-09
NT	0.259	0.259	3.86E-09

It is worth taking into account that, while EVERSTRESSFE allows to input the value of the interlayer stiffness [N/mm<sup>3</sup>], which is the same as the interlayer reaction modulus, in BISAR the value that must be input is the shear spring compliance,  $AK$  [m<sup>3</sup>/N], which is defined as the inverse value of the reaction modulus.

The values in the previous table, were the characteristic interlayer reaction modulus,  $K_{max,avg}$ , which was previously discussed in this chapter. It is important also to take into account that, these values depend on various characteristics of the specimen, such as the type of tack coat, dosage, mixture used for the layers, among others, and are specific to the cores that were extracted from the pavement test section. In such test section, it is important to remember that the upper layer was the surface course, whereas the lower one is a binder layer.

These values can be used to design/model a pavement composed by similar wearing course and binder layer in absence of experimental result, but only in a very general way. Naturally, for more accurate results, Leutner tests should be performed to characterize the interlayer condition on every specific pavement structure that must be defined, according to the method here proposed.



# 6. Chapter 6 - Conclusions

The main objective of this research was to determine a method to calibrate the interface condition in different flexible pavement design software, based on raw data measured by performing the Leutner shear test on double-layered specimens. The base of the method was centered around the constitutive models that reign the interlayer's shear response when only under shear loading, since this is the current situation when performing Leutner tests.

Additionally, in order to propose such method, it was important to understand how the interlayer condition is configured among various software, such as BISAR, EVERSTRESS, KENPAVE and EVERSTRESSFE. As discussed in this document, not all of these software allow the value of a parameter, but rather, simply allow a binary configuration between fully bonded and partially bonded. However, for those that do allow to use a given value (e.g. the interface stiffness in EVERSTRESSFE), a MATLAB script, which provides a tool to obtain the interlayer reaction modulus from data measured by performing a Leutner test (Shear load and displacement) was developed.

Such script not only processes the raw data in order to obtain the interlayer reaction modulus, but additionally provides results in terms of the peak shear stresses ( $\tau_{peak}$ ), corrected displacement at peak shear stress ( $\delta_{max}$ ) and provides the plots of the stress – displacement curves, along with the lines used to determine the value(s) of the modulus. It is important to mention that the script performs the calculations in accordance to the shear bond test standard, and therefore yield two possible values of the interlayer reaction modulus,  $K_{max}$  and  $K$ .

Naturally, since the software only allows to input one single value, and analysis on both of these values was performed, and from it, it is possible to conclude that the most adequate value of the interlayer reaction modulus to use for design/modelling purposes is that of  $K_{max}$ . Also, since when performing tests on double-layered specimens, more than one test is performed in the same type of core, a characteristic value for such type of core should be determined. This is done by finding the value of  $K_{max}$  for each test performed and then, finding the mean value of the total of tests performed. This will result in the characteristic interlayer reaction modulus,  $K_{max,avg}$  and this value is the one that should be input into the software.

In the case of BISAR, in which the value to input is not the interlayer reaction modulus itself, but rather the value to introduce is the shear spring compliance,  $AK$ . However, BISAR's manual define this value as the inverse of the reaction modulus, and therefore, it can be found by calculating  $AK=1/K_{max,avg}$ .

Additionally, the data obtained from the Leutner tests performed on the cores retrieved from the pavement test section, were analyzed in terms of peak shear stress and interlayer reaction modulus. For such cores, the type of interface treatment and dosage was varied, which allowed to calculate the input parameter to characterize the interlayer bonding condition in the programs, for various types of interlayers.

Finally, taking into account the previous considerations and in order to further assure the calibration of interlayer bonding condition, through the interlayer reaction modulus, the calculated values from the experimental data were taken into account to perform the modelling of a two-layered system to resemble the lab conditions into BISAR 3.0 and EVERSTRESSFE. During such process also the fully bonded and completely debonded condition were taken into consideration.

From the whole analysis and the modelling, it was found that firstly, the proper way to define the

interlayer condition is as partially bonded. However, the range of possible values of the interlayer reaction modulus that define such condition is large as it extends over several possible values (from  $10^{-2}$  to  $10^2$  N/mm<sup>3</sup> in the case of the interlayer shear stiffness and from  $10^{-11}$  to  $10^{-7}$  m<sup>3</sup>/N if referring to the shear spring compliance) and even small variations can affect the stresses, strains and displacements calculated by the software. For such reason, the calibration of this parameter must be done as adequately as possible.

This enforces the idea that it is even important to select a proper value between  $K_{max}$  and  $K$ , and from all the previous information, it is possible to conclude that, the method previously proposed, provides the proper way to calibrate, parting from the Leutner shear test raw data (which is one of the most commonly used methods to evaluate the interlayer shear resistance) to calculate the characteristic interlayer reaction modulus,  $K_{max,avg}$  for a give type of specimen. By doing so, an appropriate characterization of the interlayer condition is ensured, thus rendering more trustworthy asphalt pavement designs.

Additionally, regarding the analysis performed on the various types of double-layered specimens that were tested, the following conclusions were drawn.

- In terms of the peak shear strength, the cores that had a traditional emulsion as a tack coat were the most effective as compared to the rest of the cores. It could be observed that the application rate influences the results, as expected.
- Also, in terms of the peak shear strength, the cores without treatment showed the worst response under shear action as compared to the rest of the specimens.
- Regarding the calculated interlayer reaction modulus, the cores that had a traditional emulsion, applied at 0.15 kg/m<sup>2</sup> obtained the highest values, both for  $K_{max}$  and  $K$ .
- On the other hand, it is not possible to make conclusions regarding the fact that one type of emulsion is better than the other, as although the traditional emulsion at 0.15 kg/m<sup>2</sup> obtained the best results in terms of the interlayer reaction modulus, they are followed by the modified emulsion applied at 0.15 kg/m<sup>2</sup>, then by the traditional emulsion applied at 0.30 kg/m<sup>2</sup> and the modified emulsion at 0.30 kg/m<sup>2</sup>. However, the results do show that the application of a tack coat does improve the interlayer's performance in terms of the reaction modulus.

And from the software analysis and modelling, it is possible to conclude that:

- Regarding the flexible pavement design software reviewed during this study, it was found that some programs allow a more precise definition of the interlayer than other. For instance, KENPAVE allows only to define if the layers are bonded or partially bonded, and do not allow to set any condition in between.
- In the case of BISAR, two possible parameters can be defined, either the shear spring compliance,  $AK$  or the reduced shear spring compliance  $ALK$ . These parameters are related through the slip coefficient,  $\alpha$ . However, the parameter that can be calibrated through the results obtained from Leutner tests is the shear spring compliance, also defined as the inverse of the interlayer reaction modulus.
- For EVERSTRESSFE, it is possible to define if the interlayer condition is fully bonded or partially bonded. In the case of the second condition, the degree of bonding can be calibrated by defining the interlayer stiffness, which is the same parameter as the interlayer reaction modulus.

- Although various software provides the capacity to characterize the interlayer bonding condition, the most adequate ones to study the interlayer behavior are those that allow to configure horizontal loads as well as vertical ones. This is due to the fact that the shear testing on interlayers focus mainly on applied shear loads, which if cannot be calibrated in the software it would not be able to simulate the lab conditions.

# 7. Bibliography

- British Standards Institution (2019). BS EN 12697 – 48 *Bituminous mixtures – test methods for hot mix asphalts – Part 48: Interlayer Bonding*. London: BSI group.
- Bitumen Business Group (1998). BISAR 3.0 User Manual. The Hague: Shell International Oil Group B.V.
- Canestrari, F. *et al.* (2005) ‘Advanced testing and characterization of interlayer shear resistance’, *Transportation Research Record*, (1929), pp. 69–78. doi: 10.3141/1929-09.
- Canestrari, F. *et al.* (2013) *Mechanical testing of interlayer bonding*.
- Collop, A. C., Thom, N. H. and Sangiorgi, C. (2002) ‘Laboratory assessment of bond condition using the Leutner shear test’, *Proceedings of the Institution of Civil Engineers: Transport*, 156(4), pp. 211–217. doi: 10.1680/tran.2003.156.4.211.
- Cutica, S. 'Indagine sperimentale sul comportamento a taglio delle interfacce bituminose'.
- Das, R. *et al.* (2018) ‘Development and validation of a model to predict interface bonding between pavement layers’, *Transportation Research Record*, 2672(28), pp. 22–30. doi: 10.1177/0361198118759001.
- Du, J. C. (2015) ‘Evaluation of asphalt pavement layer bonding stress’, *Journal of Civil Engineering and Management*, 21(5), pp. 571–577. doi: 10.3846/13923730.2014.890664.
- Kim, H. *et al.* (2011) ‘Numerical and Experimental Analysis for the Interlayer Behavior of Double-Layered Asphalt Pavement Specimens’, *Journal of Materials in Civil Engineering*, 23(1), pp. 12–20. doi: 10.1061/(ASCE)MT.1943-5533.0000003.
- Kim, Y. R. *et al.* (2015) ‘Surface Layer Bond Stresses and Strength’, (December), pp. 1–289. Available at: <https://connect.ncdot.gov/projects/planning/RNAProjDocs/2013-04FinalReport.pdf>.
- Mohammad, L. N., Raqib, M. A. and Huang, B. (2002) ‘Influence of asphalt tack coat materials on interface shear strength’, *Transportation Research Record*, (1789). doi: 10.3141/1789-06.
- Ozer, H. *et al.* (2012) ‘Characterisation of interface bonding between hot-mix asphalt overlay and concrete pavements: Modelling and in-situ response to accelerated loading’, *International Journal of Pavement Engineering*, 13(2), pp. 181–196. doi: 10.1080/10298436.2011.596935.
- Raab, C. and Partl, M. N. (2004) ‘Effect of tack coats on interlayer shear bond of pavements’, *8th Conference On Asphalt Pavements For Southern Africa*, (September), p. 9.
- Raab, C., Partl, M. N. and El Halim, A. E. H. O. A. (2009) ‘Evaluation of interlayer shear bond devices for asphalt pavements’, *Baltic Journal of Road and Bridge Engineering*, 4(4), pp. 186–195. doi: 10.3846/1822-427X.2009.4.186-195.
- Shahin, M. Y. *et al.* (1987) ‘Consequence of layer separation on pavement performance’, *U.S. Army Construction Engineering Research Laboratory*.
- Sholar, G. A. *et al.* (2004) ‘Preliminary investigation of a test method to evaluate bond strength of bituminous tack coats’, in *Asphalt Paving Technology, AAPT*.

Song, W. *et al.* (2018) 'Effects of asphalt mixture type on asphalt pavement interlayer shear properties', *Journal of Transportation Engineering Part B: Pavements*, 144(2), pp. 1–7. doi: 10.1061/JPEODX.0000056.

Szydło, A. and Malicki, K. (2016) 'Analysis of the Correlation between the Static and Fatigue Test Results of the Interlayer Bondings of Asphalt Layers', *Archives of Civil Engineering*, 62(1), pp. 83–98. doi: 10.1515/ace-2015-0053.

Tseng, E., Street, T. and Vic, P. M. (2019) *Review of Applicable Bond Strength Tests for Assessing Delamination Potential*. Review of Applicable Bond Strength Tests for Assessing Asphalt Delamination Potential.

University of Maine (2009). EVERSTRESS FE Help. Maine: University of Maine.

Uzan, J., Livneh, M. and Eshed, Y. (1978) 'INVESTIGATION OF ADHESION PROPERTIES BETWEEN ASPHALTIC-CONCRETE LAYERS.', in *Asphalt Paving Technol.*

Washington State Department of Transportation (2005). EVERSERIES User guide pavement analysis and case studies. Washington: Washington Department of Transportation.

Williamson, M. J. (2015) *Finite element analysis of hot-mix asphalt layer interface bonding*.

Zhang, H. *et al.* (2019) 'Effects of Continuous Laydown and Compaction on Interlayer Shear Bonding of Asphalt Layers', *Advances in Materials Science and Engineering*, 2019, pp. 1–12. doi: 10.1155/2019/2184094.



# 8. Appendix

### 8.1. Appendix A – Stress – displacement curves with Kmax and K lines.

The plots here presented are obtained by performing the data analysis with the MATLAB script presented in Appendix B. Each plot represents the bonded segment of the curve for each test performed on each type of core. These results are discussed in Chapter 4.

#### 8.1.1. ME<sub>1</sub> plots.

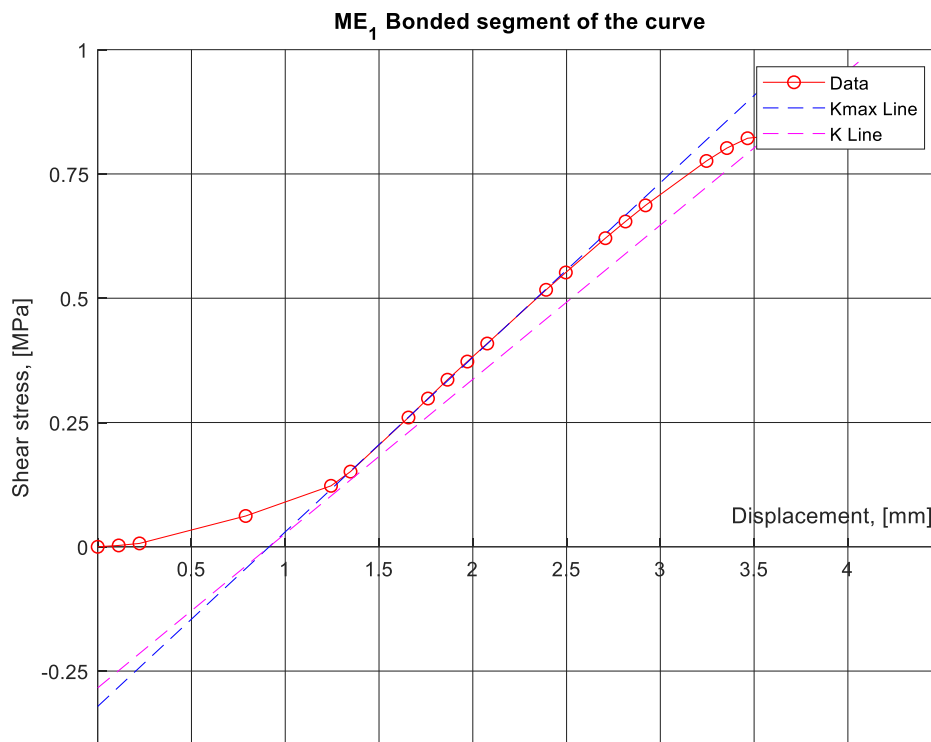


Figure 8.1: Bonded segment of the curve with Kmax and K lines, ME<sub>1</sub>\_1.

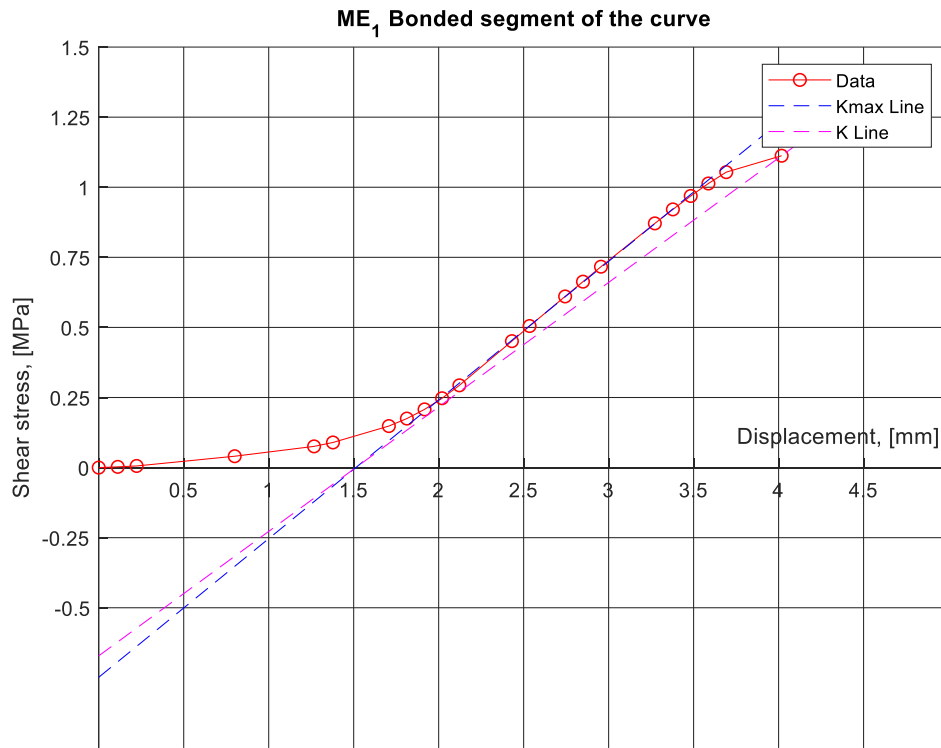


Figure 8.2: Bonded segment of the curve with Kmax and K lines, ME<sub>1</sub>\_2.

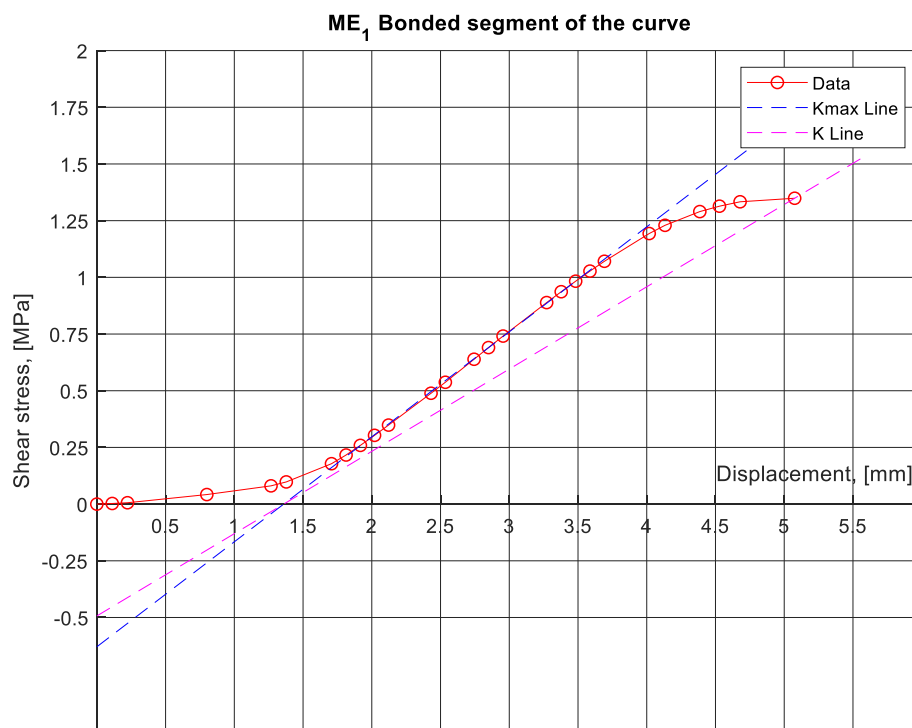


Figure 8.3: Bonded segment of the curve with Kmax and K lines, ME<sub>1</sub>\_3.

8.1.2. ME<sub>2</sub> plots.

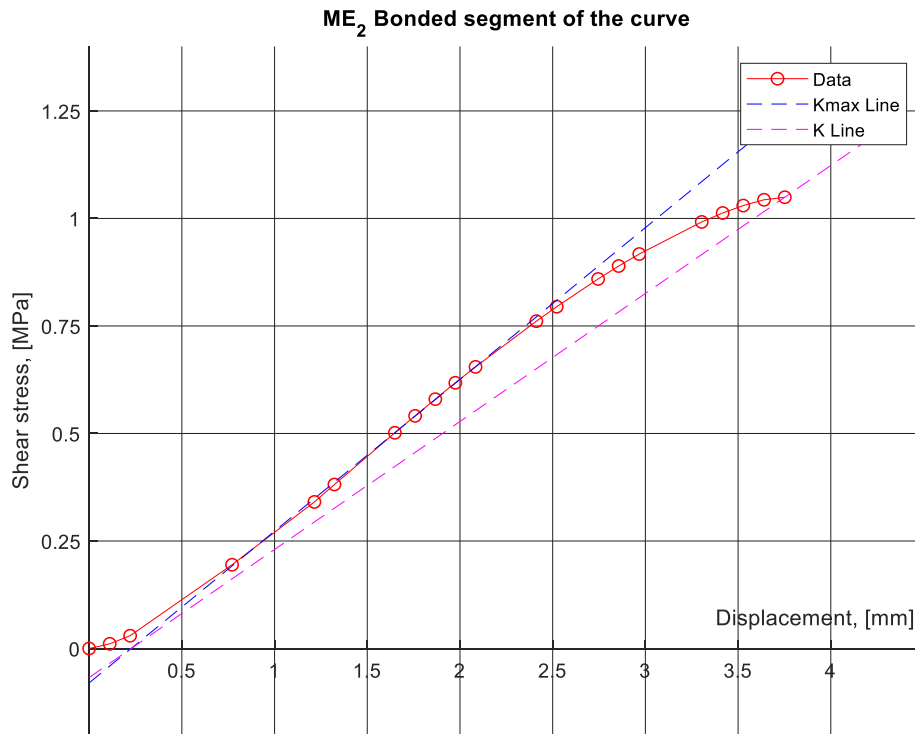


Figure 8.4: Bonded segment of the curve with Kmax and K lines, ME<sub>2</sub>\_1.

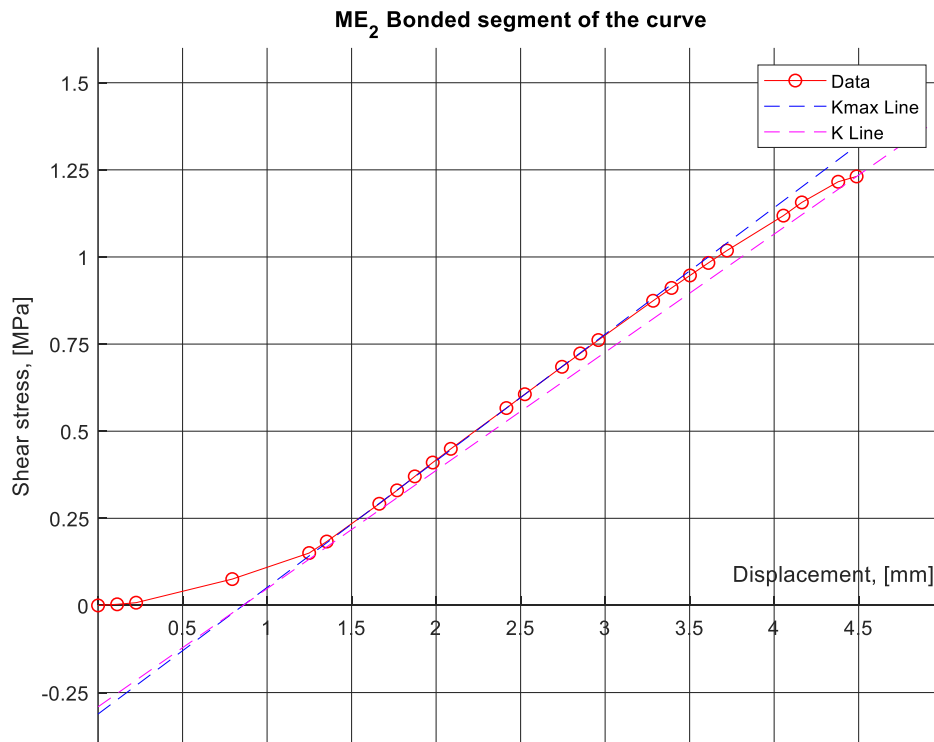


Figure 8.5: Bonded segment of the curve with Kmax and K lines, ME<sub>2</sub>\_2.

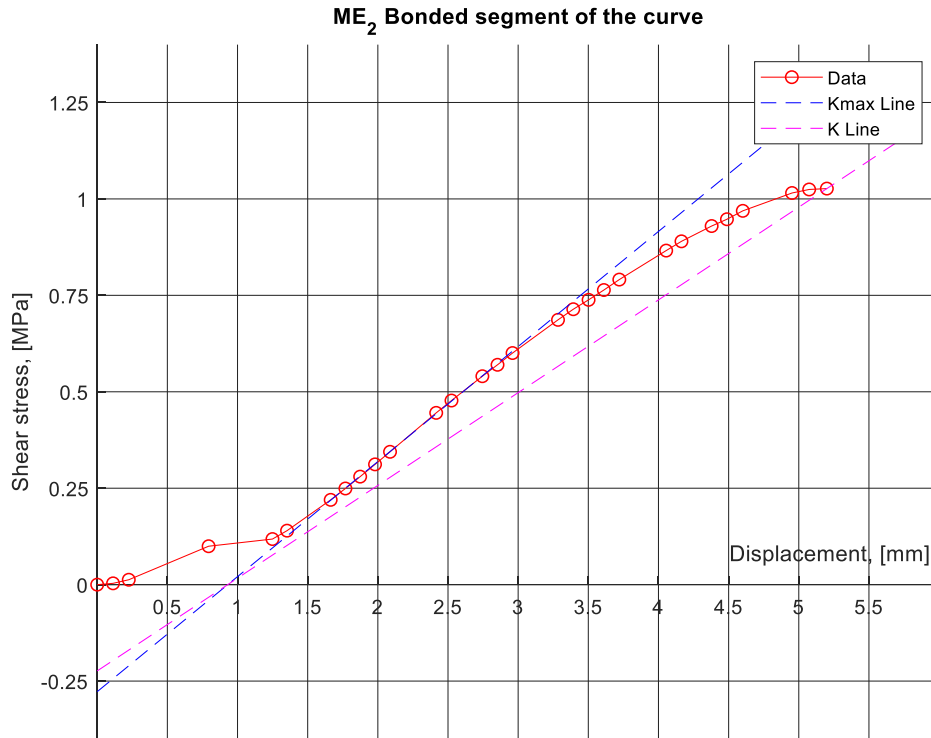


Figure 8.6: Bonded segment of the curve with Kmax and K lines, ME<sub>2</sub>\_3.

### 8.1.3. TE<sub>1</sub> plots

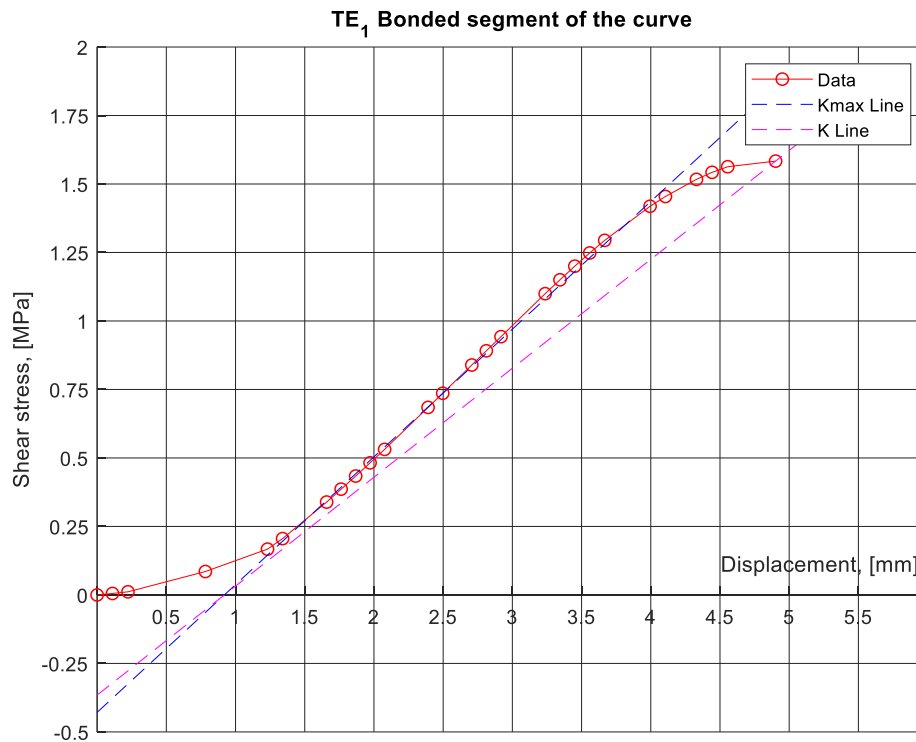


Figure 8.7: Bonded segment of the curve with Kmax and K lines, TE<sub>1</sub>\_1.

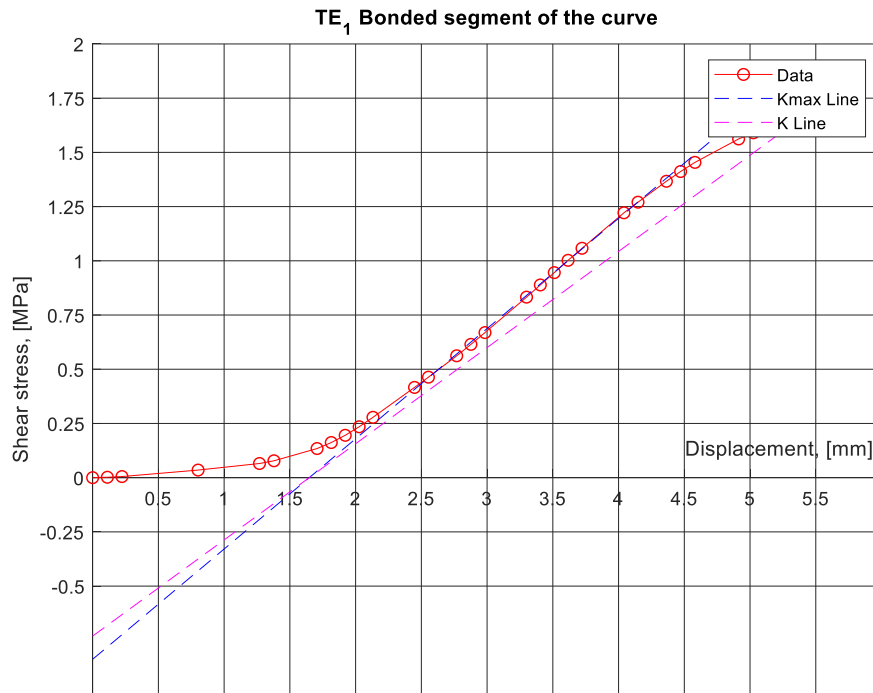


Figure 8.8: Bonded segment of the curve with Kmax and K lines, TE<sub>1</sub>\_2.

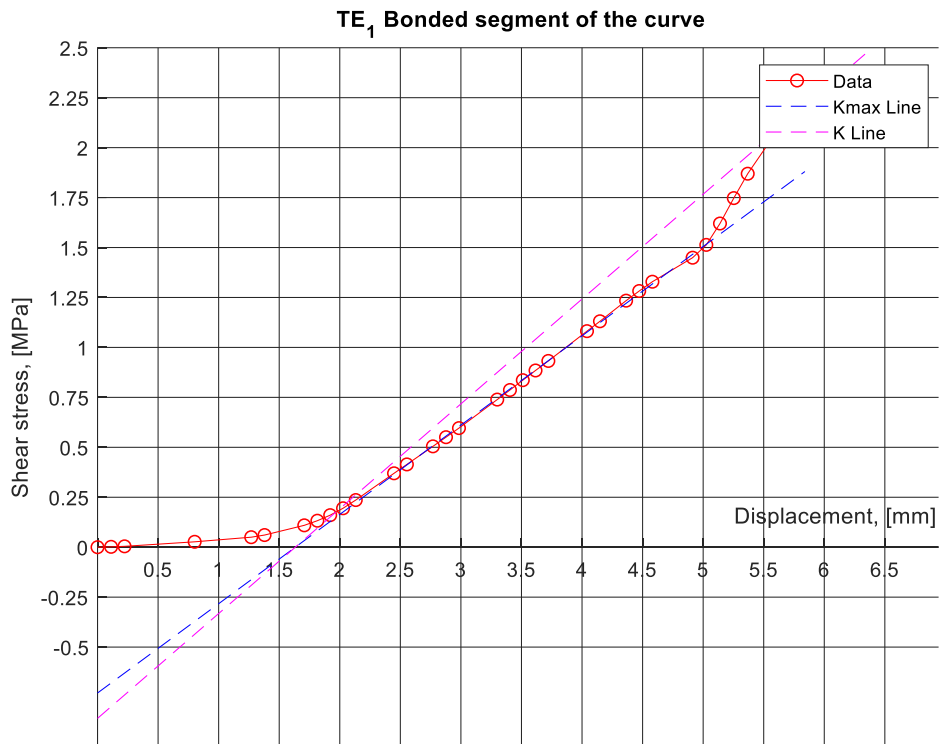


Figure 8.9: Bonded segment of the curve with Kmax and K lines, TE<sub>1</sub>\_3.

8.1.4. TE<sub>2</sub> plots.

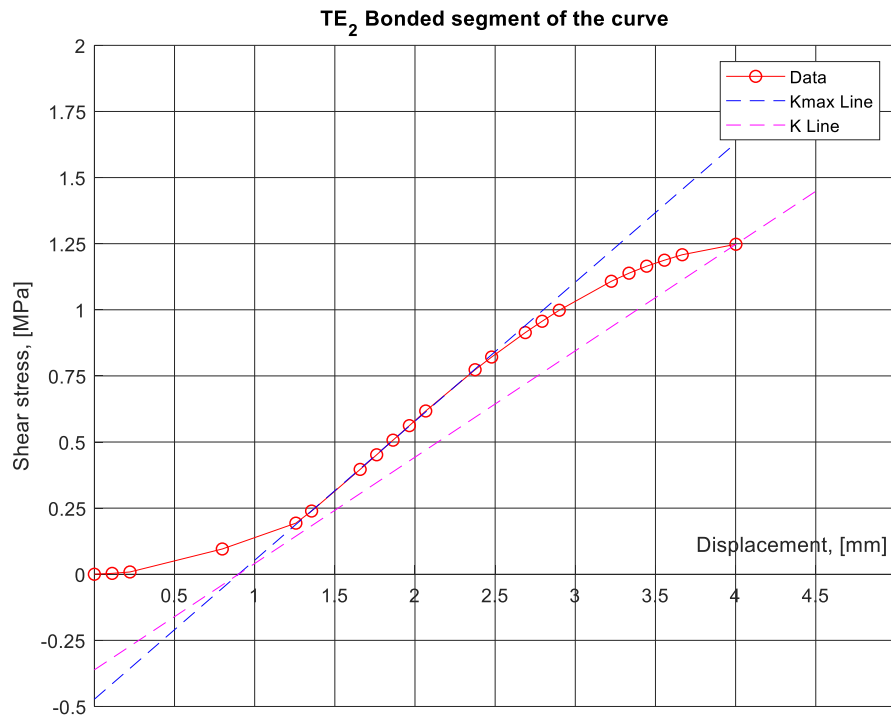


Figure 8.10: Bonded segment of the curve with Kmax and K lines, TE<sub>2</sub>\_1.

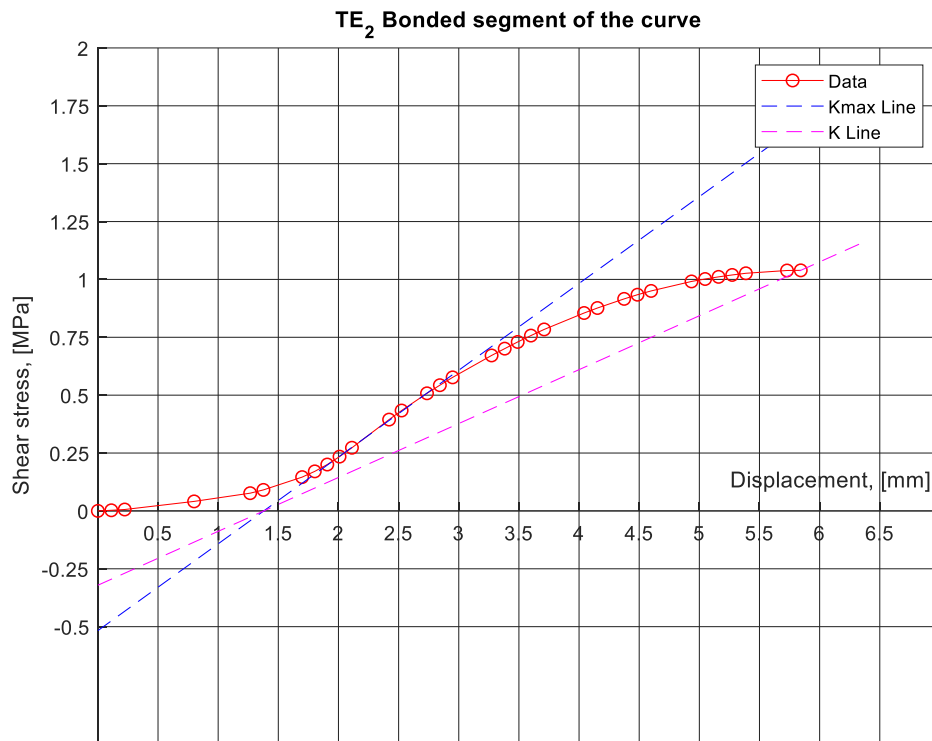


Figure 8.11: Bonded segment of the curve with Kmax and K lines, TE<sub>2</sub>\_2.

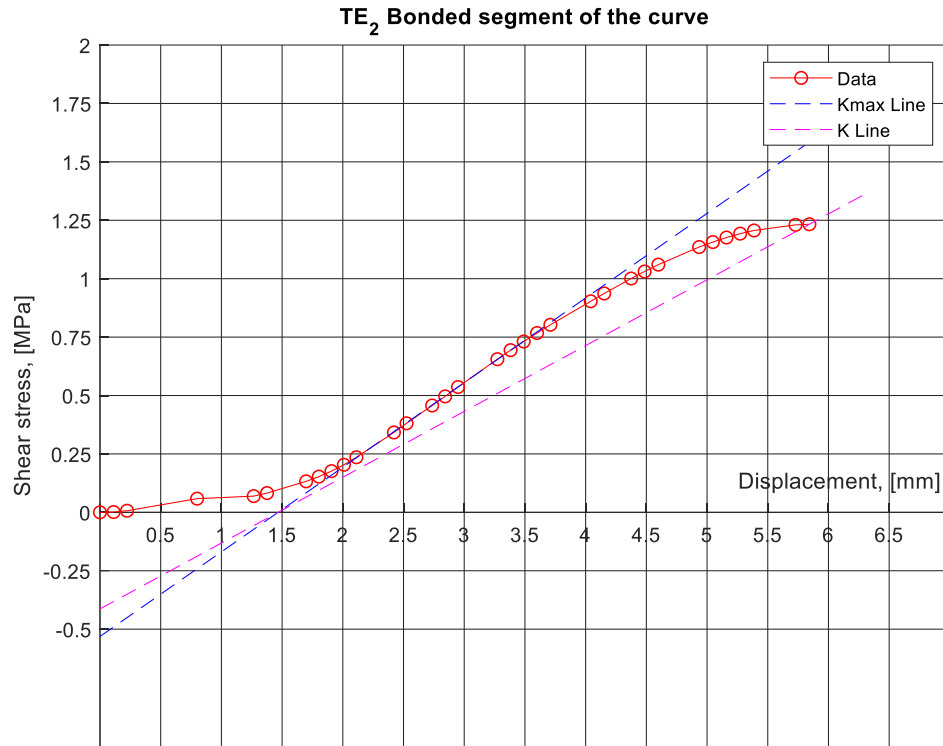


Figure 8.12: Bonded segment of the curve with Kmax and K lines, TE<sub>2</sub>\_3.

### 8.1.5. NT plots

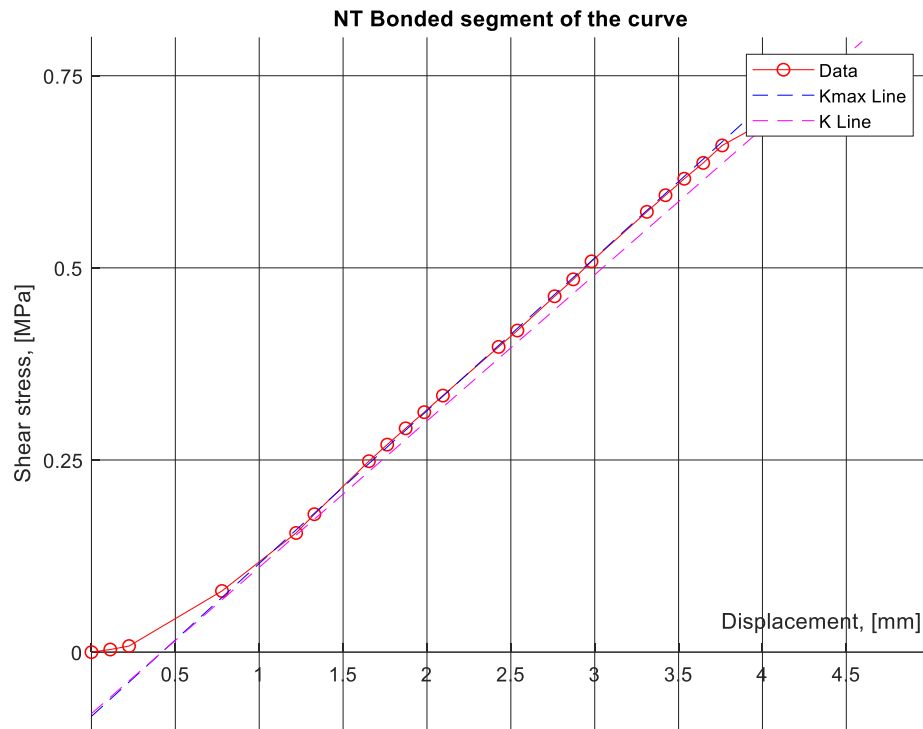


Figure 8.13: Bonded segment of the curve with Kmax and K lines, NT\_1.

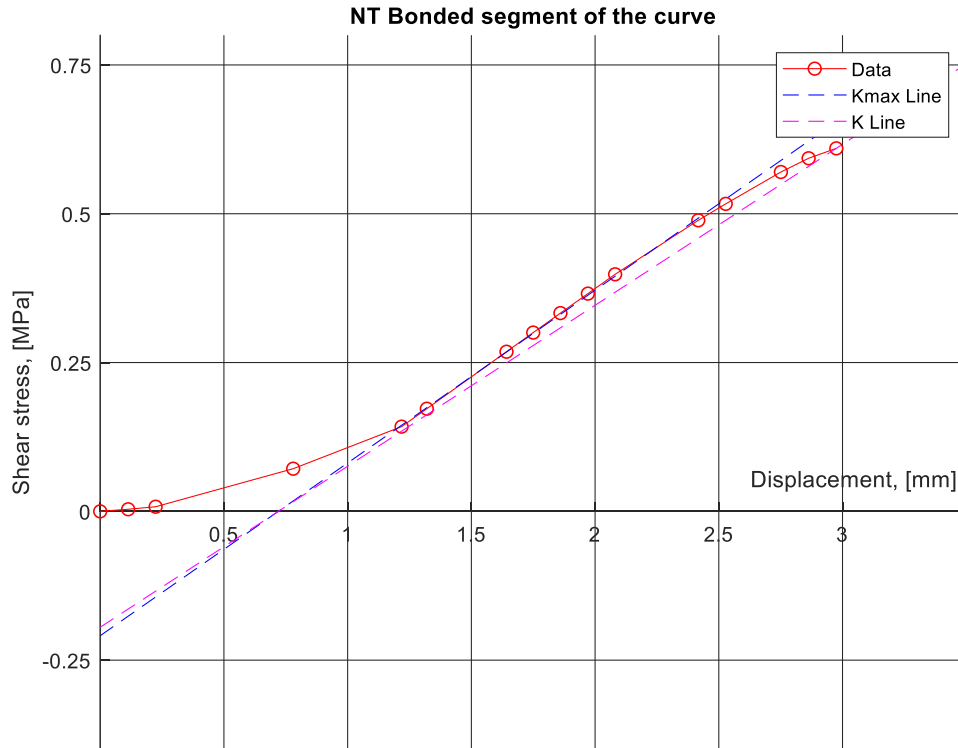


Figure 8.14: Bonded segment of the curve with Kmax and K lines, NT\_2.

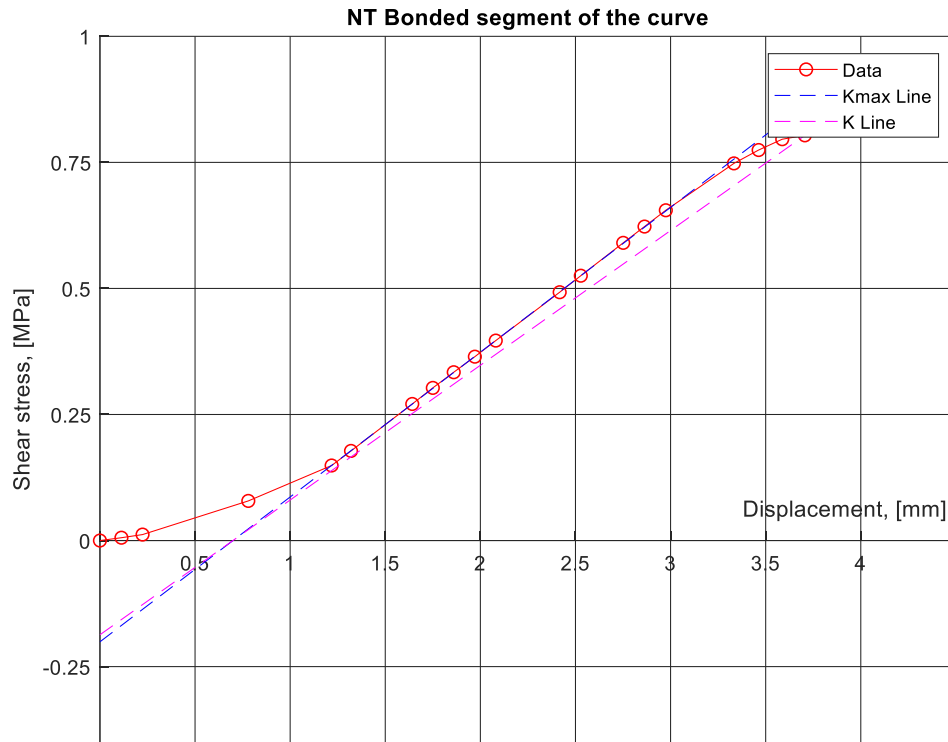


Figure 8.15: Bonded segment of the curve with Kmax and K lines, NT\_3.

## 8.2. Appendix B – MATLAB script

NOTE: The current MATLAB script was developed in the 2019 version of the program. It is possible, by modifying the *Load\_Dataset* function and the main script properly, this script can be used to perform the analysis on other datasets different to the established ones. However, it is recommended that the input data is contained in an Excel file, with the shear load in kN in the first column and the displacement (mm) in the second.

It must be acknowledged that the script allows to analyze maximum three tests per type of dataset, and the *Analyze\_Dataset1* function performs the analysis for only on test of a given dataset and *Analyze\_Dataset* performs the analysis in all of the three tests.

The files for this MATLAB script can be found in the zip attached files delivered along this document.

# 9. Acknowledgments

Special thanks to my parents and my sister, for making all of this possible, thanks to their unconditional love and support, not only during this process, but throughout all my life. I love you the most.

Also, thanks to all those who were present along this road, both to those who were physically with me and those who could not be with me because of the distance but still had my back all this time.

Finally, I would like to thank L. Tsantilis and P. P. Riviera and I would like to let them know that it was a pleasure to work not only with such excellent professionals, but also, such great individuals.

Thanks to you all for helping me become a better professional, for imparting me such vast knowledge, and most important of it all, instructing me on how to be a better human being.